THE AERODYNAMIC PERFORMANCE OF A HIGH TURNING ANGLE TURBINE BLADE PROFILE

THE AERODYNAMIC PERFORMANCE OF A HIGH TURNING ANGLE TURBINE BLADE PROFILE

by

THOMAS CHARLES MONTIZAMBERT HARRIS, B.ENG.

A Thesis

Submitted to the School of Graduate Studies

in Partial Fulfilment of the Requirements

for the Degree

Master of Engineering

McMaster University

August 1977

MASTER OF ENGINEERING (1977)
(Mechanical Engineering)

McMASTER UNIVERSITY
Hamilton, Ontario

TITLE: The Aerodynamic Performance of a High Turning Angle Turbine Blade Profile

AUTHOR: T.C.M. Harris, B.Eng., Carleton University (Ottawa)

SUPERVISOR: Dr. J. H. T. Wade

NUMBER OF PAGES: x, 160

ABSTRACT

The continuous emphasis placed on obtaining higher work outputs from Gas Turbines has led to the design of turbine blades having large turning angles.

As part of a research program co-sponsored by the National Research Council and Pratt and Whitney of Canada Ltd., this work examined the aerodynamic behaviour of the root section of the highly curved turbine blade under investigation.

An intermittant blow-down wind tunnel was used to test a two dimensional cascade of high turning angle turbine blades. The tunnel was modified to allow improved flow control at the desired operating conditions.

A computerized scheme was developed whereby the two dimensional potential flow solutions could be obtained by merely specifying the cascade geometry and inlet flow. This allowed the direct comparison of theoretical and experimental blade surface pressure distributions. The effect of overall pressure ratio on the variation of exit gas angle and total head loss coefficient was also investigated experimentally.

ACKNOWLEDGEMENTS

The author is grateful to Dr. J. H. T. Wade for his continuous guidance and support as supervisor of this work. My sincere gratitude is due also to Dr. J. H. Stannard for his constant interest and valuable suggestions.

The financial support provided through the National Research Council Operating Grant A1585 is gratefully acknowledged.

I also wish to acknowledge the assistance of the Division of Mechanical Engineering of the National Research Council who manufactured the blades for the cascade wind tunnel.

The author would also like to thank Ms. B. Bedell for her expert typing of the thesis.

TABLE OF CONTENTS

LIST OF FIGURES

NOMENCLATURE

Arabic Symbols	Description	Units
A_E	exit flow area	inches^2
c	blade chord	inches
c_D	drag coefficient	——
C	curvature of streamline on orthogonal (inverse of radius)	inches^{-1}
Cp'	pressure surface curvature	inches^{-1}
C_s'	suction surface curvature	inches
d	diameter of body causing wake	inches
d_1	diameter of first tube	inches
d_2	diameter of second tube	inches
e	error	p.s.i.
l_1	length of first tube	inches
l_2	length of second tube	inches
M	Mach number	——
N	distance along an orthogonal measured from the suction surface	
N_0	orthogonal length	inches
P	static pressure	p.s.i.
ΔP	difference between initial and final pressures	p.s.i.
q_{OUT}	outlet dynamic head	----
S	blade pitch	inches
t	pressure rise time	seconds

Arabic Symbols	Description	Units
u	velocity	f.p.s.
u_1	velocity in wake	f.p.s.
v_1	volume of first tube	$inches^3$
v_2	volume of second tube	$inches^3$
y	vertical coordinate	inches
x	distance downstream	

Greek Symbols

α	stagger angle	degrees
β	inlet gas angle	degrees
δ	mixing length/wake thickness	$inches^{-1}$
δ^*	displacement thickness	inches
δ^{99}	boundary layer thickness	inches
ϕ_N^2	total pressure loss coefficient	----

Subscripts

1	inlet section
2	outlet section
s	suction surface
p	pressure surface
o	stagnation
mid	midstream
press	pressure surface
atm, a	atmosphere
m	transducer

CHAPTER 1

INTRODUCTION

Due to the complexity and three dimensional character of the flow between gas turbine blades having high turning angles, various simplifications have been adopted in the quest for accurate design data. Primarily, the flow across individual blade sections has been treated as two dimensional flow in which a rectilinear blade cascade is used with the appropriate inlet and outlet flow conditions. Because of the limitations involved in the theoretical models of such flow, experimental investigations have been adopted as the primary source of blade design data. Reference [1] points out that "the use of two-dimensionally derived flow characteristics"..."has generally been satisfactory for conservative units". Although such three dimensional effects as radial pressure gradients can not be investigated, a great deal of important basic information on blade surface pressure distribution, flow angles, loss coefficients and, to a lesser extent, blade surface boundary layers can be derived.

Early experimental cascade results were quite sensitive to individual tunnel design and operation [1] making reproduction of results difficult. Hence, one of the major aims of this thesis was to improve the operating characteristics of the existing cascade wind tunnel to permit reproduceible results to be obtained at high pressure ratios. Chapter 3 presents the tunnel modifications and results achieved.

In an effort to achieve greater work output per stage, the turbine designer has continued to increase the axial flow velocity, pressure ratio, total turning angle and blade speed. All of these changes have resulted in supersonic flow patches on the blade surfaces. The turbine blade profile under investigation in this work is shown in Figure 1. It is the root section of a turbine blade currently being investigated under a turbine research program cosponsored by the National Research Council and Pratt and Whitney of Canada Ltd. For higher than critical pressure ratios, we obtain a high subsonic inlet condition while the discharge becomes supersonic in the expansion process just downstream of the exit plane (see Figure 29). This is a "low loss" condition because generally boundary layers are subjected to decreasing pressures on the suction surface of the blade. The blade's high turning angle also results in a profile which is structurally stiff and allows area for coolant flow passages.

Five quantities basically determine the aerodynamic behaviour of a cascade with ideal flow. One of these is blade shape expressed in terms of thickness distribution and camber (see Figure 1). Another quantity is the orientation of the blades with respect to the cascade principal axis. This is referred to as the stagger angle (α in Figure 1) and was approximately 24° for the cascade tested. The third quantity is the solidity ($\sigma = c/s$) which in our case was about 2.1.

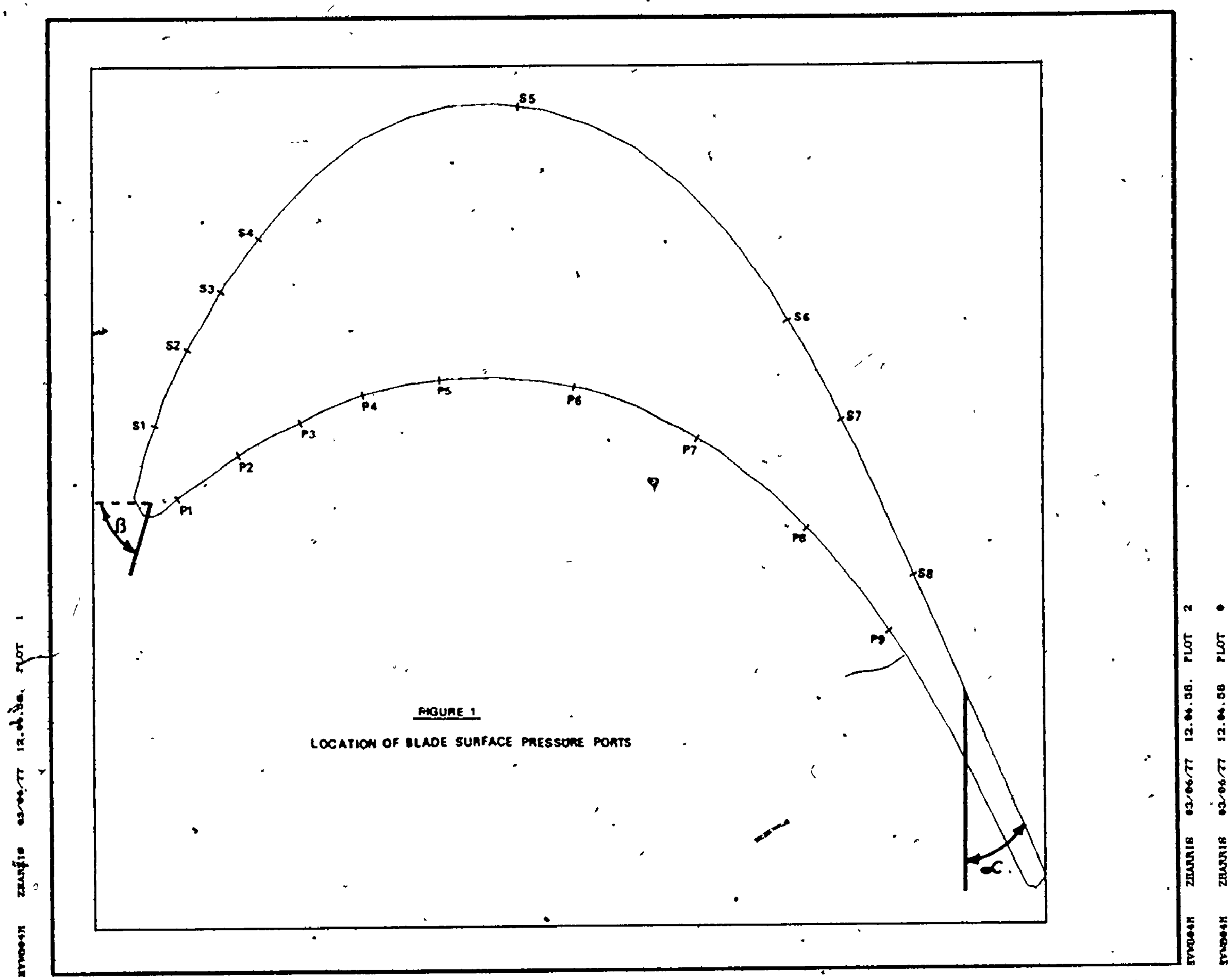

Figure 1 Profile of Turbine Blade under Investigation

The geometry of the cascade of blades is defined with these three quantities. Finally, the direction of air flow (β in Figure 1) and Mach number must be known upstream of the cascade. Theoretically, all details of the flow of an ideal inviscid fluid can be determined from these data.

Besides the objective just mentioned, this thesis had two other primary goals. The first was to test a two-dimensional cascade of turbine blades with the profile as illustrated to obtain the following information for a range of exit Mach numbers and inlet gas angles:

(i) pressure and suction surface static pressure distributions,

(ii) average passage exit flow angles,

(iii) total cascade loss coefficients.

Chapters 5 and 6 present the experimental results and discussions.

This data will assist in determining the acceptability of such high turning angle blades with regards to possible boundary layer separation due to adverse pressure gradients. Since this blade is likely to be used on the gas compressor turbine, it is important to know the exit flow angle and available flow energy for design of the next turbine stage.

The last thesis objective was the development of a computer program to specify the flow passage quasi-orthogonals (see References [2] and [3] for explanation) required for input to the existing potential flow streamline curvature program (developed by Malhotra [3]). The technique employed and the accuracy achieved are discussed in Chapter 7. The streamline curvature program was modified slightly to calculate the blade lift force and to present theoretical pressure and Mach number information in both tabular and graphical form. The graphical presentation in particular allows direct comparison with experimental results. These are also shown in Appendix VI.

The thesis objectives are summarized as follows:

(1) the improvement of the wind tunnel operating characteristics

(2) the testing of the specified turbine blade profile

(3) the development of a computer program which constructs and specifies the potential flow orthogonal grid.

CHAPTER 2

LITERATURE SURVEY

The rapid rate of growth and development of the gas turbine industry in recent years has been brought about most significantly because of two factors:

(i) metallurgical advances have allowed the use of high temperatures in the operating parts of the turbine leading to a cooled turbine blade.

(ii) the accumulated knowledge in aerodynamics and thermodynamics has made possible the design of more efficient compressors and turbines.

The present day concept of a gas turbine system was first patented in 1884 by John Parsons of England [4]. At this time and until the 1920's turbines were designed assuming one dimensional flow through the blade passages. However, the need for higher axial flow compressor efficiencies led to the development of two dimensional flow theories. Early theoretical models considered each blade as an isolated airfoil and consequently, actual design work relied heavily on the results of two dimensional cascade testing [5]. As mentioned in Chapter 1, these results were very sensitive to the specific tunnel used making correlations of isolated data very difficult. The problems experienced were primarily due to failure to obtain true two dimensional flow. In the late 1940's, British experimentors Carter and Howell were among the first to make effective use of early cascade investigations.

Recently the use of effective tunnel boundary layer control (i.e., suction, blowing, etc...) has resulted in more consistent test data which shows better correlation with theoretical results. This is primarily due to to the minimization of boundary layer induced secondary flow effects. However, most of the available cascade test data has been obtained at low speeds (Mach numbers of 0.1 are usual) and this is of questionable value when higher velocity characteristics are required [1]. Since this thesis presents high subsonic and low supersonic cascade results, the data presented is considered to be a contribution to turbine design.

The first turbine blade profile results from the blow-down wind tunnel used in this thesis were obtained by Stannard [2]. He demonstrated that flow in the tunnel exit plane was sufficiently two dimensional for the cascade results obtained to be meaningful. Stannard continued to investigate the high turning angle blades shown in Reference [2] and demonstrated the effects of variations of angle of attack and pressure ratio on the blade's surface pressure distributions. Due to tunnel limitations, he was able to get good flow control for long time spans (12 seconds or more) only at pressure ratios of approximately 2.0 and below. Thus, there existed a need to extend the tunnel operating time and improve its stability for high pressure ratios. References [2], [5], [6] were used as guides in attempts to do this. Reference [6] also discusses error analysis of effects induced by moisture and turbulence in the cascade inlet flow.

Reference [7] presents several two dimensional cascade test results from the National Gas Turbine Establishment in Britain and discusses the various generalized plotting techniques. These plotting techniques require the selection of a design point for each set of flow conditions. Howell [8] arbitrarily defines the design point as that where the fluid deflection is 0.8 times the stalling value of deflection. The latter is defined as the point where the loss coefficient is twice that of minimum loss. Lichtfuss and Starken [9] examined the effect and position of expansion and shock waves in the throat region.

A thorough review of the available low speed exit angle data and theoretical predictions is found in Reference [1]. They mention the need for high Mach number testing before acceptable models for the determination of exit flow deviation can be formulated.

The theoretical prediction of flow of a viscous fluid through a cascade is highly complex and, as yet, cannot be determined in its generalized form [1]. In most cases, the effects of viscosity are concentrated at the blade surfaces and the problem can be treated using boundary layer theory. The work of Stannard [2] and Le Foll [10] are examples of improvements to the basic potential flow solution by including boundary layer effects. Outside a narrow region near the blade surfaces, the flow is practically irrotational and potential flow calculations have been shown to provide useful information regarding the flow in a blade passage despite completely ignoring viscosity. Even when thick boundary layers or separation exists, potential flow derived pressure distributions are indespensible for boundary layer calculations. For these reasons, two dimensional flow solutions are probably the most important single theoretical tool with which to analyze cascade flow [1].

Reference [5] is a good example of recent attempts at combining potential flow theory, viscous flow effects and empirical results. Both References [1], [3] provide an extensive survey of the existing plane potential flow theory and available methods. These reviews indicate that the available design theory, although not simple, is useable and has established a firm understanding of the ideal flow through two dimensional cascade blade sections.

The streamline curvature technique selected for use in this thesis, is a development of methods dating back to the 1950's [1]. This method is slightly inaccurate under transonic conditions but has the advantage of being inexpensive and quick in operation [2]. It can be classified as a "direct" instead of "inverse" potential flow technique. Reference [1] includes a complete dissertation on this point. The method was programmed for use on the computer by Malhotra [3] and several improvements were incorporated by Stannard [2].

CHAPTER 3

THE CASCADE WIND TUNNEL

3.1 General Description

As discussed in Reference [2], an intermittent "blow-down" system was designed primarily to avoid the higher capital and running costs associated with a continuous flow tunnel. Reference [11], for example, cites how a reduction in power requirements of greater than 90% is accomplished when a blow-down instead of a continuous flow tunnel is used. Since a detailed description of the cascade wind tunnel and related equipment is included in Reference [2], only a brief outline will be given here. An overall view of the test equipment is shown in Figure 2.

A large V-twin oil free compressor compresses atmospheric air to approximately 110 p.s.i.g. This air is delivered at a rate of 500 S.C.F.M. through a water cooled after-cooler, and an air drier to four cylindrical storage vessels. These vessels provide a storage capacity of 1080 cu. ft. Originally, one 4" diameter pipe with two control valves connected the reservoirs to the tunnel. The first valve is an air actuated butterfly valve for primary on-off control of the air flow. The second is a variable position ball valve, also air actuated. As outlined in section 3(iii), several modifications were

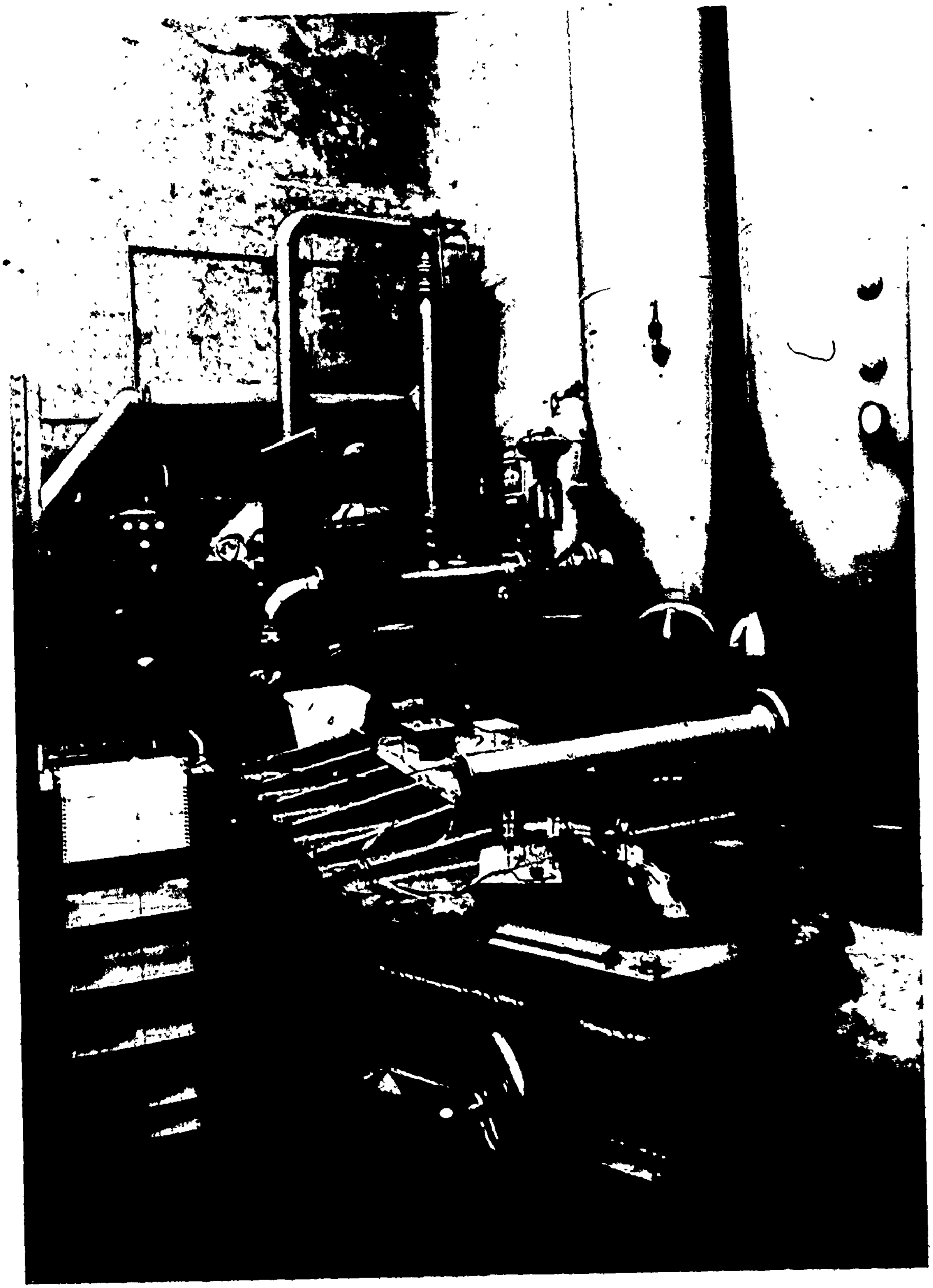

Figure 2 Overall View of the Test Equipment

considered necessary in order to obtain the maximum utilization of the tunnel. The position of the ball valve during a discharge is controlled by an automatic feedback controller which compares the measured plenum pressure with the "set point" pressure. This latter quantity is manually set to the desired plenum pressure before a run. The controller is equipped with proportional, integrating and derivative feedback loops, all of which are described in detail in Reference [2]. Since the control system only adjusts the ball valve position when plenum pressure fluctuations of about 0.7 p.s.i. occur, good flow control at pressure ratios below 1.3 is difficult to attain. This is especially true at large exit areas where it was frequently necessary to make several runs, to extract the necessary flow information with proper accuracy. Since the plenum pressure stability was extremely sensitive to variations in initial control setting, considerable patience was required to attain acceptable standards.

Figure 3 is a sketch of the original tunnel layout including relevant dimensions. The cascade angle of attack is varied by rotating the calibrated turntable on which the blade cascade is mounted. Reference [2] describes several of the modifications made to permit turbine blades to be tested. Initially the tunnel was used at lower pressure ratios to test compressor blade cascades. Hence, Stannard [2] reinforced and improved many of the component parts. The result was that the tunnel could withstand the greater operating loads experienced when used at pressure ratios suitable

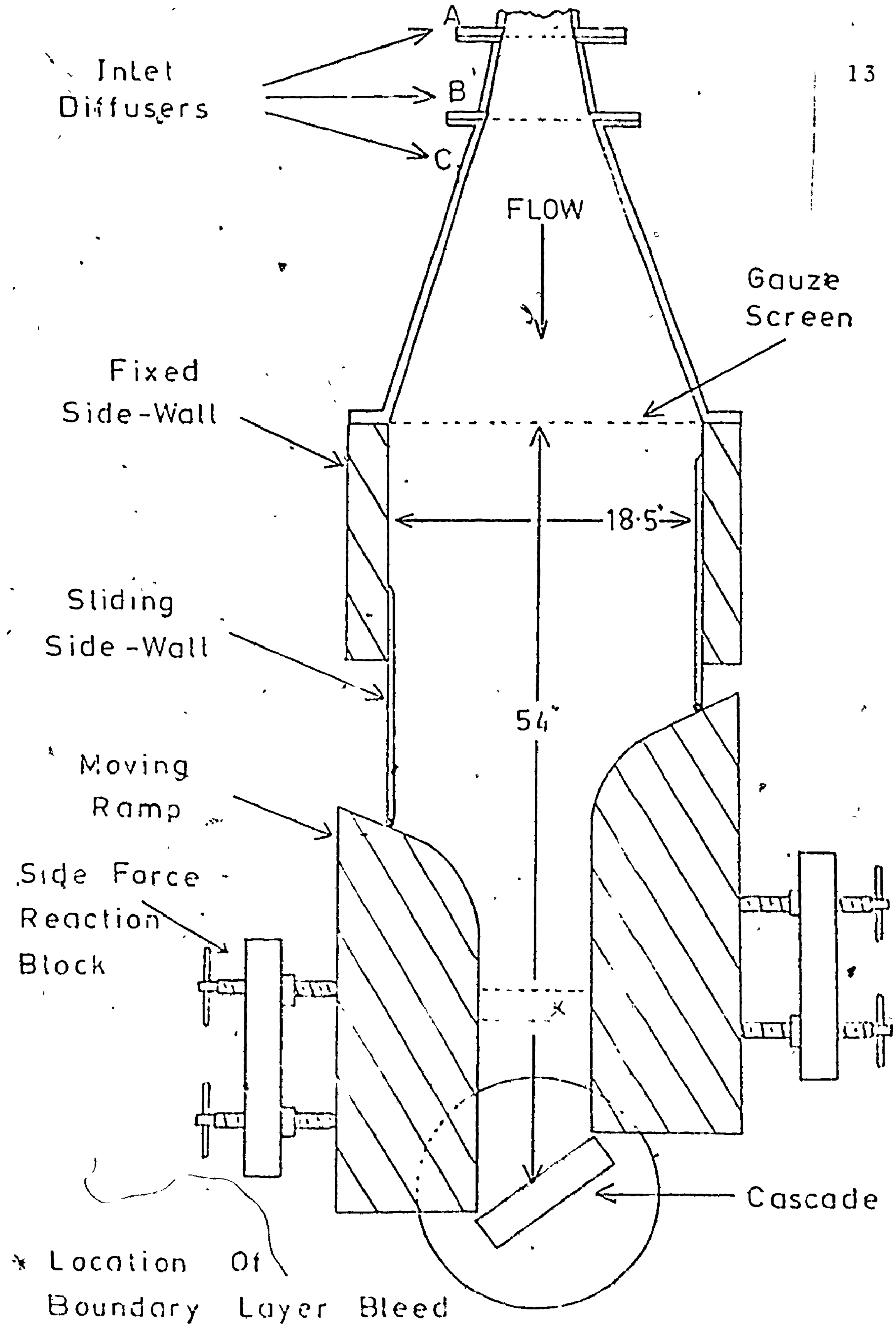

Figure 3 Original Tunnel Layout
Reference [2]

for turbine blade testing with exhaust to atmosphere.

3.2 Required Improvements for New Testing

After extension of tests to pressure ratios greater than 2.0, it was decided that the cascade wind tunnel, as described above and in Reference [2], required several alterations for the following reasons:

(a) Running times for high plenum to exit pressure ratios were too short (in the order of 7 - 10 seconds) to allow a sufficient number of measurements to be made using the existing scanivalve equipment.

(b) At pressure ratios greater than 2.0, control of the plenum pressure was difficult and flow conditions were not easily reproduceable.

(c) Vibrations induced during a tunnel discharge were transmitted to the force - balance pressure transducer mounted above the plenum. This resulted in undesirable "noise" in the transducer output.

(d) An insufficient number of brass blades to be tested were available to fill the whole of the exit area at the required pitch and inlet gas angle.

(e) The total temperature variation during a discharge was required for boundary layer calculation.

(f) Control of the main shut-off valve was required at the test section location for ease of operation.

3.3 Tunnel Alterations

The tunnel running time was improved by making several modifications. The first reduced the leakage problem. As can be seen in Figure 9, additional 1/2" bolts were installed next to the fixed and sliding side walls. These bolts are capable of holding down the tunnel top alone and, thus, effectively reduced the side leakage. Following this, the turntable top was reinforced by a 3/4" stainless steel plate This prevented leakage which was occurring over the top of the blade holder. Probe holder brackets and O-ring probe seals were included on the plate as can be seen in Figure 4.

The second problem concerned the control valve and its non-linear characteristics at the extreme end of its travel. After a lengthy test period, it was decided that no combination of control settings would result in an acceptable and reproduceable plenum pressure variation during a discharge. The electronics of the feedback control system was thoroughly tested and found to be in good condition. It was finally determined that the problem was the result of the characteristics of the main Foxboro control valve itself. It can be seen in Reference [2] that at valve openings above 90%, the plenum pressure becomes extremely sensitive to changes in valve position. Since valve openings this large were required to give the desired pressure ratios, the controller valve system was unstable, continually overshooting and undershooting the set point pressure. Thus, it was necessary to shift the valve operating condition to a less sensitive part of its

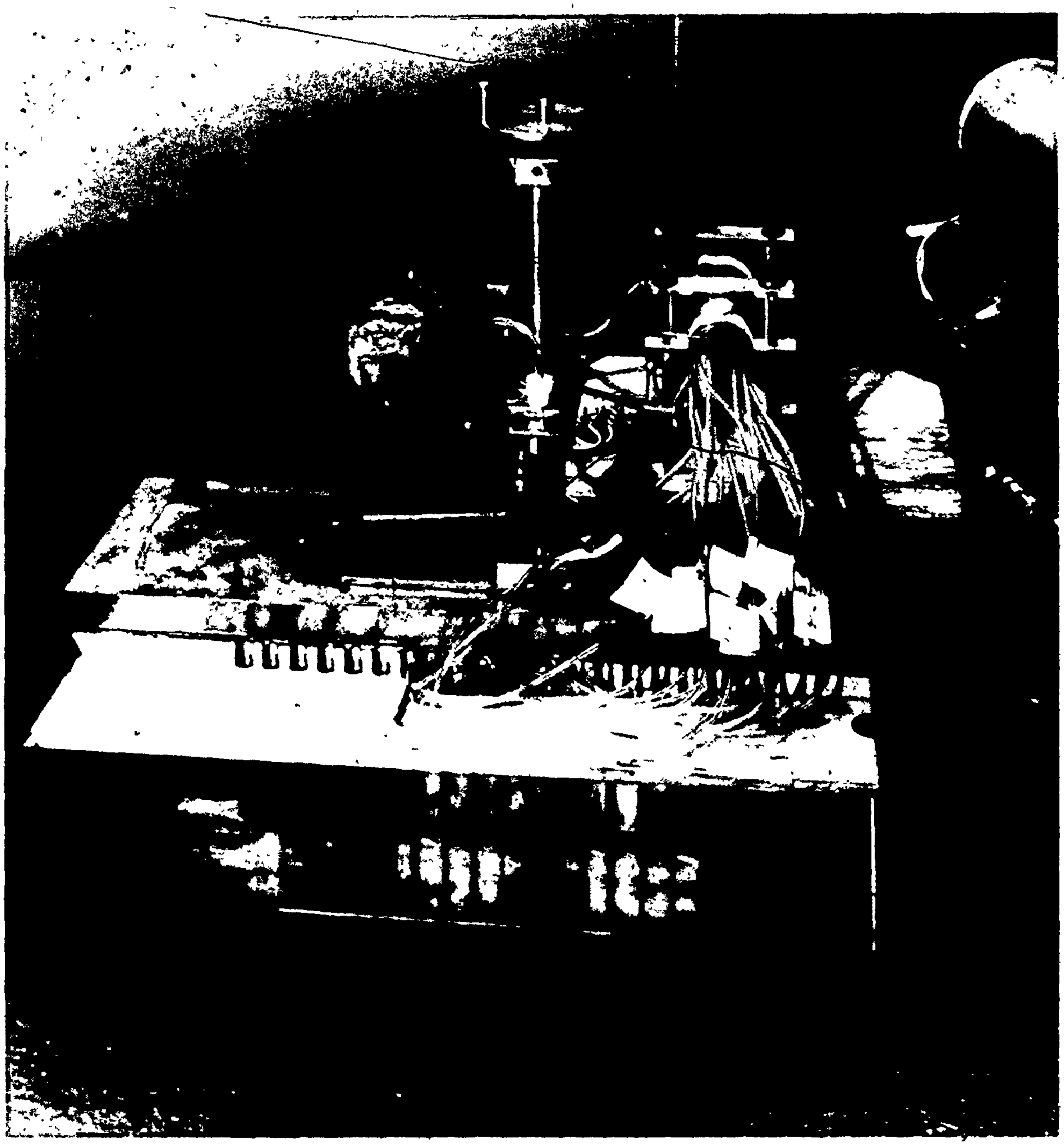

Figure 4 Test Section Instrumentation and Blades

travel - to say 50-90%. To do this, and still maintain the desired plenum pressure, a 2" by-pass piping system was installed around the control valve as shown in Figure 5. The butterfly valve which was installed in the by-pass allowed control of the amount of by-pass and was completely closed when pressure ratios lower than 2.0 were required. Figure 6 shows a typical plenum pressure variation before the by-pass was installed. Also shown is a similar run using the by-pass with its butterfly "memory valve" set to the 9/16 open position. This variation of plenum pressure was considered satisfactory. It should be noted that the test rig is generally a high subsonic and low supersonic discharge apparatus and hence good pressure control below an exit Mach number of about 0.45 is beyond the capability of the present equipment.

Problem (c) was solved by mounting the pressure transducer such that rubber separated it from the tunnel. A Tygon hose was used in place of the existing 1/2" steel pipe for the pressure connection.

The fourth problem required the installation of 1/2" stainless steel side ramps on the inside surfaces of the moving side ramps (see Figure 7). Plastic body filler was smoothed in to permit a gradual contraction from the plenum. This considerably reduced the number of blades required. The remaining blades used at the cascade's outer edge were those tested in Reference [2], staggered such that the minimum area between any two blades was the same as that between the blades under investigation. This criteria was difficult

Figure 5 By-pass Piping System and Butterfly "Memory" Valve

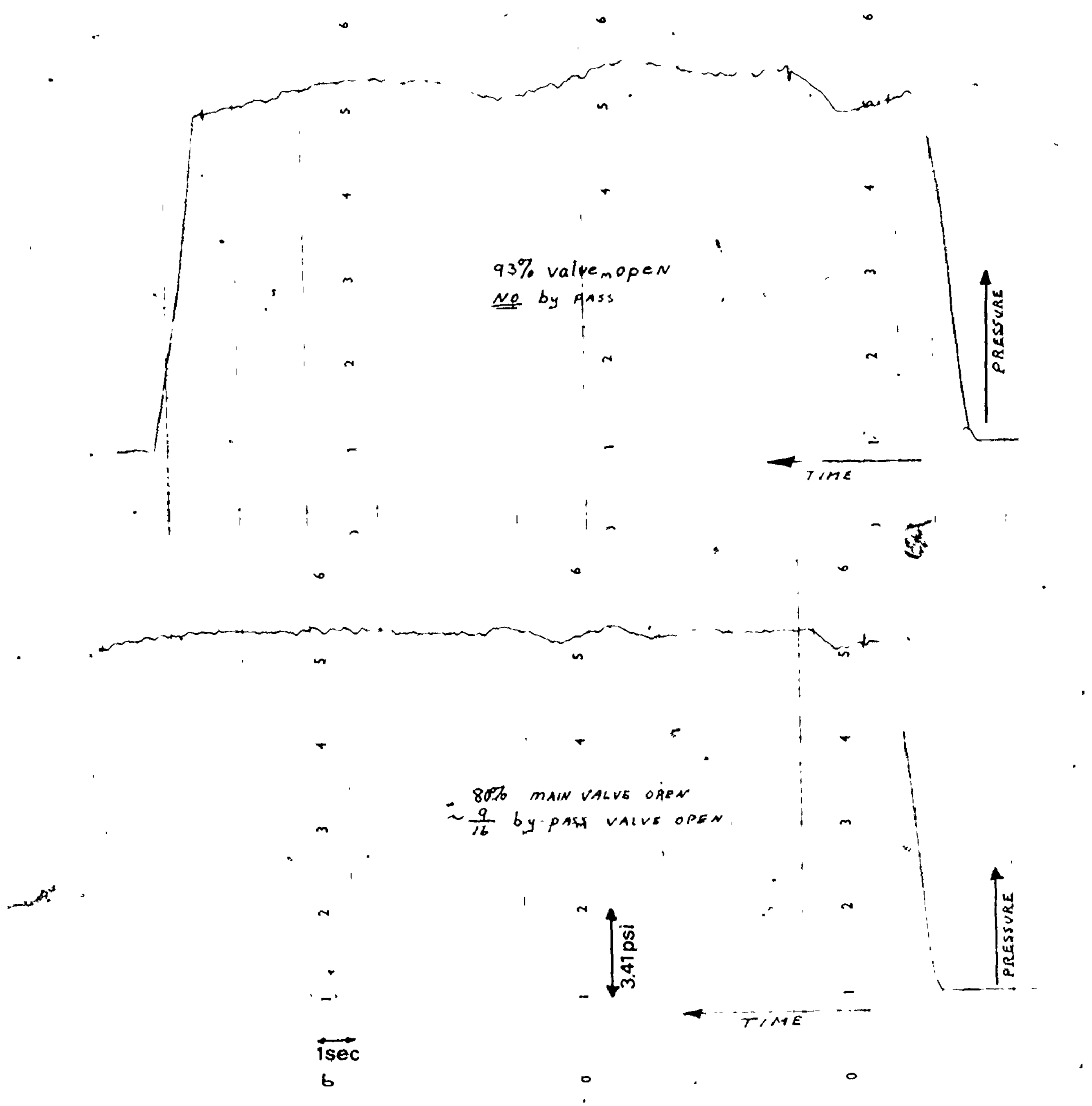

Figure 6 Effect of Added By-pass

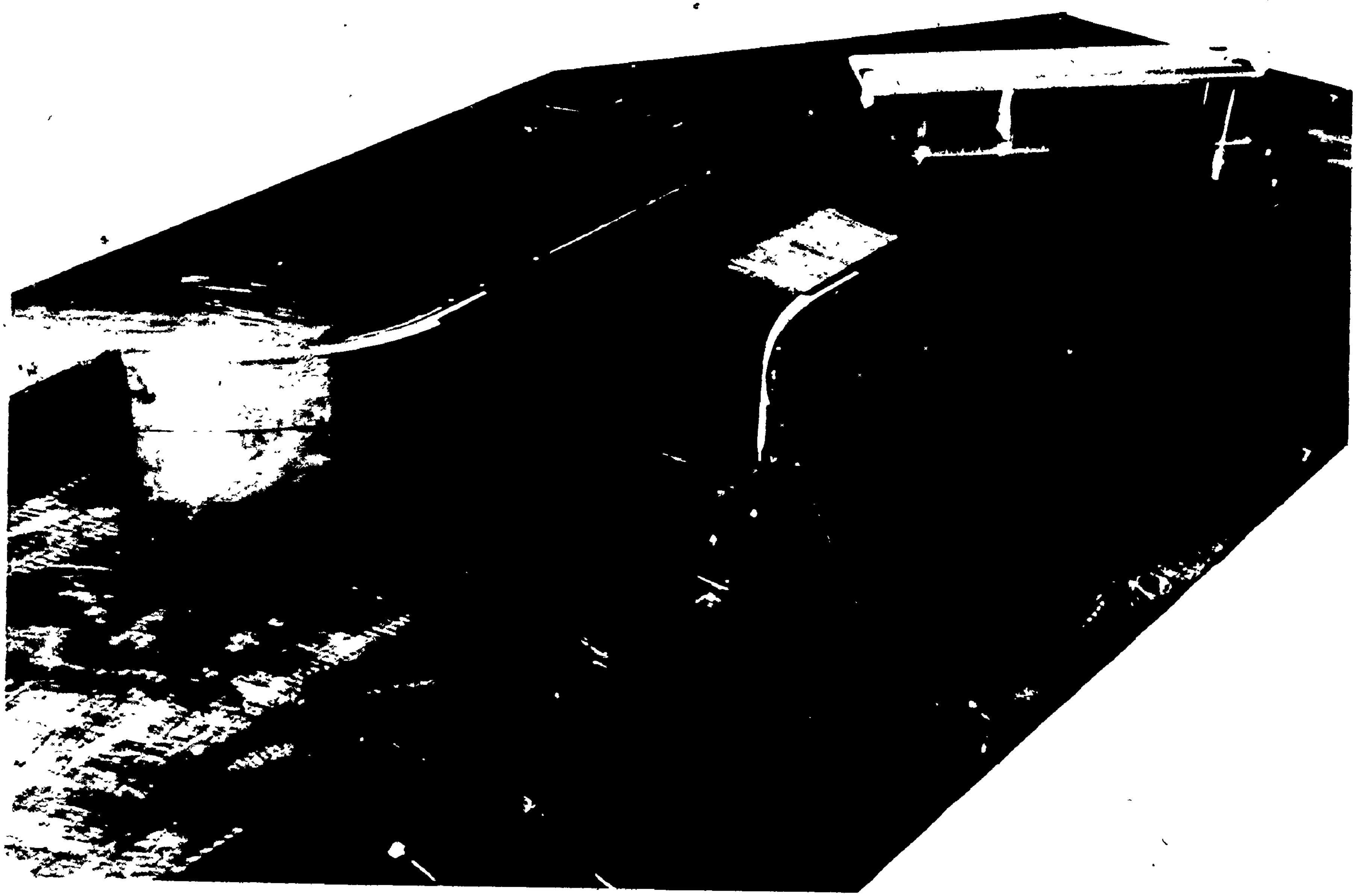

Figure 7 View of Added Side Ramps with Tunnel Top Removed

to satisfy as, due to the differing blade shapes, the minimum area was not always at the trailing edge. Thus, instead of attempting surface to surface measurements to position the blades, a computer program was written to plot the surface of the blades being tested beside the filler blade surfaces rotated through various angles (see Figure 8). The minimum length between the different blade surfaces was measured and the correct angle selected. The positions of the filler blades relative to each other were determined in a similar fashion. Aluminum templates, as in Reference [2], were made and used to ensure the correct stagger angle.

A half cylinder total temperature probe was constructed using the specifications recommended in Reference [12]. The temperature sensor was a copper-constantan thermocouple and an ice bath was employed as the reference temperature. The probe was inserted through an O-ring seal into the center of the plenum region (see Figure 9). Temperature-time variations during a discharge are shown in Figure 10.

Finally a switch was installed at the test section which by-passed the main control valve switch, thus transferring control to the test section location. This greatly simplified one-man testing procedures.

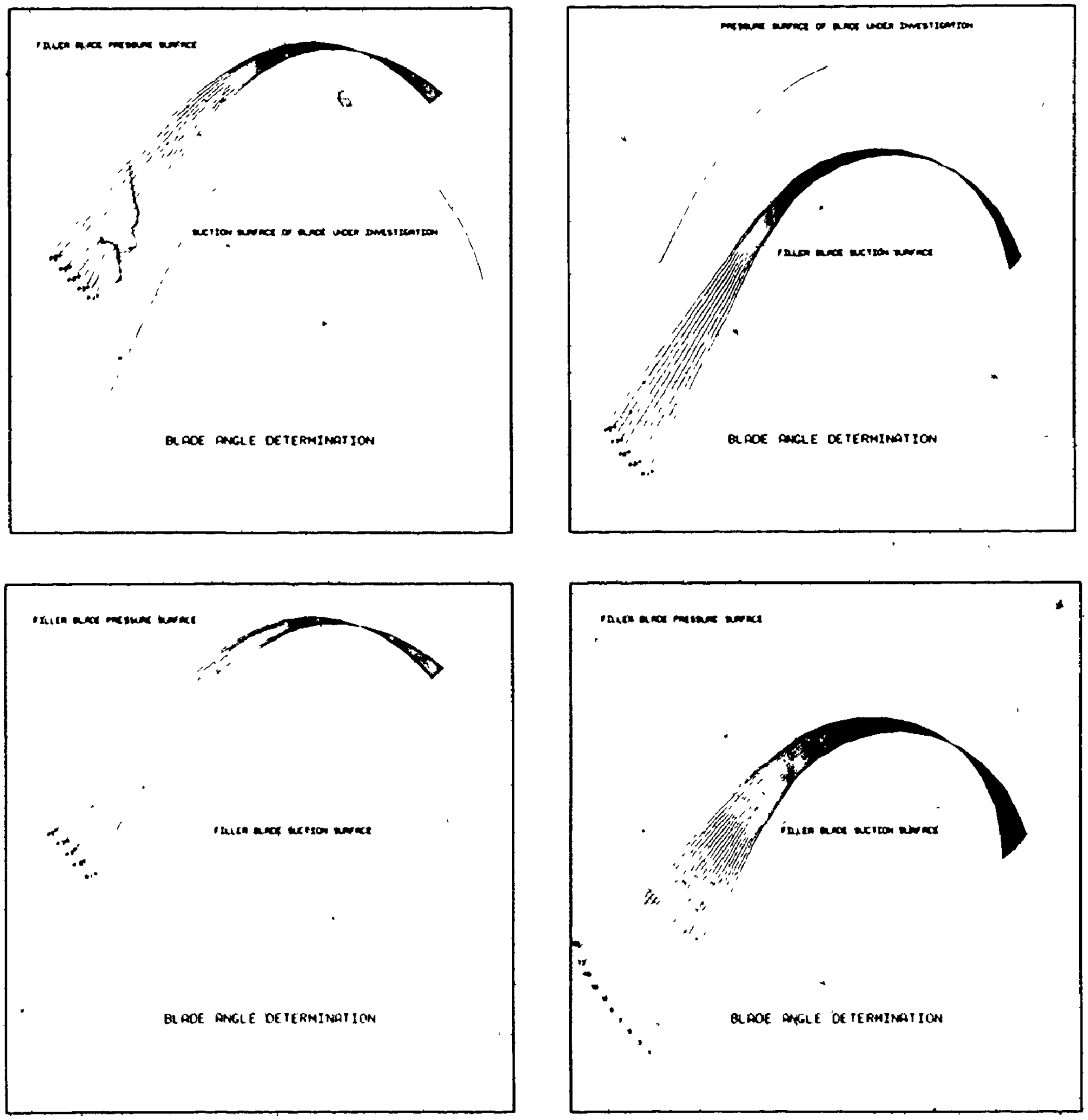

Figure 8 Filler Blade Stagger Angle Determination

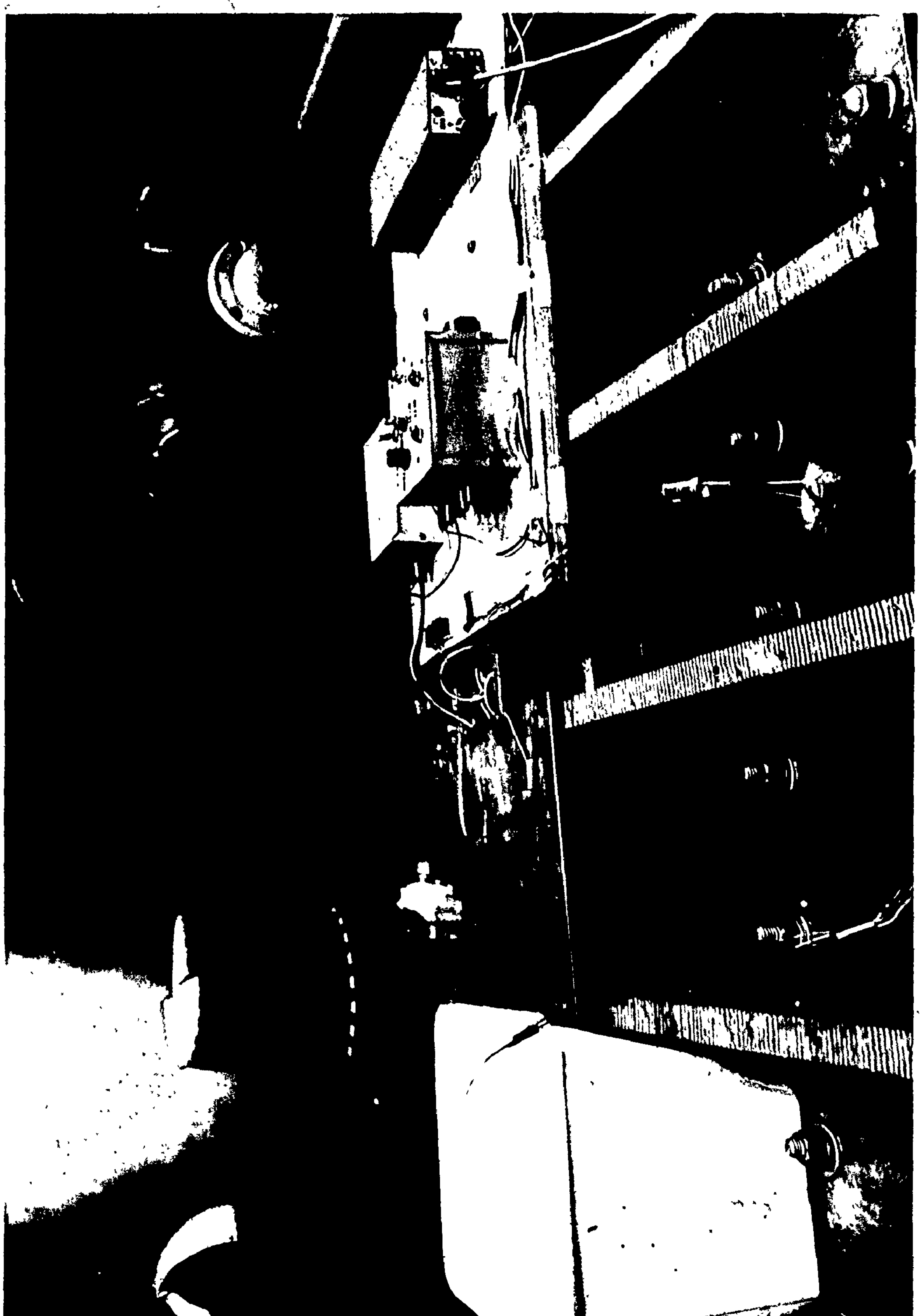

Figure 9 Plenum Region Tunnel Top

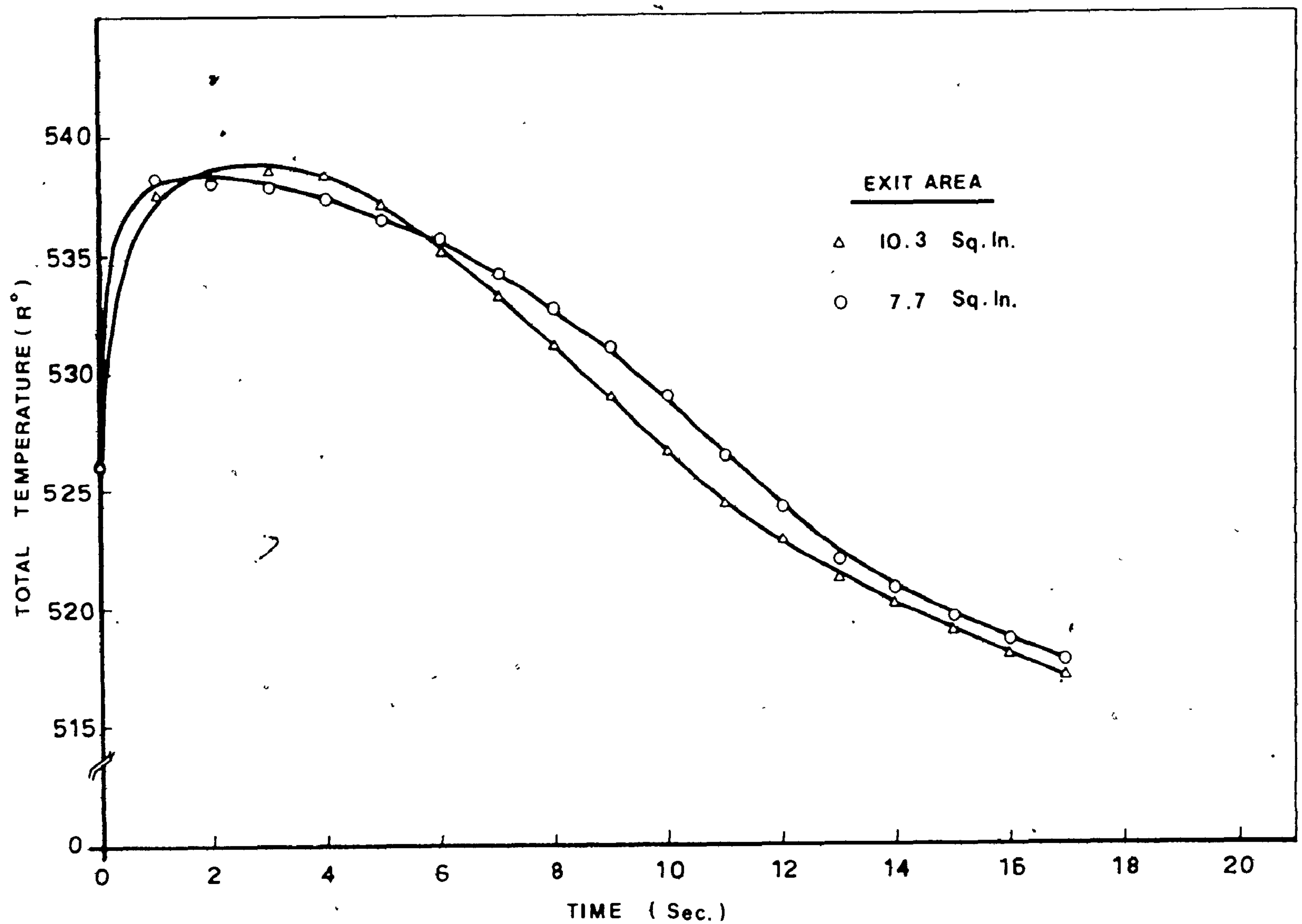

Figure 10 Temperature-Time Variation During a Test Run

CHAPTER 4

INSTRUMENTATION AND EXPERIMENTAL METHODS

4.1 Transient Flow Instrumentation

The principal objection to the use of blow-down wind tunnels is the fact that steady flow conditions, during which time meaningful measurements can be made, are available for a relatively short time span. In the tunnel used for this investigation acceptable flow conditions lasted for a maximum of 15-20 seconds for pressure ratios above 2.5 (at moderate angles of attack). The N.A.E. five foot wind tunnel described in Reference [11] provides run times of about 20 seconds. Hence, instrumentation on such tunnels must be capable of high response rates to allow rapid measurements. References [2], [13] discuss several of the possible methods of obtaining experimental data under these conditions. The technique selected was the use of a motor driven scanning valve (trade name Scani-valve) alternately connecting several pressure ports to one central transducer. Advantages of such a system include low cost, reduced calibration requirements and a fast response time due to the low volume of the transducer and the internal passages. Ready availability was another factor in its selection.

The following sections of this chapter describe the instrumentation and ancillary equipment.

4.2 Pressure Measurement

The upstream plenum static pressure was continually measured using a force balance type pressure transducer* mounted on the tunnel top. Its operating characteristics are outlined in Reference [2] and Figure 9 shows its location. For exit flow measurements, a diaphragm type pressure transducer** was used, mounted inside a Scani-valve*** chamber (a discussion of different pressure measuring systems is given in Reference [2]). The scanivalve transducer was calibrated using bottled Nitrogen and a Wallace and Tiernan-gauge**** as a standard. The calibration curve is shown in Figure 11. The plenum pressure transducer was calibrated "on site" using the Scani-valve which had previously been calibrated and air pressures as supplied by the shop air system through a reducing valve. Figure 12 shows its calibration curve. Electrical outputs from both transducers were recorded on a two pen chart recorder***** manufactured by the

---

* Foxboro E11AH series absolute pressure transmitter

** Druck PDCR-22-Scani-valve Inc., San Diego, California.

*** Model type 8393 Scani-valve, Scani-valve Inc.

**** Type FA 145

***** Rikadenki two pen recorder, model #B28L

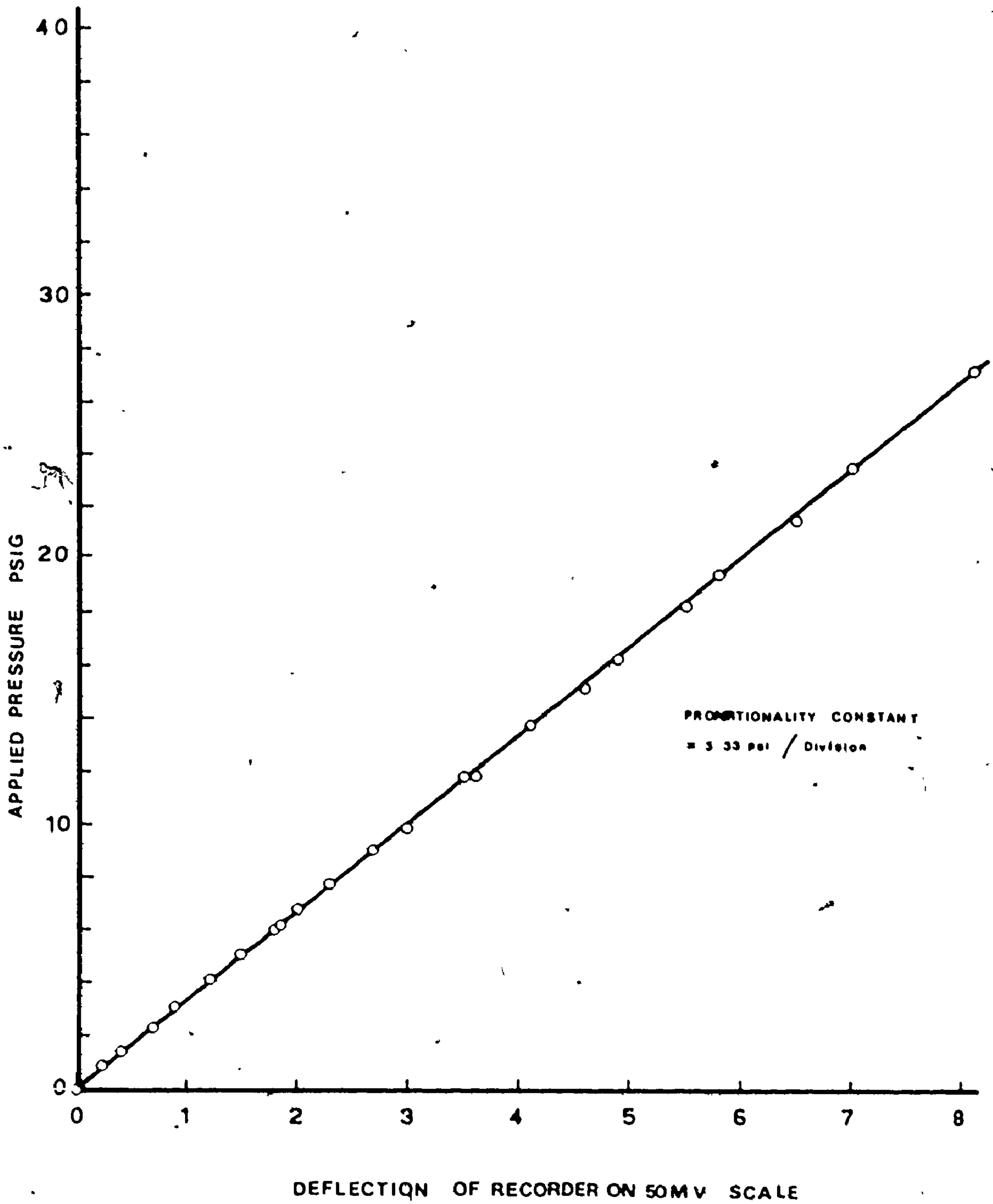

Figure 11 Scani-valve Pressure Transducer Calibration Curve

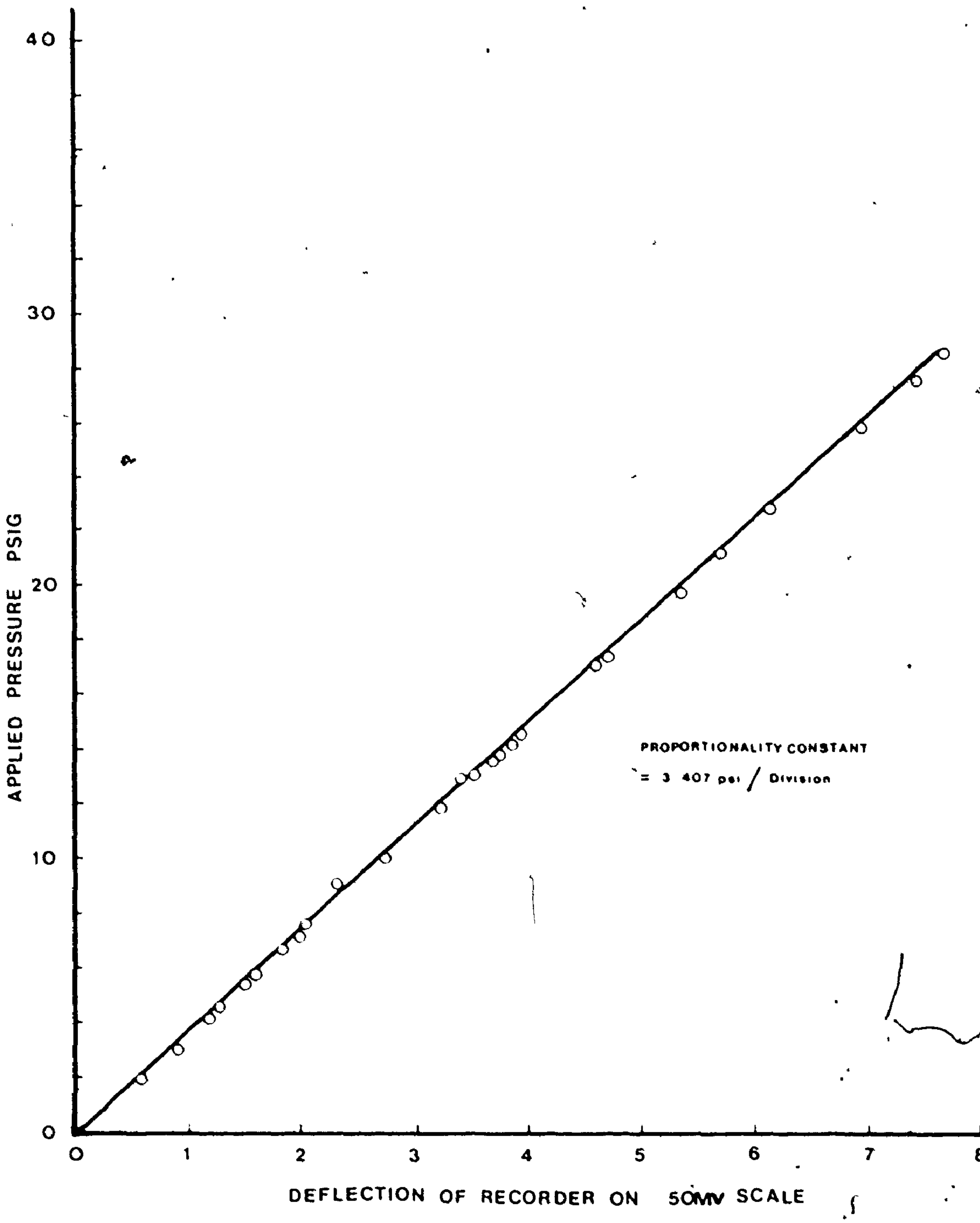

Figure 12 Plenum Pressure Transducer Calibration Curve

Rikadenki Corporation. This allowed the continuous monitoring of upstream plenum pressure as well as the variable of interest (either thermocouple or Scani-valve outputs). Thus a time history of the flow during a discharge was recorded.

4.3 Blade Instrumentation

The main emphasis of the wind tunnel testing was placed on obtaining the static pressure distribution on the two surfaces bounding a cascade flow passage. Thus, both the pressure and suction surfaces for one passage were instrumented as in Reference [2]. Figure 13 shows the two blades to be instrumented placed in the aluminum cascade holder. Stainless steel tubing .035 inches O.D. was epoxied into each slot and extended approximately one inch beyond the blade's upper edge. Before the epoxy solidified, .020 inch holes in the tube walls were lined up with each static pressure port (also .020 inches in diameter). The epoxy was later polished with emery paper to reproduce the original surface finish and contour as nearly as possible so as not to interfere with flow through neighbouring passages. This technique allowed pressure transmission from a blade surface port to the tubing outside the blade and eventual connection by a short length of tygon tubing to a scani-valve port (see Figure 4).

As discussed in Reference [2], the rise time of such a system could place an upper limit on the speed at which the scani-valve could accurately read pressures. Using the formulae

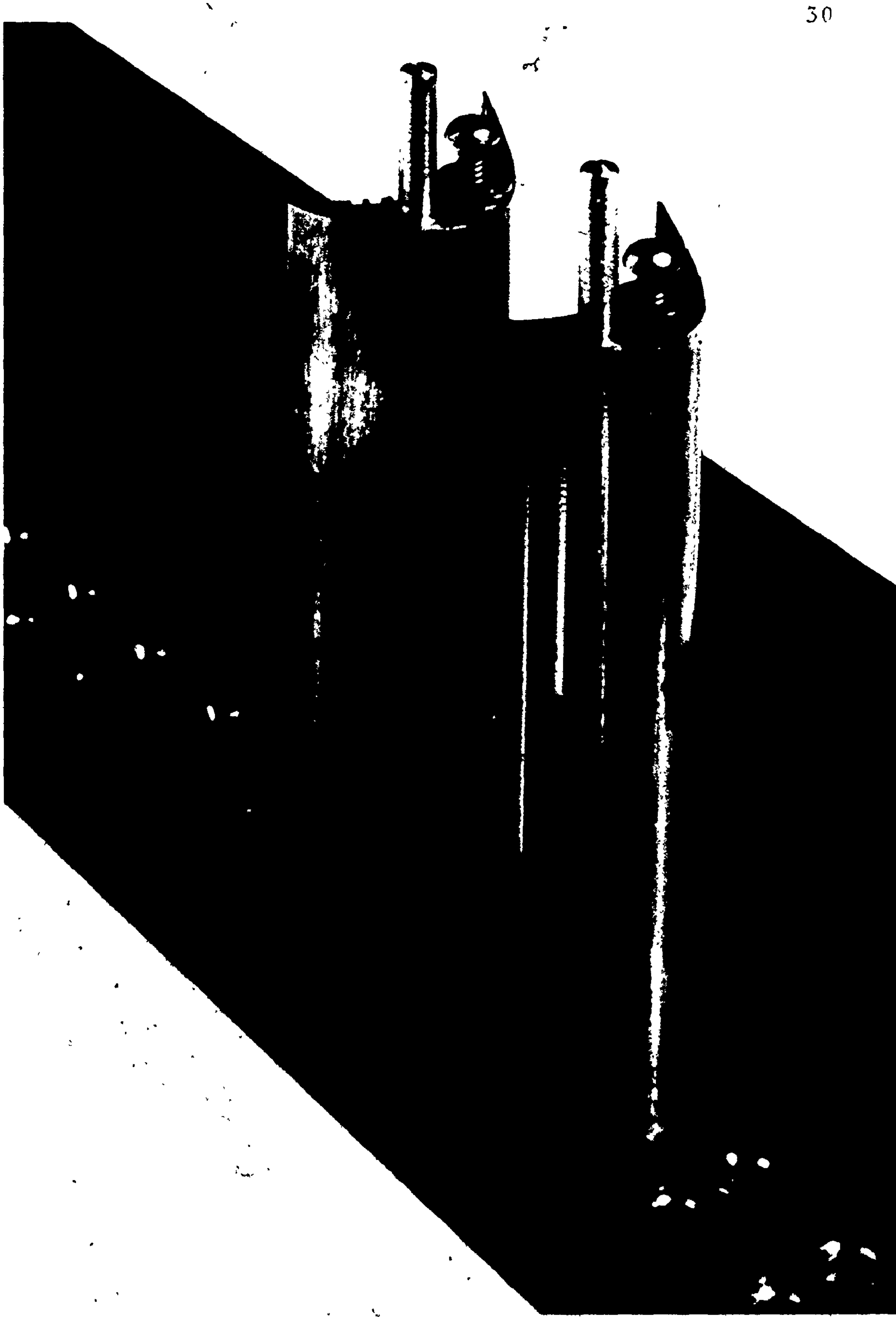

Figure 13 Turbine Blades to be Instrumented

taken from Reference [14]

$$t = \frac{l_1 \alpha}{3P_f d_1 (c+1)} \{V_1 + V_2(c^2+3c+3) + 3 V_m (c+1)^2\} \quad (1)$$

where

$$c = \frac{l_2}{l_1} \{\frac{d_1}{d_2}\}^4 \text{ and } \alpha = 2.47\text{x}10^{-7} \log\{\frac{\Delta P(2P_f + e)}{e(P_1 + P_f)}\} \quad (2)$$

the rise time to 99.5% of the final pressure is approximately 10^{-7} seconds. In this equation, we have reduced our pressure communication system to the equivalent of two tubes. Since the full scale response of the two pen recorder takes 1/6 second, the pressure rise time was not a critical factor.

Prior to testing, a computer model developed by Pratt and Whitney Aircraft of Canada Ltd. had predicted an interesting suction peak near the leading edge on the suction surface. The theoretical analysis assisted us in selecting the positions of the static taps in this area. Due to the suction surface's high curvature, the small dimensions of the model and the necessity of having the static holes perpendicular to the blade surface, it was physically impossible to locate the static taps any closer than shown in Figure 1.

The pressure taps on the pressure surface were evenly spaced because theoretical pressure variations were smooth and showed no major points of interest. As discussed in Reference [2], the procedure employed was to allow odd scanivalve ports to be open to atmosphere, thus allowing differentiation between similar pressure readings.

Generally, static pressure measurements were accepted only if the corresponding plenum pressure was not more than 2% away from the designated "set point" pressure. Reference [2] shows a typical recorder output obtained during a run.

Finally it should be noted that the blades received did not all have identical profiles. After milling the blades to the desired height, the two with slightly different profiles were placed at the outer edges of the cascade, far from the instrumented passage. The comparison of the two profiles was obtained using an optical comparator and is shown in Figure 14.

4.4 Upstream and Downstream Total Pressure Measurements

Although the plenum static pressure history was recorded during a run, it differed slightly from the total pressure upstream of the blades. Hence a total head probe (as shown in Reference [2]) was positioned about one chord length upstream of the instrumented cascade flow passage. The probe was connected to two scani-valve ports so that the total pressure could be checked twice. As the gas inlet angle was varied, the probe was rotated to maintain a parallel alignment with the flow direction. The dimensions of this probe, are such that a yaw angle of 7^{o} degrees is required before significant error in total pressure measurement is experienced [15].

When determining the inlet boundary layers on the top

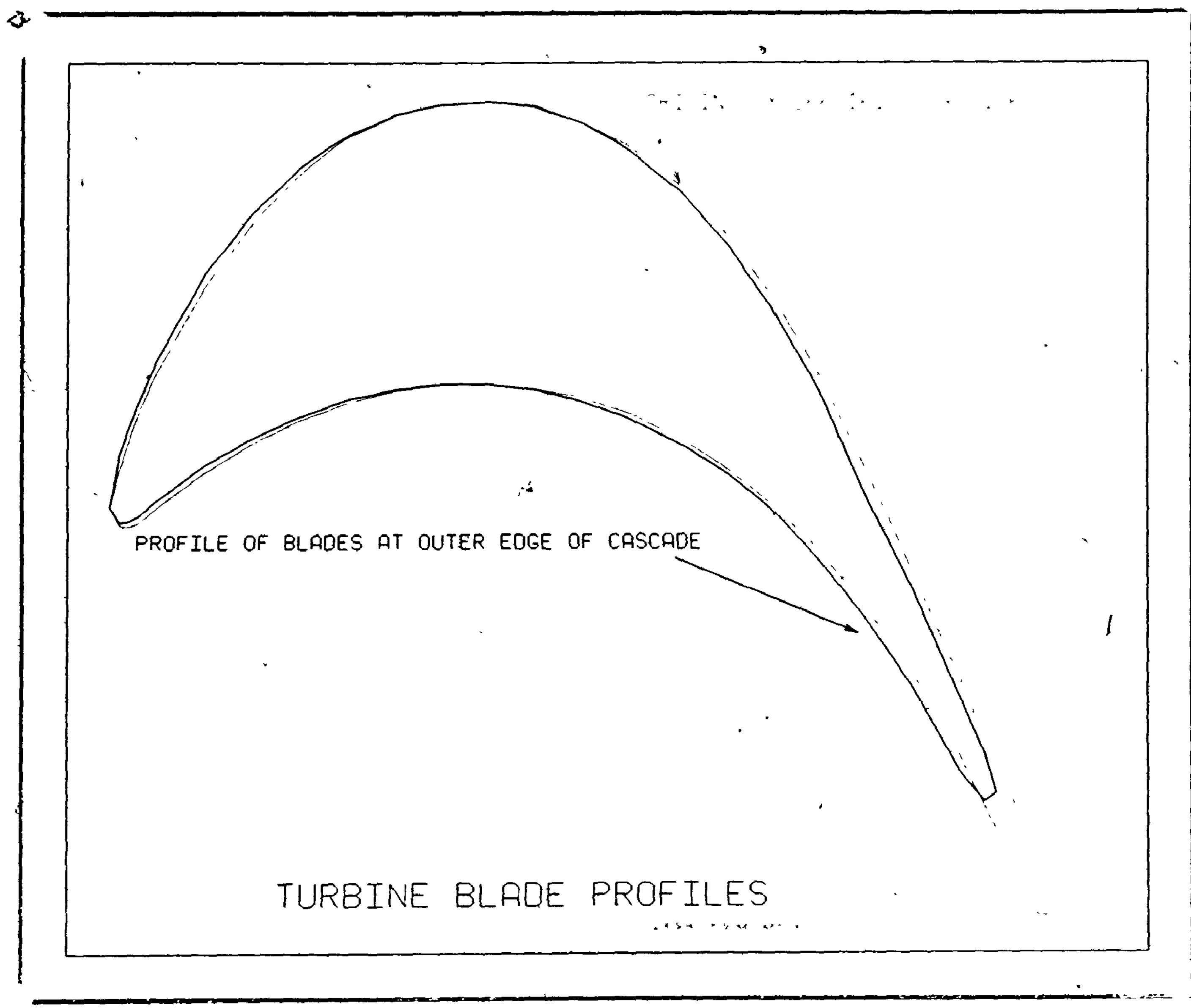

Figure 14 Turbine Blade Profiles

surface of the tunnel the total head probe and traversing mechanism used in Reference [2] was installed approximately one chord length upstream of the cascade. The probe head and tunnel wall were made part of an electrical circuit so that the illumination of a light bulb indicated contact of the probe with the surface. This technique, along with the use of a micrometer drive on the traversing mechanism, allowed considerable accuracy in probe positioning. The boundary layer profiles obtained were corrected for both displacement error and total head error within two probe diameters of the wall as explained in Reference [16].

Exit total pressures were measured in one of three ways depending on the discharge Mach number.* Initially, exit plane traverses were preformed in a similar fashion to that described in Reference [2]. The total head probe was located at an axial distance of about 1.4c downstream of the trailing edge as shown in Figure 15. This is approximately 3.0c measured parallel to the flat backed portion of the blade. At the lower range of Mach numbers tested, it was difficult to detect changes in total head which would indicate the presence of a wake. However, at the higher Mach numbers, the wakes were clearly visible in the recorder traces, though not large. This is not surprising, as we would expect the velocity deficit to increase with the Mach number at a specific location downstream of the trailing edge. Reference [17] gives the following formula:

---

* Mach number determined with inlet total pressure

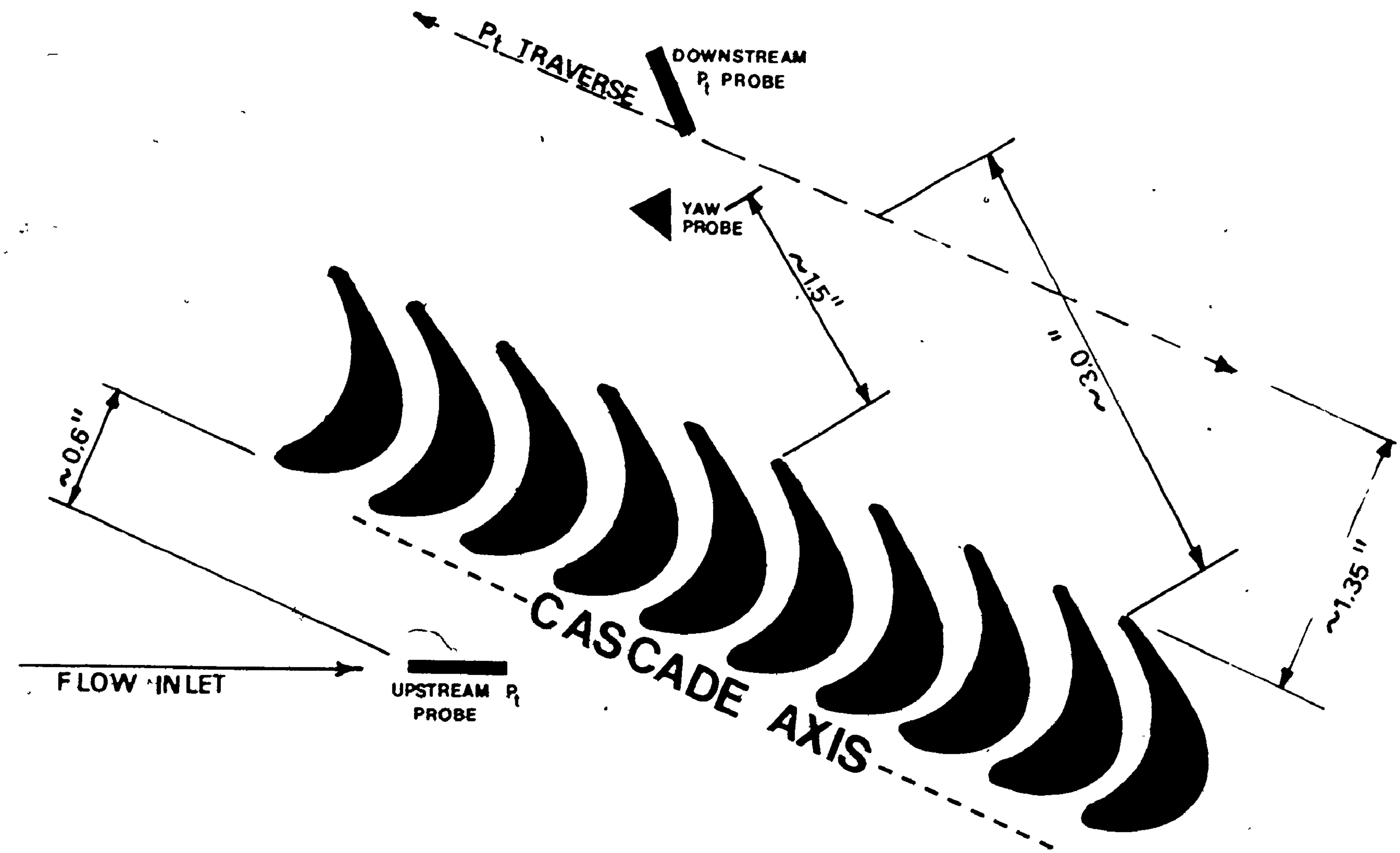

Figure 15 Location of Pressure Measurement Probes

$$\frac{u_1}{u_\infty} \propto \left(\frac{c_D d}{\delta x}\right)^{1/2} \quad (3)$$

for a two-dimensional wake. Hence, as u_∞ increases, a specific velocity deficit, u_1, appears further downstream. Reference [17] also explains that the "strength" of the wake decreases downstream as can be seen from the above equation.

Since the lower velocity wakes were considered negligible at the probe location, total pressures were measured using a subsonic Kiel probe for exit Mach numbers of 0.43 and 0.78. Due to the Kiel probe's relative insensitivity to yaw, meaningful pressure measurements could be obtained without high accuracy in probe alignment. The probe's size was comparable to that of a flow passage, so it was also positioned about 1.4c axially downstream of the trailing edge to avoid changing the exit flow conditions.

For an exit Mach number of 0.95, the wake was still significant but the total head probe described previously was employed as the Kiel probe is not recommended for use beyond the critical Mach number of the probe (approximately 0.7).

Effects of a wake started to become evident at supersonic discharge Mach numbers. Hence, for both exit Mach numbers of 1.06 and 1.29 the total head traverses were used to get an average outlet total pressure. Traverses obtained under these conditions are shown in Figures 27 and 28. The total head measurements for a Mach number of 1.29 include a slight correction as specified by the Rayleigh Pitot Tube Equation.

For incompressible flow wake traverses, Reference [1] gives a loss estimation technique using the experimental values of wake momentum deficit thickness and form factor. However, they continue to state that a high Mach number flow technique is currently unavailable as the magnitude of the compressibility effect on the above two quantities is unknown. Reference [1] concludes by remarking that compressible flow total pressure loss coefficients are still determined primarily through experimentation.

4.5 Exit Angle Measurement

One of the basic requirements of the testing was the determination of the gas exit angle for various exit Mach numbers and inlet gas angles. Since part of the testing included supersonic exit flow, the cobra type yaw probe used in Reference [2] was not acceptable. Although a conical probe was considered most desirable for this type of flow, complications in both its manufacture and support in the tunnel exit plane prohibited its use. Instead, an equilateral triangular wedge yaw probe was designed as shown in Figure 16. The pressure ports were inspected under an optical microscope and found to be free from machining burrs and were acceptably perpendicular to the wedge's surfaces. The probe was calibrated in a vernier angle positioner using the air jet as described in Reference [2]. The probe holder had a positioning accuracy of $\pm .1^{\circ}$. During later tests it was found that adjustments this small would result in measurable pressure

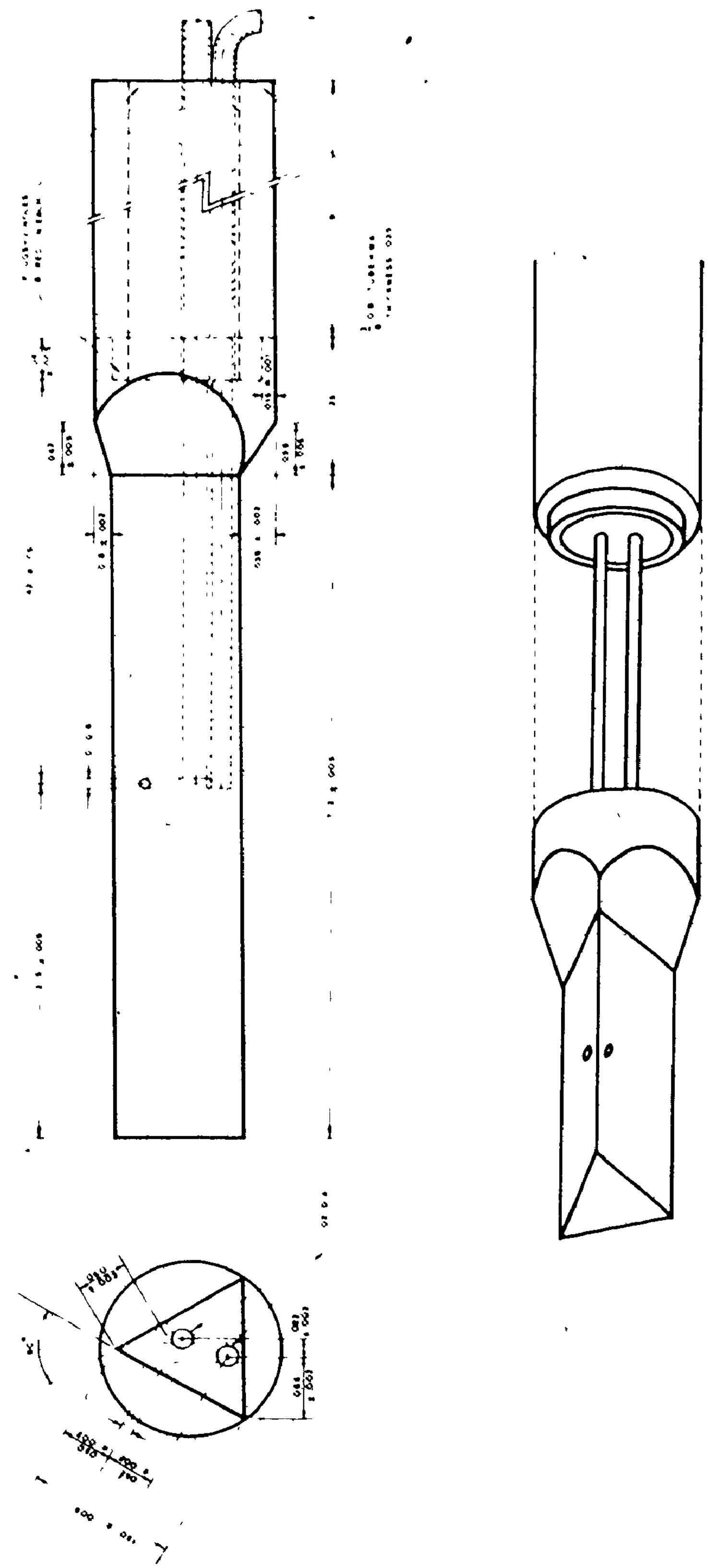

Figure 16 Wedge Yaw Probe

Figure 17 Exit Angle Measurement

variations. The calibration graph is shown in Figure 18.

While calibrating, it was not difficult to ensure that the yaw probe holder was perpendicular to the direction of air flow. This was not true on the tunnel top however. A line was scribed on the turntable upper surface and the probe holder was aligned by eye with this each time exit angle measurements were made. Also a level was used to ensure that the holder was horizontal. However, it was desired to establish the magnitude of the error introduced through removing and repositioning the holder. To do this, the exit angle was measured for one set of flow conditions, the holder removed and then re-attached. The measurement was repeated and compared to that read previously. From this test, the conclusion was drawn that positioning could be responsible for an error of as much as 0.3°. Thus, direct numerical comparisons between different flow conditions are not especially reliable. Instead, the trend that is followed with variation of exit Mach number and inlet angle should be observed.

Since the wedge probe was of considerable size when compared to the flow passage width, it was decided to take the exit angle measurements at a distance of 1 3/8" or about 1.5c downstream of the trailing edge (see Figure 15). This would also negate the effects of the exit plane expansion fan and associated oblique shock wave patterns. Due to the probe's size, variations in exit gas angle across a flow passage could not be investigated and the values given are, thus, average exit angles.

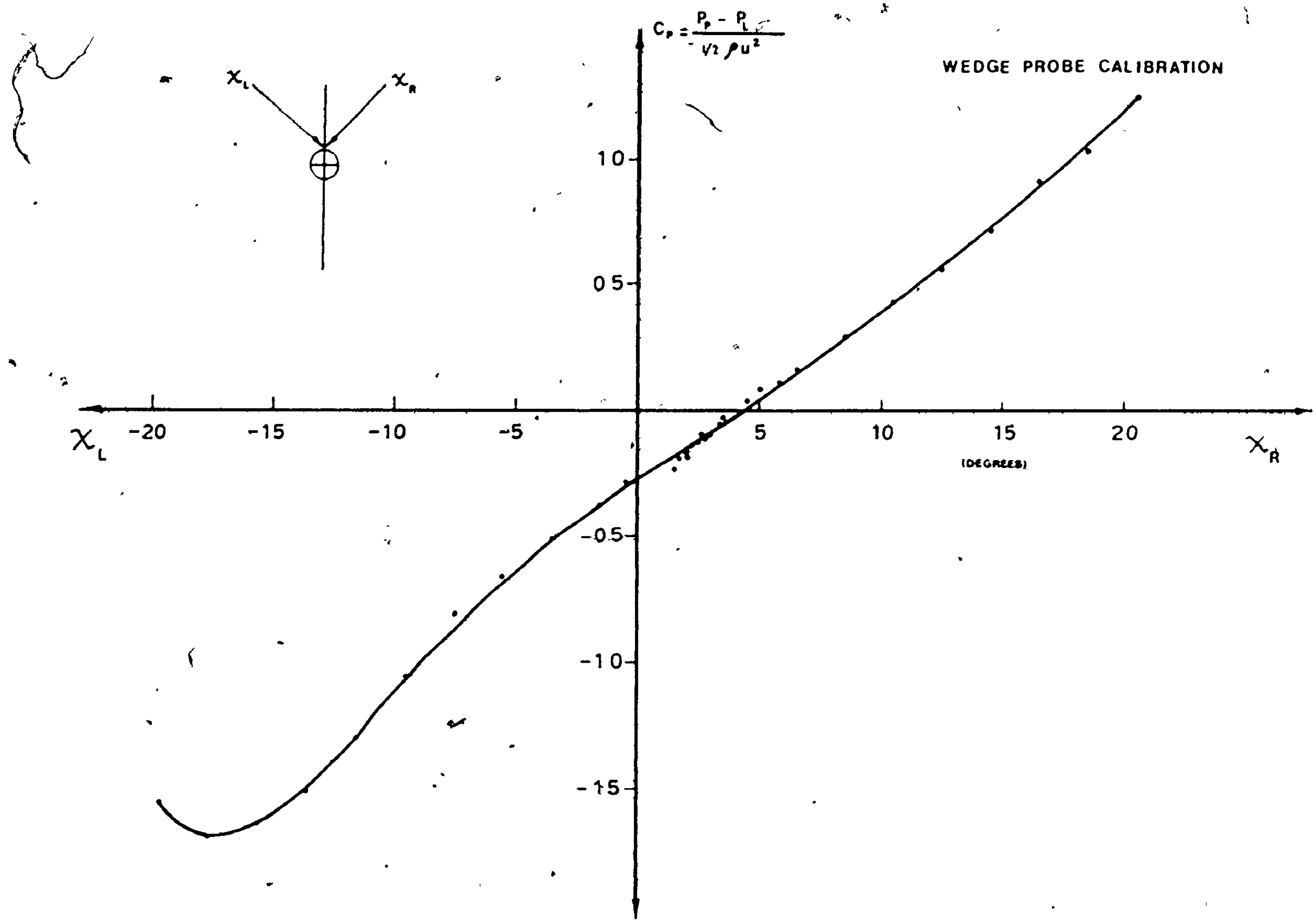

Figure 18 Wedge Probe Calibration

The experimental technique is described as follows. The left and right hand wedge surface ports were alternately connected to scani-valve ports. During a discharge, the two pressures were read in succession and later compared. Small adjustments were made in the angular position of the probe until the two pressures were approximately equal. The exit angle was then read off the instrument's vernier scale and appropriate corrections applied.

It is important to recognize that a nulling technique, as described above, was necessary as calibration was performed in low subsonic flow (about 80 f.p.s.) while testing was primarily in high subsonic and low supersonic flow. The calibration curve was useful, however, to determine the approximate extent to which the probe should be rotated between readings.

CHAPTER 5

EXPERIMENTAL RESULTS

The following figures present the experimental results in a graphical form.

Figure 10 showed the total temperature-time profile measured in the plenum chamber. The 7.7 square inch exit area corresponds approximately to that of the turbine blade cascade. Both curves were obtained at pressure ratios of approximately 2:1. The temperature variation was required for later boundary layer calculations.

Figure 19 shows the tunnel inlet boundary layer profile non-dimensionalized for the same exit areas as shown in Figure 10. The measurements were carried out on the top wall of the tunnel approximately one chord upstream of the cascade. Boundary layer displacement thickness and other relevant quantities are listed on the graph.

Figures 20, 21, 22, 23 and 24 illustrate the static pressure distribution on the instrumented blade surfaces for a range of inlet gas angles and pressure ratios (or Mach numbers). As the variation of total pressure upstream of the cascade was determined, during each run all the surface pressures have been non-dimensionalized by dividing by the instantaneous total pressure. Seven inlet angles were tested and, of these, 70^{o}, 67.5^{o}, 64^{o} and 58^{o} are plotted. Appendix III

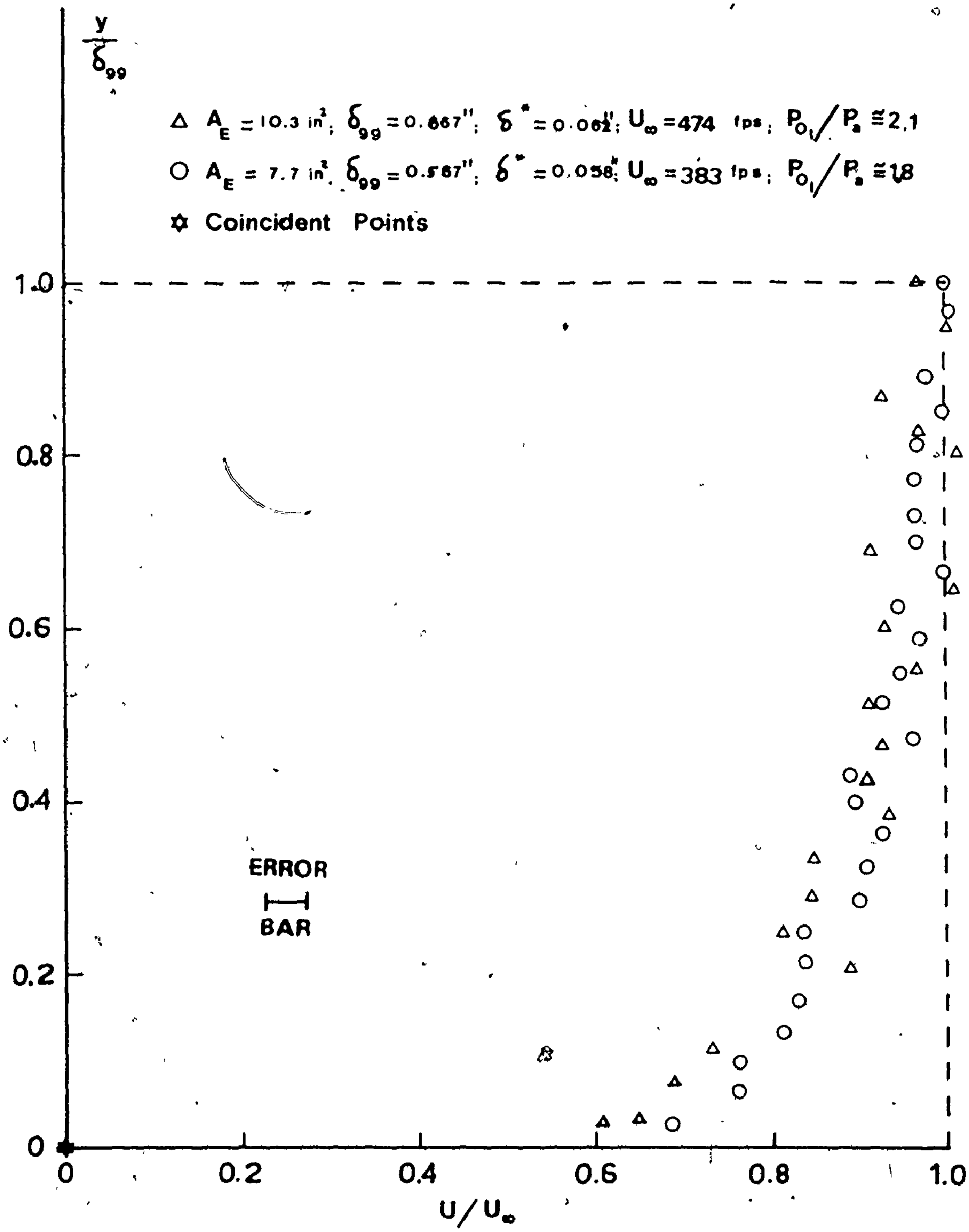

Figure 19 Boundary Layer Profile

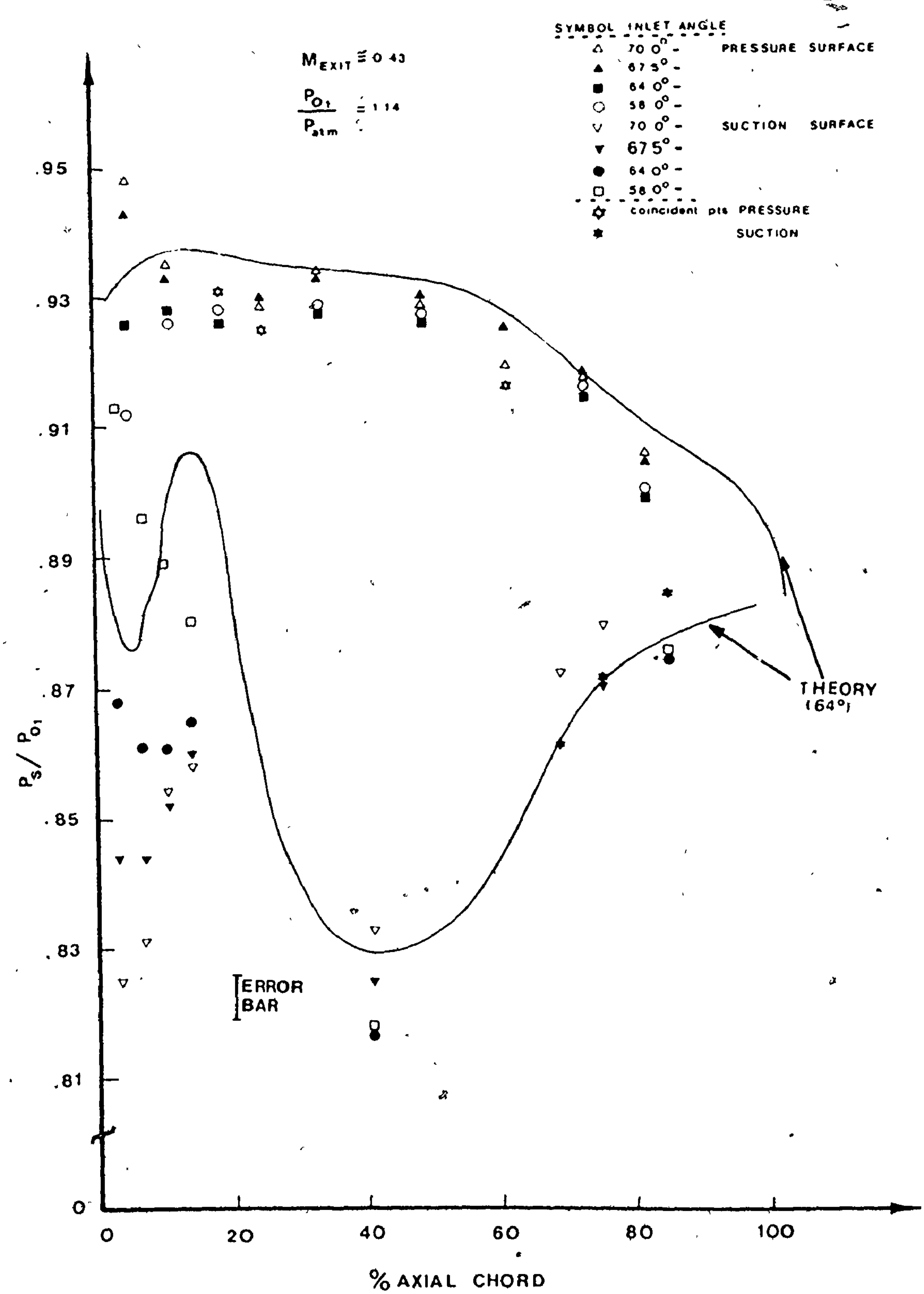

Figure 20 Blade Surface Pressure Distribution

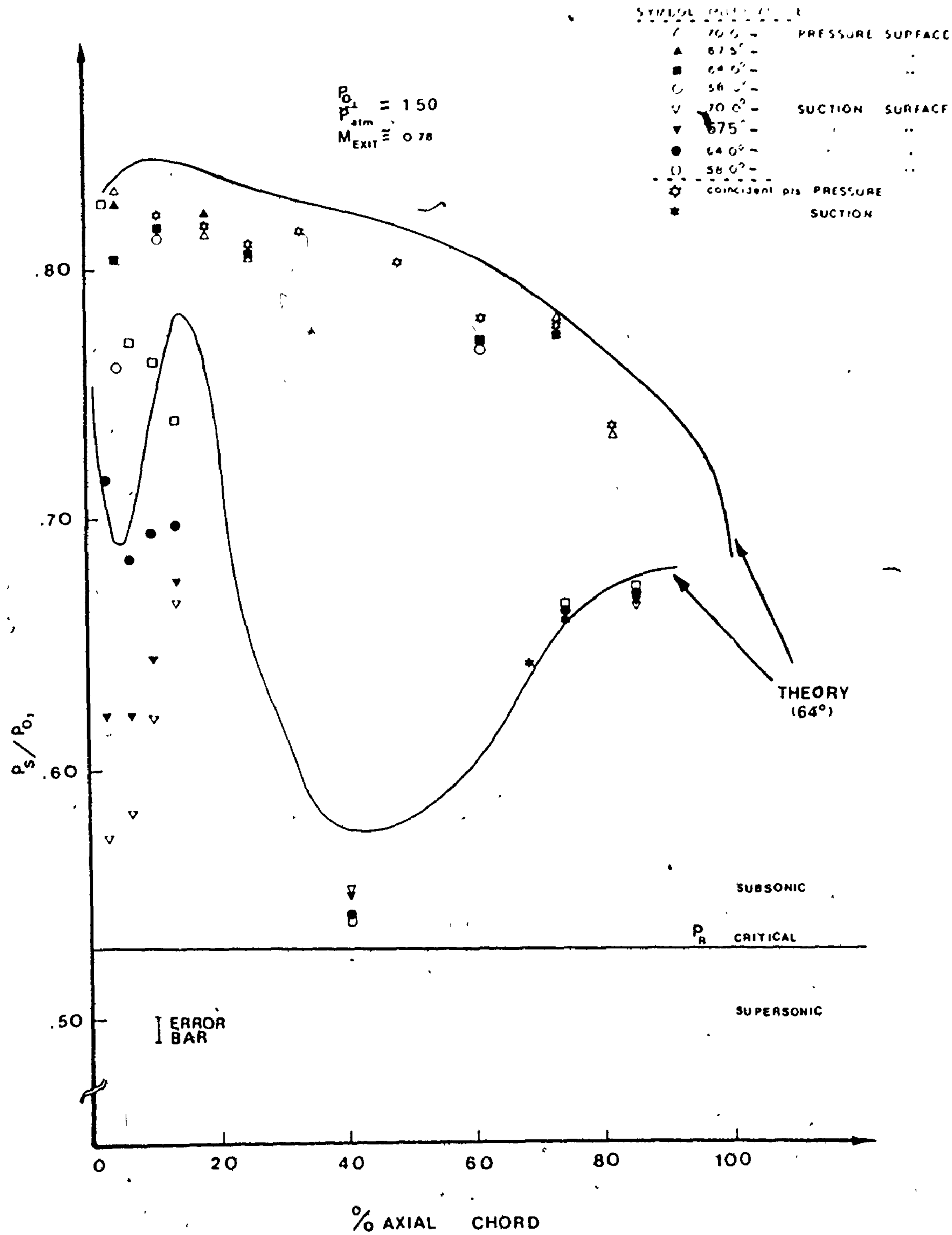

Figure 21 Blade Surface Pressure Distribution

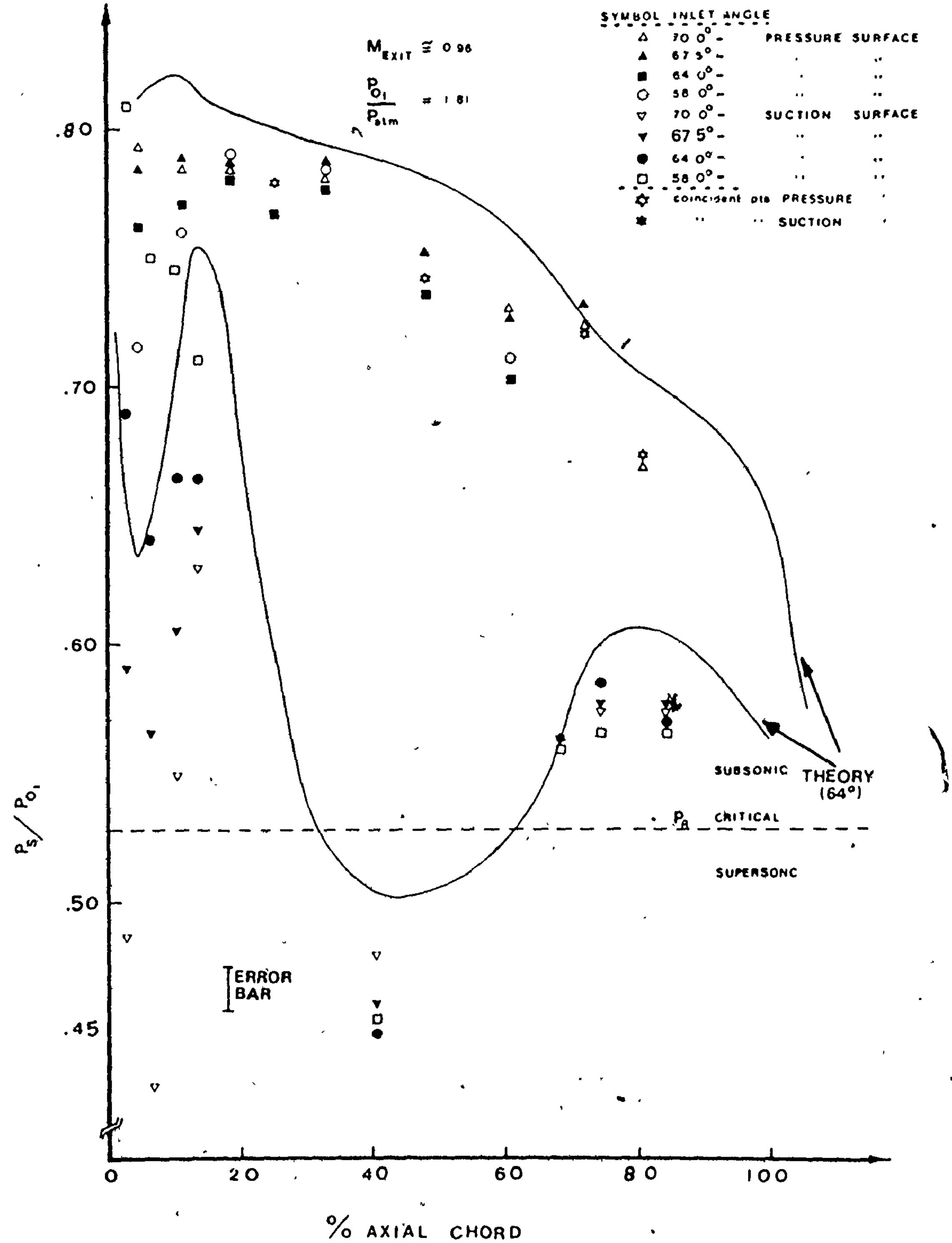

Figure 22 Blade Surface Pressure Distribution

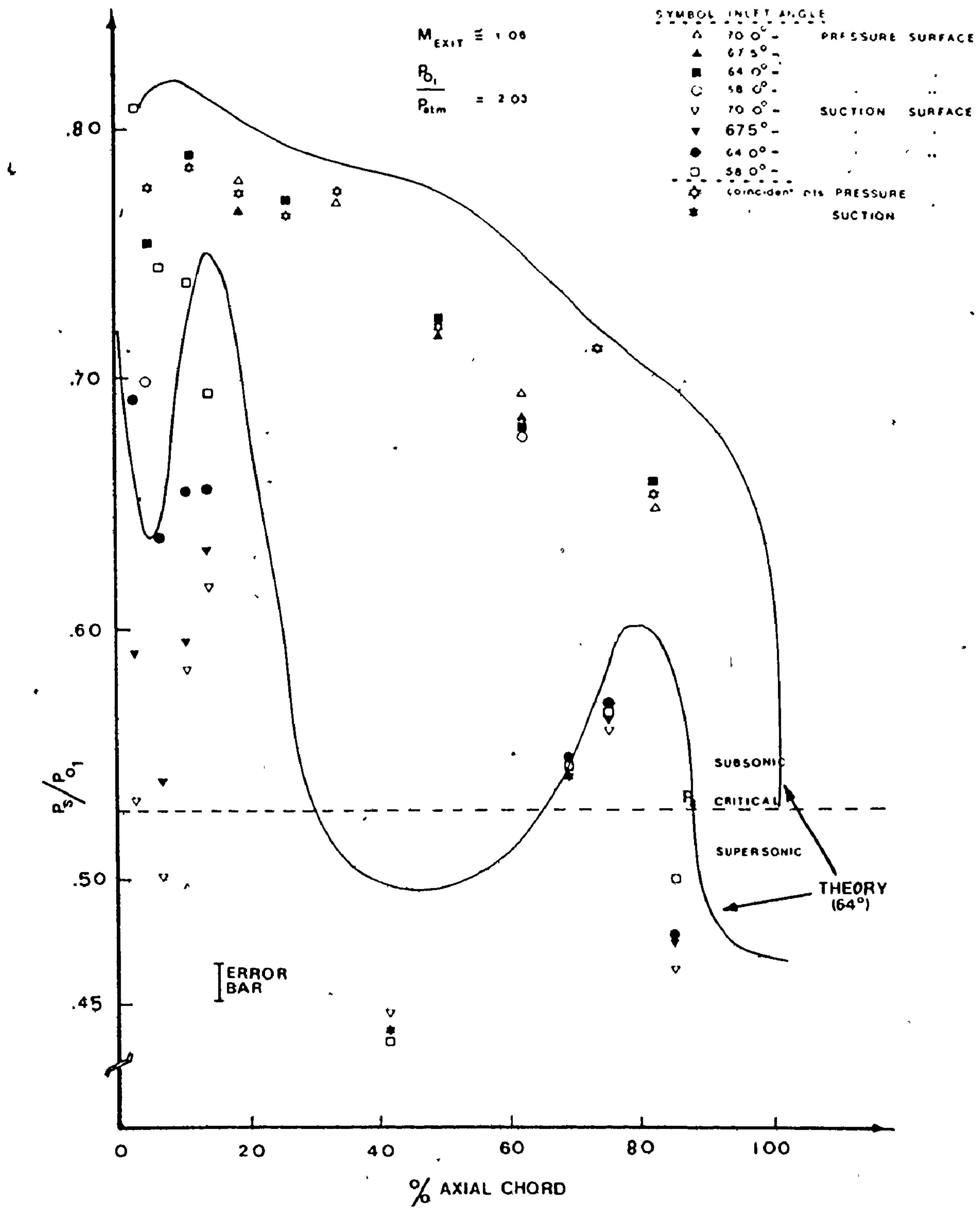

Figure 23 Blade Surface Pressure Distribution

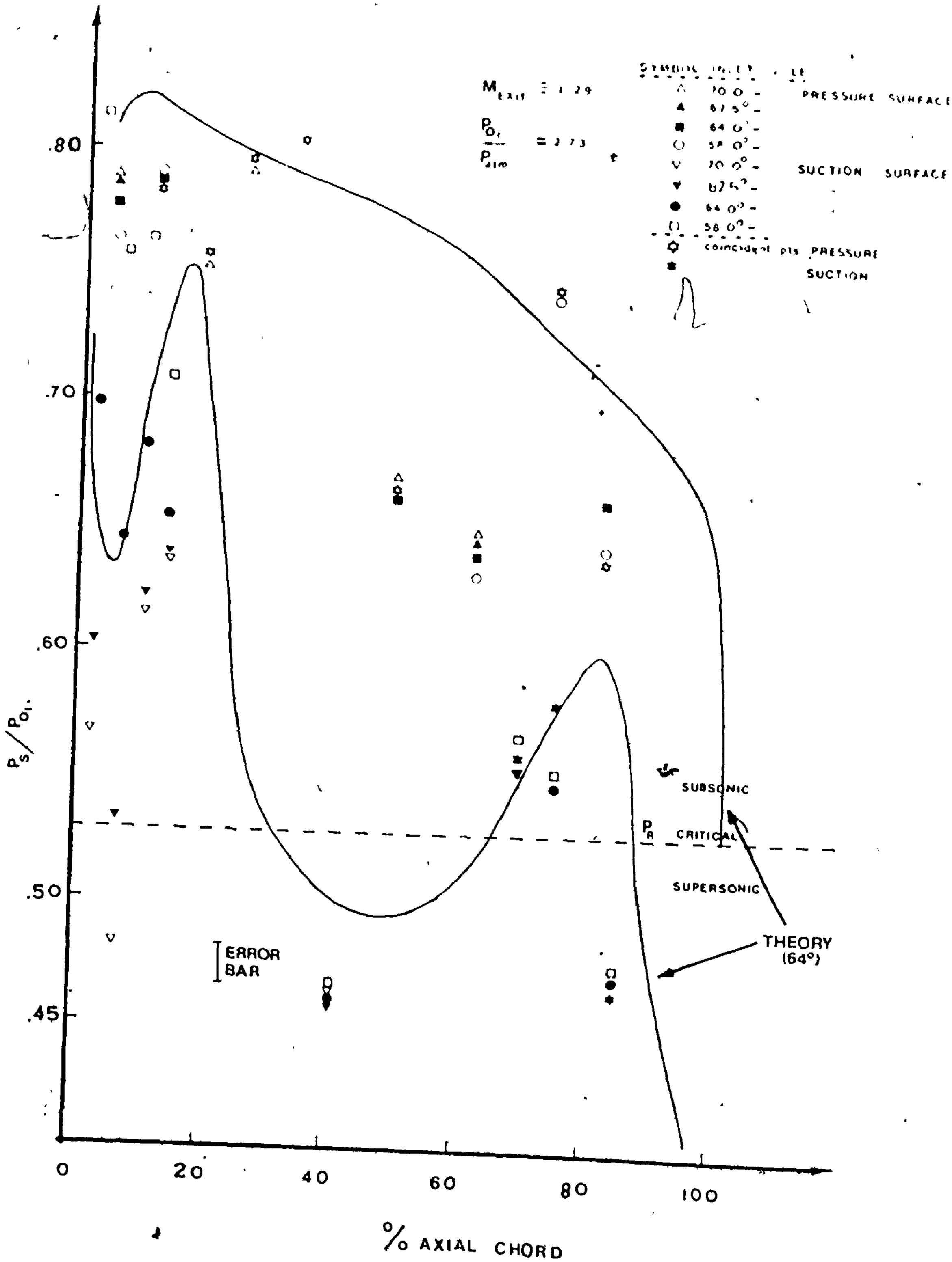

Figure 24 Blade Surface Pressure Distribution

shows the results of tests with 69°, 66° and 62° inlet angles. It should be noted that flow control was excellent at all pressure ratios tested except at a ratio of 1.14 ($M_{exit} \cong 0.43$). This pressure ratio is considered beyond the nomial limits of tunnel operation and the results are presented to show trends only, not specific numerical results.

In all of the graphs coincident data points are marked by a white star on the suction surface and a black star on the pressure surface. Different inlet angles are denoted by the same symbols on all plots.

Figure 25 illustrates the variation in exit gas angle with exit plane Mach number for a range of inlet angles. The data points marked by stars indicate coincident points. The measurement accuracy of the gas angle is approximately ± 0.3 degrees as indicated by the error bar.

The total head loss coefficient ($\phi_N{}^2$) has been plotted against exit Mach number for various angles of attack in Figure 26. In this thesis, the total head loss coefficient is defined as follows:

$$\phi_N{}^2 = \frac{P_{0_1} - P_{0_2}}{q_{OUT}} \tag{4}$$

which can be shown to reduce to

$$\phi_N{}^2 = \frac{P_{0_1} - P_{0_2}}{M_{EXIT}{}^2} (9.72 \times 10^{-2}) \tag{5}$$

when P_0 is measured in psia.

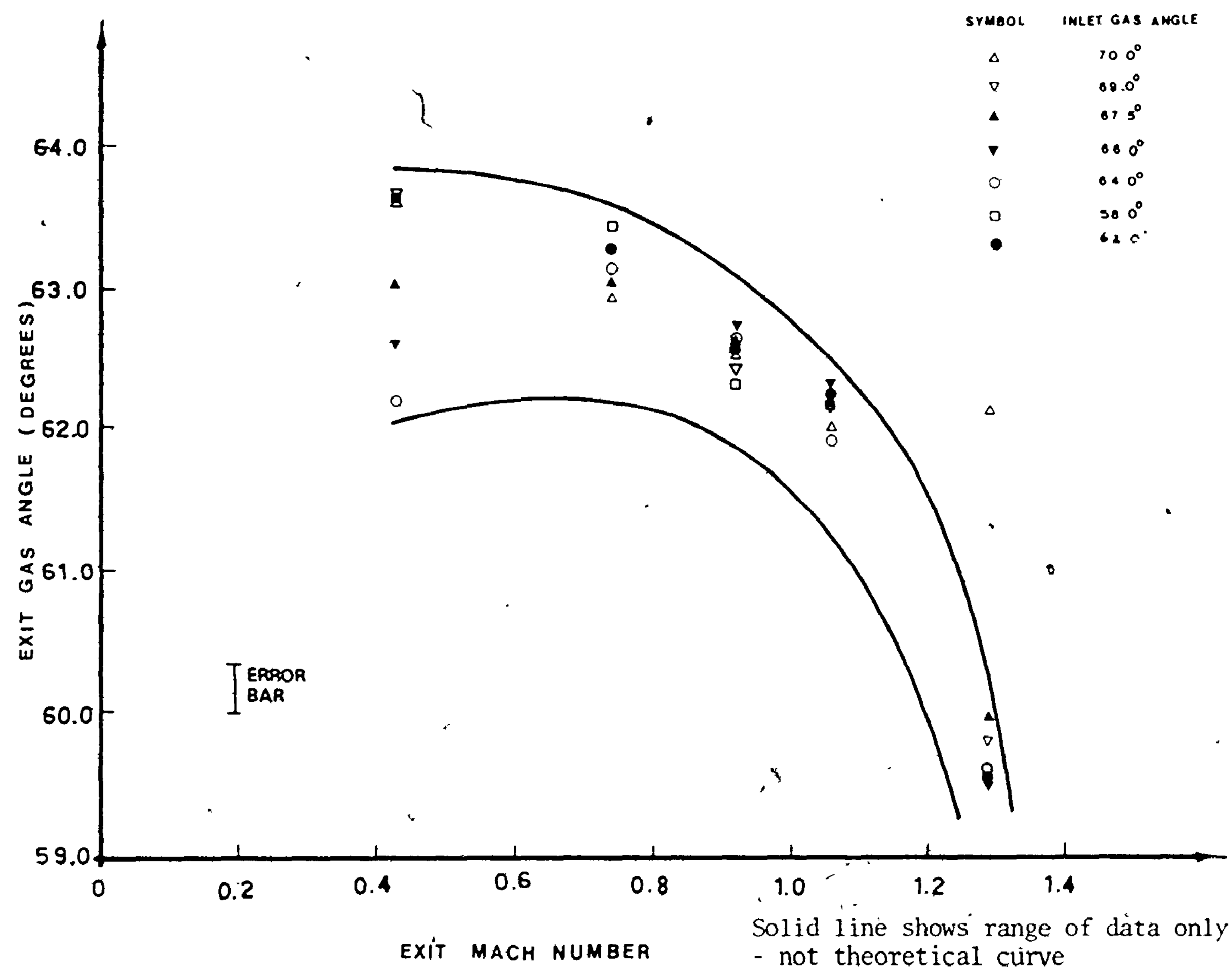

Solid line shows range of data only
- not theoretical curve

Figure 25 Exit Gas Angle Variation

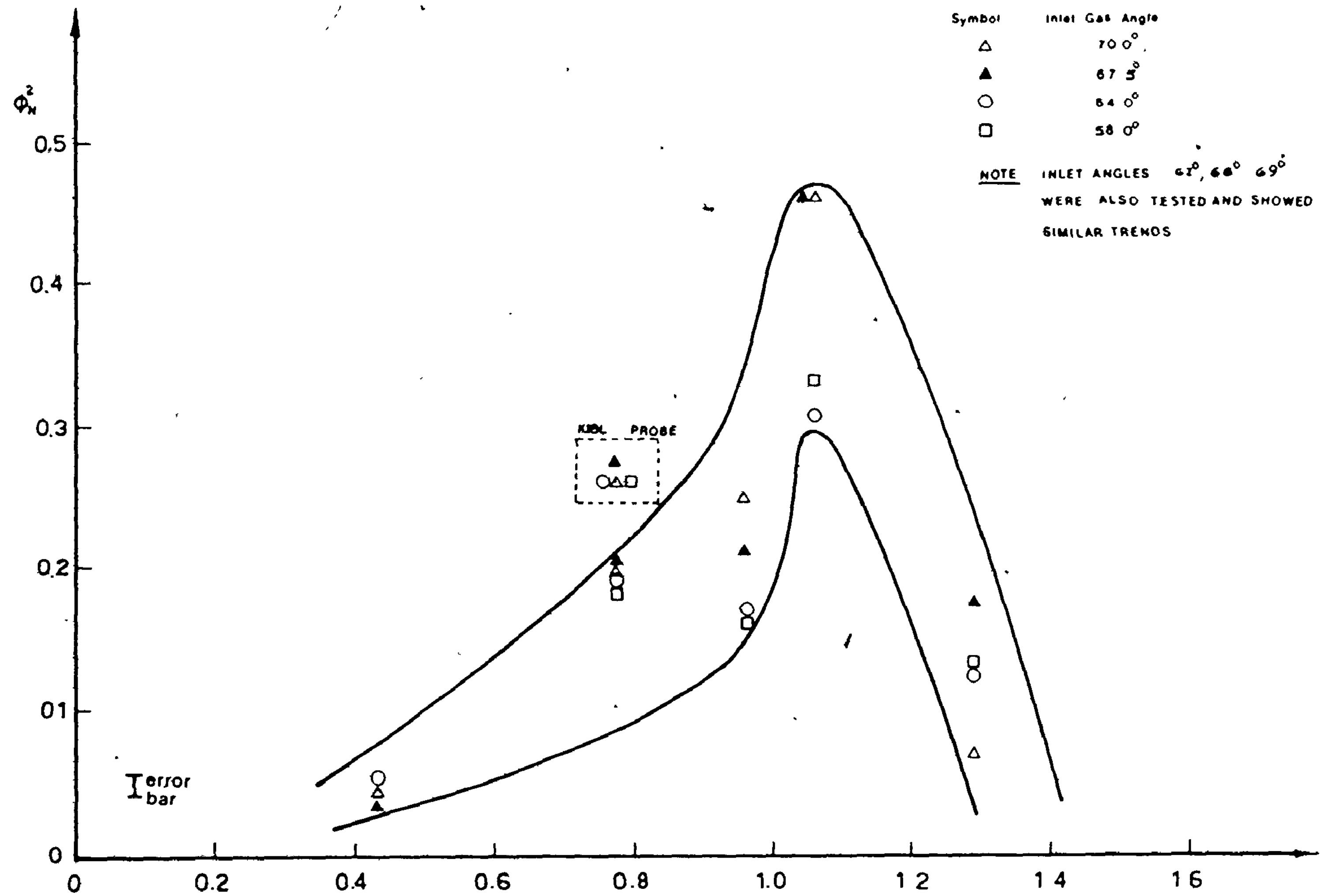

Solid line shows range of data only
- not theoretical curve

Figure 26 Total Head Loss Coefficient Variation

Figures 27 and 28 show the total pressure profiles downstream of the trailing edge for exit Mach numbers of 1.05 and 1.29. The average total pressure was calculated in these cases and used in Figure 26. As in the pressure distribution plots, inlet angles of 62.0°, 66.0° and 69.0° were also tested.

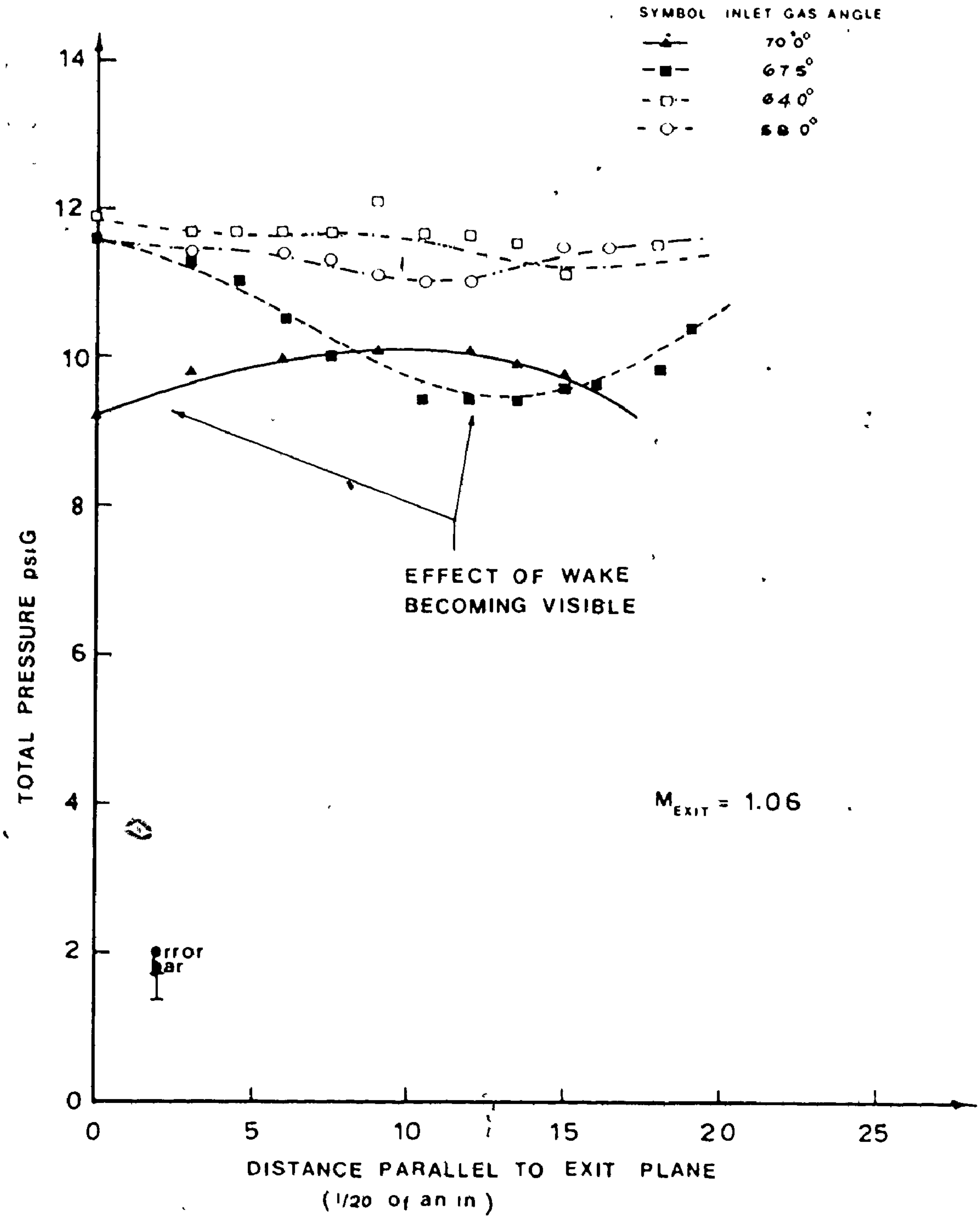

Figure 27 Total Pressure Traverses

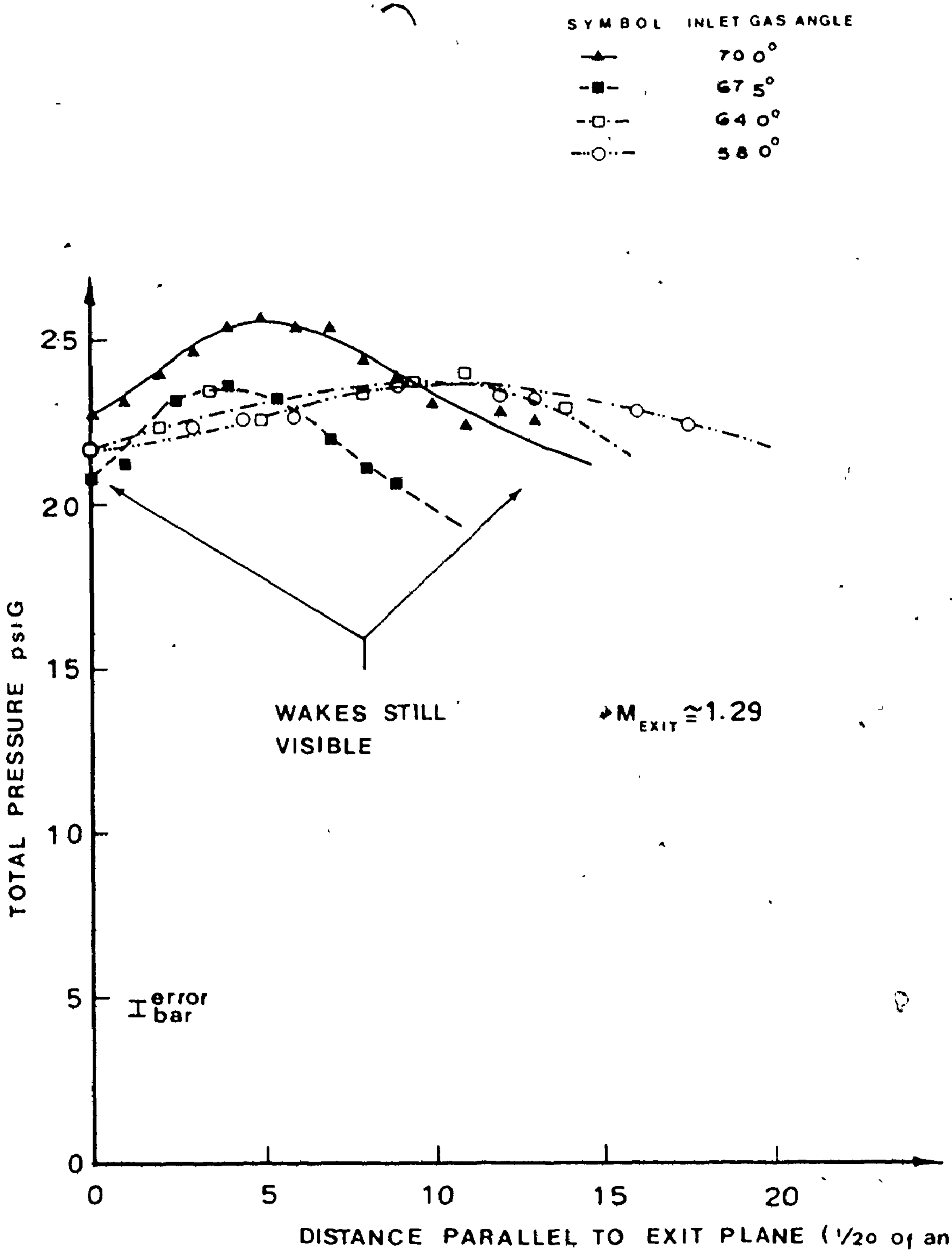

Figure 28 Total Pressure Traverses

CHAPTER 6

DISCUSSION OF RESULTS

6.1 Boundary Layer Profile

A fifth order polynomial was fitted by a least squares technique to the data of Figure 10 so that the total temperature could be determined at any time during a run. This information was used in the determination of flow velocity for the boundary layer profiles shown in Figure 19. Modelling the boundary layer with a 1/7 power law equation, displacement thickness of .0625 and .0578 inches were determined for the two exit areas. It was originally considered that boundary layer blowing would result in considerably better two dimensionality of flow upstream of the cascade. However, upon calculation of the displacement thickness, the removal of the boundary layer was deemed unnecessary as pressure measurements were made at the mean blade height, well removed from the region of boundary layer effects. Thus, two dimensional flow was assumed over all of the passage.

6.2 Pressure Distributions

Initially the pressure distribution plots will be examined to distinguish various trends developing as the two independent variables, inlet gas angle and pressure ratio, are varied. Comparisons between the experimental results and those predicted by the streamline curvature technique will be discussed in Chapter 7.

Firstly it should be noted that the pressure surface distribution is practically independent of inlet angle except in the leading edge region. Here, the increase of inlet angle causes the flow to impinge more directly onto the surface and consequently results in greater static pressures. As the pressure ratio increases, the effect becomes less pronounced. As expected the suction surface shows the opposite trend with the degree of suction increasing with inlet angle. This effect generally becomes more pronounced as the pressure ratio is increased. It is interesting to note that for an isolated aerofoil the opposite situation occurs [19]. It should be pointed out that the extreme suction peak initially predicted is indeed present but is an effect very localized to the suction surface leading edge region. Although the large amount of suction would have the beneficial effect of increasing the total tangential force on the blade, the extremely adverse pressure gradient which immediately follows could cause boundary layer separation. This possibly explains the extensive region of low pressure over the mid-chord position of the suction surface. At the lower angles of attack, the suction peak diminished, finally becoming non-existent at 58°. In fact, at the higher pressure ratios, the first suction surface pressure tap registered a considerably higher pressure than the corresponding pressure surface measurement. This, of course, would result in a reduction of the lift offered by this blade section.

Figure 21 also shows the development of a lump near the trailing edge of both surfaces as the pressure ratio increases. This effect becomes most visible as the Mach number in the exit plane becomes supersonic and a considerable flow expansion process follows the throat. This effect was illustrated in Reference [2] when testing was carried out on turbine blades having high turning angle. However, the blades examined in Reference [2] do not exhibit the low pressures over the central portion of the suction surface which was observed during their tests. Although this feature appears to make the new blades more desirable, other aspects of blade performance should be included before one can arrive at a final conclusion.

Finally, attention should be drawn to the apparent decrease in suction measured by the first three taps on the suction surface as the exit Mach number rose from 0.96 to 1.06 with the blade at an angle of attack of 70.0°. This unusual feature is possibly due to a separated boundary layer (at M_{EXIT} = 0.96) re-attaching as the momentum of the incoming fluid is increased.

6.3 Exit Gas Angle

The correct determination of exit flow angle presents a problem because the air is not discharged at the angle of the blade mean line at the trailing edge but instead at some

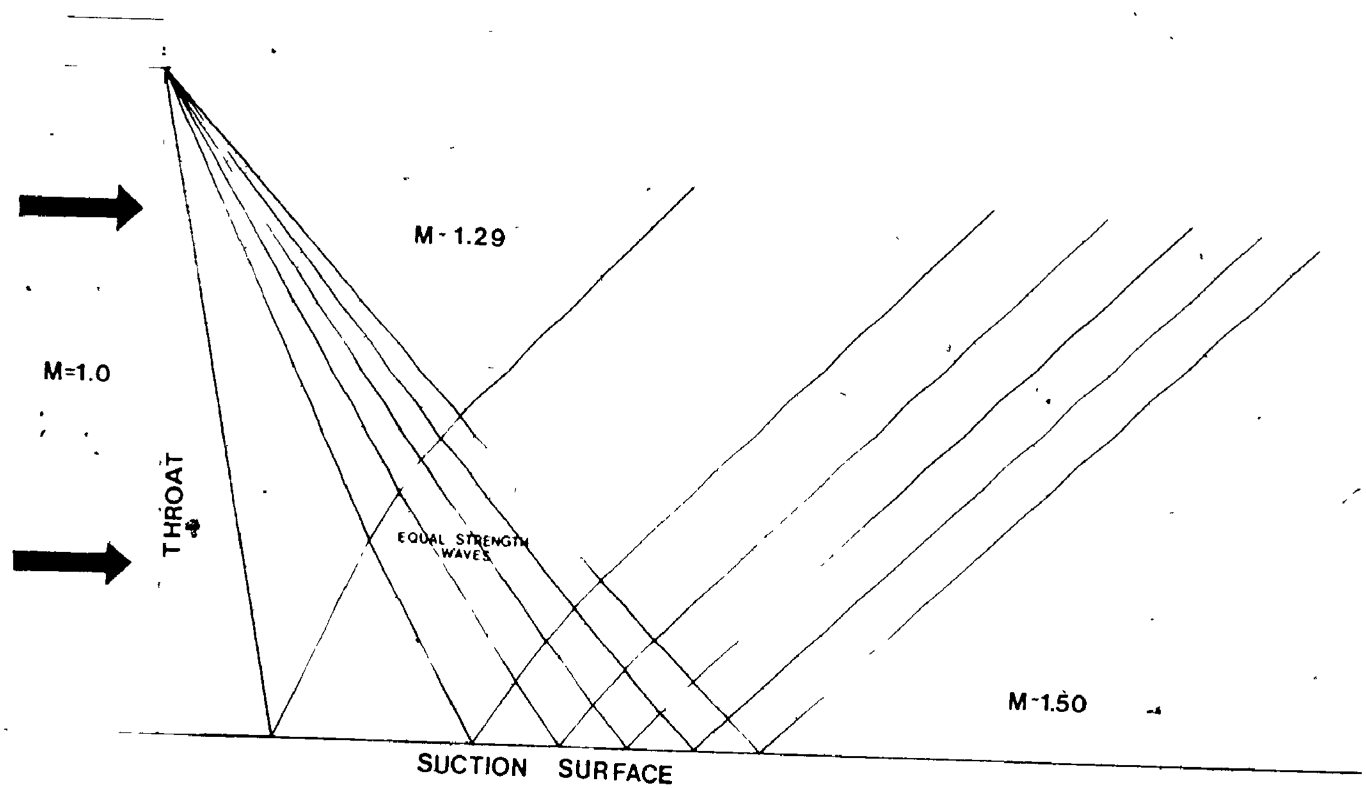

Figure 29 Exit Plane Expansion Fan
(20X Scale)

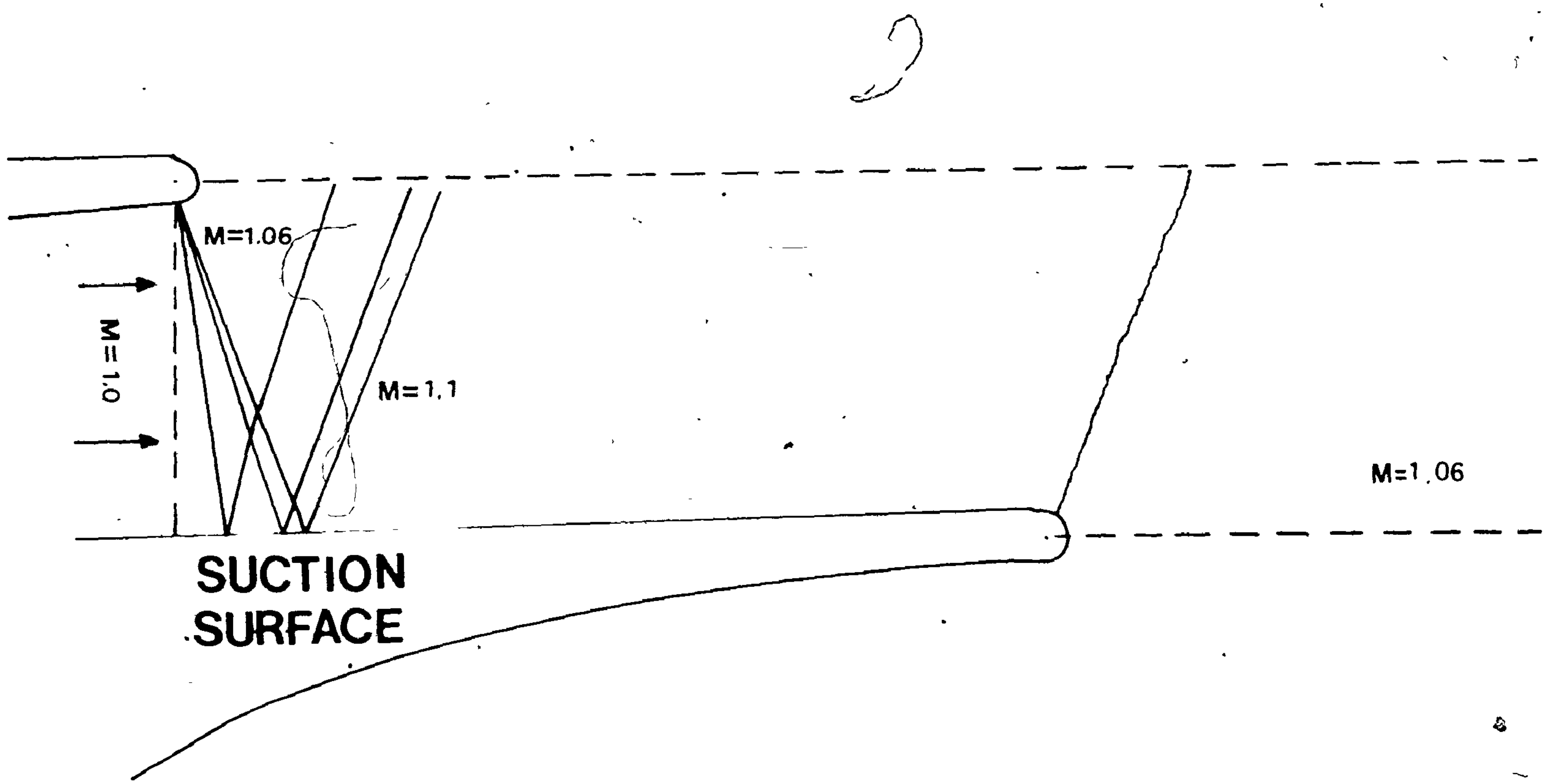

Figure 30 Exit Plane Expansion Fan
(10X Scale)

deviation from it. Since flow deflection is a measure of the guidance capacity of the passage, one can expect that cascade geometry will be an influential factor. In addition, variations of inlet Mach number can also affect the exit angle because of the associated changes in blade circulation, boundary layer development and compressibility effects [1].

Figure 25 shows a distinct trend of decreasing exit gas angle as the discharge Mach number rises for all angles of attack tested. This is not surprising when one considers that as the momentum of the flow increases, it would follow the blade shape to a lesser extent. At an exit Mach number of 0.43 the data points are widely spaced and there is some inconsistency when compared to the results obtained at higher pressure ratios. As discussed previously, tunnel control at such low pressure ratios is difficult and, hence, this data showed a large scatter. Perhaps these low Mach number results can best be used in demonstrating the effect of inlet angle variation.

Another irregularity worth noting is the increase in exit gas angle, for a 70° angle of attack, when the Mach number varied from 1.06 to 1.29. This is contrary to the decreasing trend seen for other inlet angles. To investigate the cause of this unusual result, a detailed total pressure traverse was performed for the specified flow conditions. As illustrated in Figure 28, the wake structure is more pronounced at a 70° angle of attack. This suggests that less boundary layer separation has occurred than for the other inlet angles tested. In those cases, the greater extent of separation has led to more mixing of the exit plane flow and hence less distinct wakes. As a result the flow near the trailing edges is "blown out" and does not follow the passage contours well. On the other hand, for an inlet angle of 70°, the boundary layer appears to stay attached to the blade surfaces over a greater distance. Therefore, the flow is directed more to follow the surface contour, and the gas exit angle does not decrease.

Reference [1] presents the effect of inlet Mach number and incidence angle variation on gas exit angle. Although it is emphasized that these results are for low speed flow ($M_{EXIT} < 0.6$), it is interesting to compare them with the results of this investigation. The only data we have which could be considered low speed is that obtained at an exit Mach number of 0.43. Reference [1] points out that for cascades of high solidity (the present cascade has a very high solidity - approximately 2.1) the discharge angle is predicted to change little with inlet angle variation. This is where our results differ considerably from theirs. They predict that for solidities above about 1.0, the change of exit angle should be less than 10% of the corresponding inlet angle variation. The results presented here exhibit a change of about 20%. This difference is probably due to the fact that Reference [1] is presenting the results of compressor blade testing and, thus, the blade turning angles are far less than that of our turbine blade profile. The only correlation in this respect is seen at higher exit plane Mach numbers.

Reference [2] also illustrates that the effect of Mach number variation on the exit gas angle is small up to the limiting value of the inlet Mach number. Then a large decrease in deviation is shown as Mach wave formation within the flow passage becomes significant. This may be part of the explanation of the sudden drop in exit angle between exit Mach numbers of 1.06 and 1.29.

Finally, Reference [18] predicts that the exit angle should increase with inlet gas angle. This is approximately what is observed in Figure 25.

In all of the discussions up to this point, perfect inlet angle control was assumed. As indicated in Reference [1] the skewed nature of the moving side ramps leads to some inlet angle variation across a section upstream of the cascade. The modifications discussed earlier appear to have decreased the variation from the original 2° measured in Reference [2] to approximately 1° measured for the current arrangement. Thus, a further improvement to the accuracy of the results was accomplished.

Several times during the exit angle test, a flow visualization technique was used to check the validity of the probe measurements. A mixture of fine aluminum powder and SAE 20 grade oil was painted onto the lower surface of the blade holder downstream of the blades. After a very short run time, a distinct pattern emerged on the surface and the approximate exit angle was measured. Although outlet angle could not be determined to an accuracy of better than $\pm .5^{\circ}$, this technique generally verified the more accurate yaw probe results.

6.4 Total Head Loss Coefficient

Cascade losses may be primarily the result of boundary layer growth on the suction and pressure surfaces of the blades [1]. These surface boundary layers combine at the blade's trailing edge to produce wakes as shown in Figure 31. As a result, a local deficit in total pressure is created and a mass averaged total pressure loss is determined in the section wake. As discussed earlier, when the wake was significant at the downstream measurement location, the total pressure variation across a blade spacing is considered when determining the total head loss coefficient.

Figure 26 illustrates the variation of total head loss coefficient for a range of exit Mach numbers and inlet gas angles. As expected, measured losses increased with exit Mach number until the exit plane flow is approximately sonic. This trend is predicted in References [18] and a sudden increase in losses is observed when approaching the limiting inlet Mach number. This is due primarily to the first appearance of supersonic flow patches on the blade surface and the possible development of shock waves (see References [9] and [17] for a detailed discussion on shock

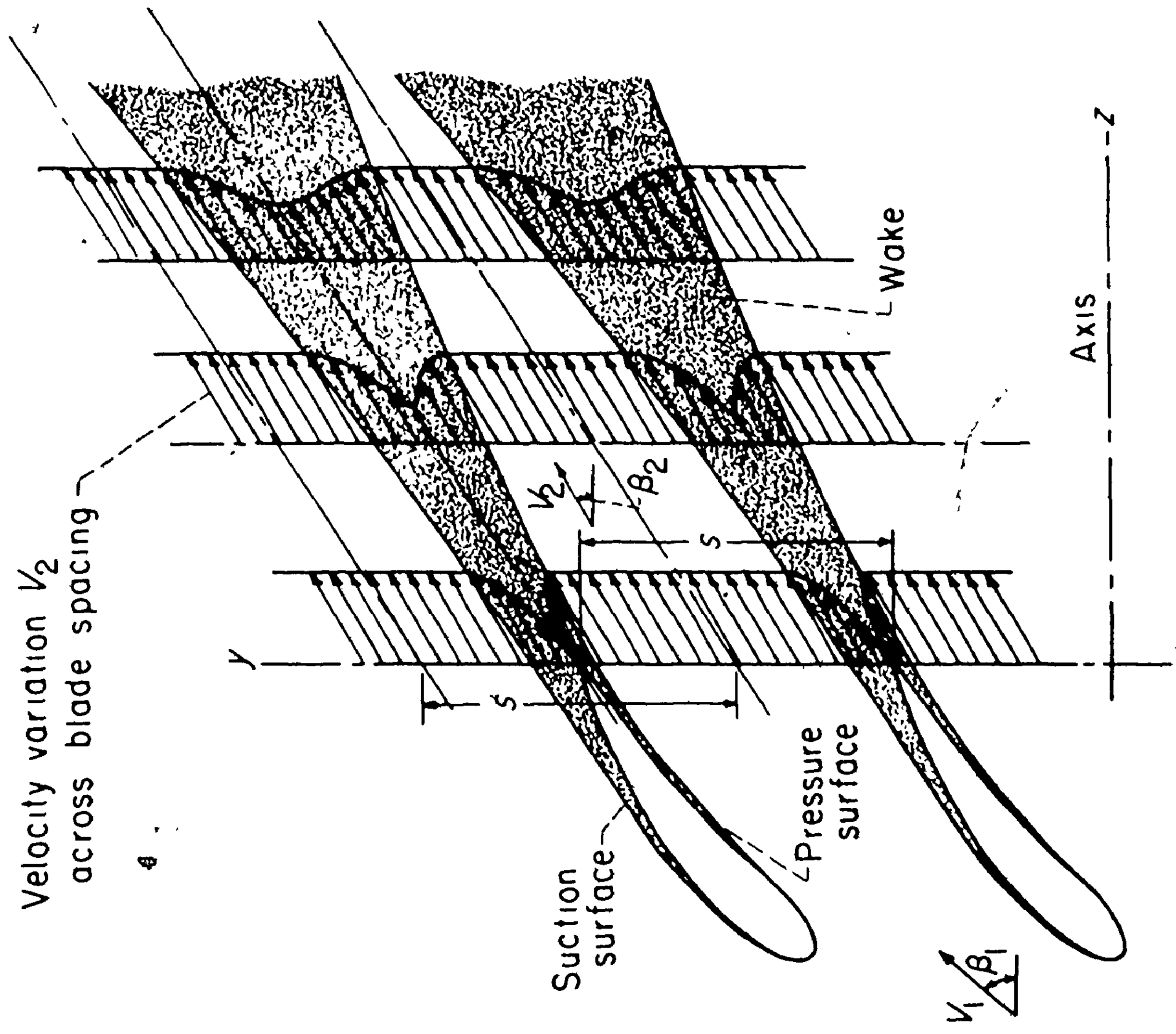

Figure 31 Wake Behind Blades
(Reference [1])

wave effects in cascade flow). However at the highest supersonic exit conditions, the loss coefficient decreases abruptly becoming less than all previous values except those at the lowest pressure ratio. The theoretical model presented in Reference [1] predicts a similar drop in losses for supersonic exit flow. They show a considerable decrease commencing at an exit Mach number of about 1.75, which is above the range currently attainable by our experimental rig. The cascade losses associated with boundary layer induced shocks is discussed in Reference [18].

Initially, the data collected at an exit Mach number of 0.78 was the result of tests conducted using a Kiel probe. These results are outlined with a box in Figure 26. This data did not correlate well with the remainder of the experimental results, and hence, was considered suspect. Since the use of a Kiel probe is not recommended for such high flow velocities the data was checked by traversing a total head probe across the exit flow as described earlier. The new results fell considerably below those obtained with the miniature Kiel probe and were more consistent with the rest of the data. This is an excellent illustration of the importance of correct instrumentation in high speed gas measurements particularly as one approaches the critical Mach number based on the geometry of the probe.

CHAPTER 7

THE COMPUTER MODEL

The two dimensional potential flow in a cascade passage has been modelled using the streamline curvature technique described in References [2], [3] and [20].

7.1 The Quasi-Orthogonal Grid

Initially, a system of quasi-orthogonal lines were determined which intersected every streamline at 90° between the flow boundaries exactly once. Since the exact location of the streamline would not be established at this stage, it should be emphasized that the network obtained is only a grid for the computational scheme. Later refinements can establish both the streamline and equipotential lines more accurately. The problem that this thesis investigated concerned the pressure and velocity distribution on the blade surfaces, which, by definition, are indeed true streamlines. The accuracy attained was considered acceptable.

The orthogonals are then divided into an arbitrary number of equal widths. Reference [2] showed that nine portions gave good accuracy without unduly complicating the computation. An elementary stream-tube system, as shown in Figure 32, was defined by drawing smooth curves between corresponding positions on each orthogonal. The designer is

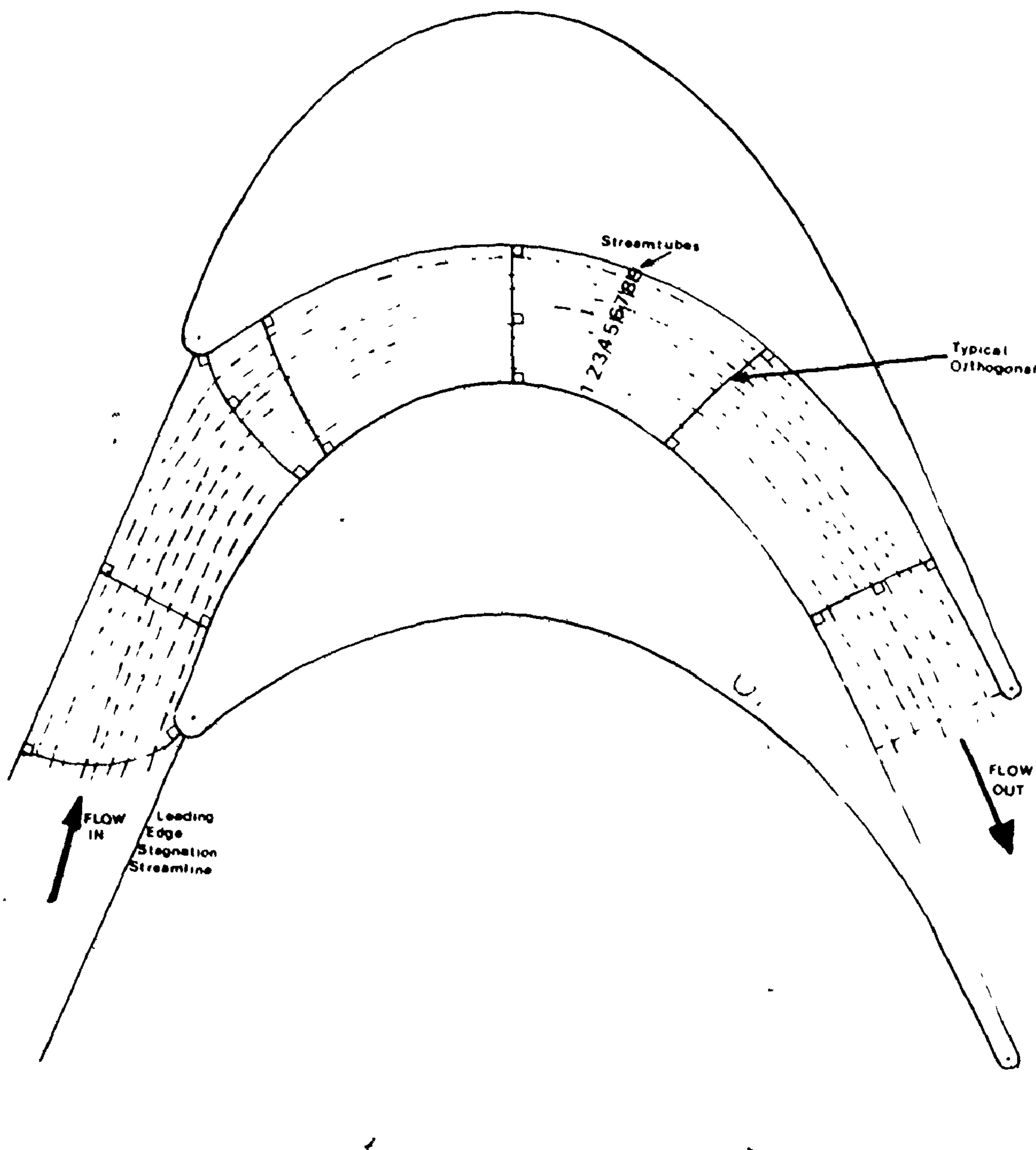

Figure 32 Streamtube System

free to select any number of orthogonals and may choose to locate most where the curvature is changing rapidly.

7.2 The Streamline Curvature Method

The basic assumptions implicit in this method are as follows:

The flow is considered:

(i) inviscid but compressible

(ii) steady

(iii) to have negligible radial velocity

(iv) two dimensional

(v) isentropic

(vi) to have its mid-passage line defined as a streamline.

From manipulation of the continuity and momentum equations describing the flow across any orthogonal and the momentum equation for flow along a streamline, the velocity variation across the passage may be determined. By assuming that the streamline curvature varied in a linear fashion along each orthogonal (Stannard [2] found that this gave the most consistent results), the velocity variation expressed in terms of the mid-channel velocity, and the pressure and suction surface curvature can be written as follows [2]:

$$\frac{V}{V_{mid}} = e^{\left[-\frac{N_o}{2(C_p{}'-C_S{}')}\left\{C^2 - \frac{(C_p{}'+C_S{}')^2}{4}\right\}\right]} \qquad (6)$$

Then by iterating, using V_{mid} as the variable, one can converge to a total mass flow equal to that allowed by choking or some other design inlet mass flow. The computer program used in References [2] and [3] was used in this thesis with modifications to calculate lift force per inch blade depth and to display surface static pressure and Mach number distributions graphically.

Stannard [2] made several improvements to the original technique formulated by Malhotra [3]. He extended the calculations to the leading edge region by assuming the inlet stagnation streamline to be a straight line focussed on the center of the leading edge curvature. With this extension the orthogonal lines can be drawn from the highly curved portion of the leading edge to this streamline. An additional improvement was his analysis of choked flow in the exit plane. The velocity distribution along an orthogonal is expressed in terms of the pressure surface velocity (assuming linear variation of curvature) as:

$$\frac{V}{V_{PRESS}} = e^{\left[\frac{N_o}{2}(C_P{}' + C_S{}' - 2C_S{}' \frac{N}{N_o} - (C_P{}' - C_S{}') \frac{N^2}{N_o^2})\right]} \qquad (7)$$

The calculation is started by assuming that the flow on the pressure surface is just choked. The assumption of linear variation of curvature across the throat results in some error in mass flow calculation, but Stannard [2] demonstrated that good correlation with experimental data is still obtained.

Although important viscous effects are ignored in this technique, it is shown in Reference [2] that the extended computational method is good enough for design purposes. The program's small size and short running time make it ideal for an iterative design procedure. The potential flow solution may be used to determine the boundary conditions for a more detailed analysis of viscous and secondary flow effects.

7.3 The Computer Model

The modified streamline curvature program requires the following input to determine the two dimensional potential flow solution:

(i) the location of each orthogonal

(ii) the curvatures of the blade surfaces at the ends of each orthogonal

(iii) the length of each orthogonal.

In References [2], [3] the orthogonal grid was constructed by hand using drafting methods. The technique used was basically as follows. The perpendicular was drawn from the desired quasi-orthogonal start point on the suction surface (point a in Figure 33). Then a point on the pressure surface was selected which appeared close to being on the same orthogonal (point b in Figure 33). The perpendicular was then drawn from the selected pressure surface point and extended to intersect with the perpendicular from the suction surface. Successive approximations were made of the pressure

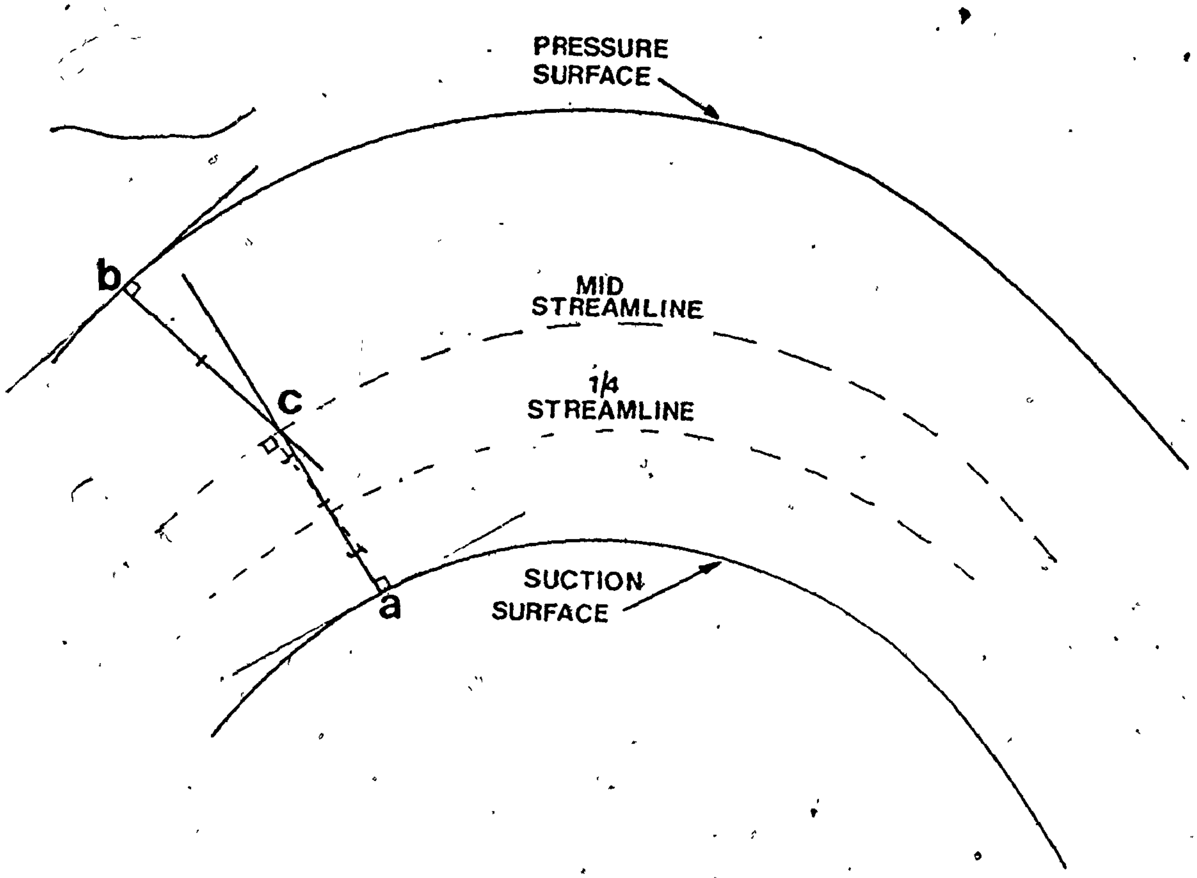

Figure 33 Orthogonal Construction

surface point location until the intersection point of the two perpendiculars was equidistant from the blade surfaces. This fixed the location of point b on the same orthogonal as point a. The procedure was continued until a sufficient locus of mid points, c, were determined to allow a curve to be fitted to the approximate mid-passage streamline. Then the same technique was repeated using the original start point and our newly defined curve as a "pressure surface". This determined the quarter passage streamline. As before this fixes c on the same orthogonal as a and b. Similarly the midstreamline is used as a "suction surface" when determining the 3/4 passage streamline.

Obviously this procedure can be continued until a sufficient number of orthogonal points are determined to allow the fitting of a curve. Since, in the case of a turbine passage, the orthogonals are close to being straight lines over most of the blade surface (the leading edges excepted), fitting a curve to pass through the three points is probably quite accurate. The problem is solved when the lengths of the orthogonals and the curvatures at their end points have been determined.

This technique is extremely tedious and time consuming when performed by hand particularly when it can be seen that for each change in geometry the procedure must be repeated.

The blades under investigation in this thesis were drawn at 20 times scale and the orthogonals constructed by hand. To determine the three points for one orthogonal took several hours, and it was soon recognized that a full grid would require two days of work. Even if two parameters, such as blade pitch or stagger angle were varied, the method would become tedious.

The second problem of a manual grid construction was in the determination of blade surface curvature. Reference [2] describes how the curvatures were determined using a boom compass on a large scale drawing. This method is sensitive to both the accuracy of drafting curve fitting and especially to the positioning of the compass when small curvatures are to be determined. Once again, this technique is quite time consuming.

Hence it was decided to write a computer program which would accurately determine blade surface curvatures and orthogonal locations and lengths. The required input to the program are the blade pitch and coordinates and the other variables as discussed in a detailed user's manual in Appendix II. The designer receives the following output for the main flow passage and the highly curved regions at the leading edges :

(i) the location of the orthogonal start and end points on each blade surface.

(ii) the curvatures of the blade surfaces at each end of the orthogonal.

(iii) the orthogonal length.

(iv) a plotter output which shows the blade under investigation and the orthogonal grids for the main part of the passage and one complete leading edge.

Some of the more important aspects of the program will now be discussed. Initially the matrix of blade surface co-ordinates was orthogonalized and a least squares fit of the data performed. A subroutine selected the polynomial order based on the criteria outlined in Appendix IV. A detailed print out of the method of polynomial selection may be obtained by using the program presented in Appendix V. After several discussions with Dr. P. C. Chakravarti [22], it was decided that a transformation technique using a linear curvature variation across the region between the two polynomials was much too complicated. It was then decided to use a computerized search which performed the same task as that originally done manually. It should be remarked that this technique will not always give satisfactory results for unusual shapes such as when the two curves have extremely different curvatures. However, for any practical blade shape the method works well. The optimum polynomial is fitted for each streamline as the technique locates them. Finally, polynomials are also fitted to the orthogonal points for length determination.

Not only was the computer program more accurate, especially in curvature determinations, than the manual method, but its speed and relatively low cost allowed the analysis of many cascade and blade geometries in a fraction of the original time required. This ultimately permits the designer to rapidly compare the two dimensional potential flow solution for many proposed blade arrangements.

The orthogonal-generation program developed in this thesis was used to produce the flow passage data of the blade profile being investigated. Later this information was input into the streamline-curvature program to determine the theoretical pressure distribution shown in Figures 20-24.

7.4 Comparison of Theoretical and Experimental Blade Surface Pressure Distributions

Initially the potential flow solutions for the design inlet angle of 67.5^{o} were obtained from the streamline curvature program. However, Figure 35 shows that for this inlet geometry, the length of several orthogonals drawn from the suction surface to the leading edge stagnation streamline was less than that of the throat at the blade's trailing edge. One would therefore expect the gas flow to choke on this orthogonal (for sufficiently high pressure ratio) and the passage to contain supersonic flow. It is likely that the flow would return to subsonic within the passage by means of internal shock.

Before deciding if this is an accurate prediction of the actual results, it is important to consider several facts. Firstly, this result can not be verified along the whole passage using the streamline curvature technique as it generally outputs the subsonic solution. Also, the program does not include predictions of the effect of discontinuities due to shock formation. As discussed in Reference [2] the leading edge stagnation streamline is not exactly a straight line but curved somewhat, thus inducing a different angle of attack (and hence different orthogonal lengths). It should also be recognized that the positioning of the blades is not perfect and real orthogonal lengths are difficult to specify to better than ± 5% (this was also the approximate difference between the width of the geometric throat at the trailing edge and the shortest orthogonal). Finally, boundary layer growth along the passage boundaries could still result in choking at the trailing edge due to a reduction in effective flow area. Because of these facts, the results obtained at the design angle of attack probably do not accurately model the actual physical situation. Hence it was decided to compare the theoretical and experimental pressure distributions obtained at a gas inlet angle of 64.0°. In this case, the shortest orthogonal originated at the trailing edge and there was no doubt that choking would occur there first.

As seen in Figures 20-24 the theoretical curve for an inlet gas angle of 64° is compared with the experimental data. The general shape of the curves is similar to that obtained experimentally especially at the lower pressure ratios (note the excellent fit for a pressure ratio of 1.14 where a greatly expanded ordinate scale was used).

The first major discrepancy between the predicted and actual results occurs near the leading edge on the suction surface where a substantial pressure peak is predicted at all pressure ratios. This peak was actually found to be much less pronounced during experimentation. The adverse pressure gradient may have been too extreme for the boundary layer to negotiate and it consequently separated before attaining the predicted higher pressures. The potential flow solution was, of course, incapable of predicting such viscous effects as boundary layer phenomenon. Following this, it appears that the boundary layer reattached and then separated again at an axial position of about 30% of the chord. This is a likely explanation of the unpredicted low pressures experienced at mid chord on the suction surface.

Observations of the conditions on the pressure surface supported these explanations. Immediately following the two regions of proposed separation on the suction surface, similar drops in pressure occurred on the pressure surface. When separation occurred, the effective passage flow area decreased, resulting in flow acceleration. Hence, until the suction surface boundary layer reattaches, the pressure experienced on the other side of the passage would be correspondingly lower than that of the passage flowing full (as assumed in potential flow models).

A further discrepancy is observed near the throat where separation again may have been responsible for reduced pressures. The pressure distribution on the flat backed portion of the suction surface was obtained using the results of the expansion wave system shown in Figure 29.

Figures 41a, 41b show the theoretical pressure distributions at the leading edge for a range of pressure ratios. Although no experimental pressures were found at these locations, the theoretical analysis of flow in this region is important to fully understand the effects that appear downstream (separation especially). The strange results shown in these two figures are fully explained in Appendix VII, where several changes to the streamline curvature program are suggested.

CHAPTER 8

CONCLUSIONS

The experimental results and theoretical analysis presented in this thesis allow the following general conclusions to be drawn:

(a) improvements made to the cascade wind tunnel permit the collection of reproduceable flow data at plenum to atmosphere pressure ratios as high as 2.9.

(b) the orthogonal generation computer program developed in this work successfully gives rapid and accurate results for use in potential flow calculations.

(c) at low pressure ratios, the streamline curvature program, as modified in Reference [2], gives results which correlate well with experimental values. However, for transonic and supersonic exit flows, boundary layer separation is believed to have occurred on the suction surface of the specified blade, resulting in an unpredicted rapid pressure drop. This feature may be considered unacceptable on the gas turbine blade under investigation.

In support of conclusion (a), Figure 6 shows this improvement in plenum pressure variation due to the by-pass installation. Further improvement was also accomplished by flow area reduction when the 1/2 inch side ramps were installed. The addition also resulted in the reduction of mean flow deviation upstream of the cascade to approximately 1^{o} off the tunnel axis.

The orthogonal generation program, shown in Appendix II gave the desired output on punched cards. The punch format was so specified as to allow direct interfacing with the streamline curvature program used in Reference [2]. Various blade configurations with different inlet gas angles may now be analyzed in a small fraction of the original time required to manually construct the potential flow grid. The blade surface pressure and Mach number distributions are now displayed in both tabular and graphical form (see Figures 42,43 in Appendix VI).

Figures 20-24 compare the theoretical and experimental results for an angle of attack of 64^{o}. As indicated by the included error bars, the data is sufficiently accurate to allow the formulation of conclusions as to the effect of boundary layer separation.

In summary, the overall conclusion may be made that modelling of high speed flow between turbine blades having large turning angles is only approximately by potential flow theories. However, the computerized technique of orthogonal production and curvature determination makes possible an extremely quick preliminary analysis of two-dimensional flow properties.

REFERENCES

1. Johnsen, I. A. and Bullock, R. O. (Editors) "Aerodynamic Design of Axial Flow Compressors", NASA SP-36, 1965.

2. Stannard, J. H., "The Aerodynamic Design and Testing of High Turning Angle Turbine Blades", Ph.D Thesis, Dept. of Mechanical Eng., McMaster University, 1975.

3. Malhotra, R. K., "The Two-Dimensional Development and Analysis of Blade Profiles having Large Turning Angles", M.Eng. Thesis, Dept. of Mechanical Eng., McMaster University, 1971.

4. Jennings, B. H. and Rogers, W. L., "Gas Turbine Analysis and Practice", McGraw-Hill, 1953.

5. McBride, M. W., "Refinement of the Mean Streamline Method of Blade Section Design", A.S.M.E. publication # 76-WA/FE-11.

6. Howarth, L. "Modern Developments in Fluid Dynamics - High Speed Flow", Volume II, Oxford - At the Clarendon Press, 1953.

7. Shepherd, D. G., "Introduction to the Gas Turbine", 2nd Ed., 1960, Constable and Company Ltd.

8. Howell, A. R., "Fluid Dynamics of Axial Flow Compressors", Proc. I.Mech.E., 1945 - reprinted by A.S.M.E., 1947 "Lectures on the Development of the British Gas Turbine Jet Unit".

9. Lichtfuss, H. J. and Starken, H., "Supersonic Exit Flow of Two Dimensional Cascades", A.S.M.E. publication # 72-GT-49.

10. Le Foll, J., "A Theory of Representation of the Properties of Boundary Layers on a Plane", Proc. of Seminar on Advanced Problems in Turbomachinery, V.K.I., 1965.

11. Tupper, K. F., Dilworth, P. B. and Jenkins, L. A., "The N.A.E. Five Foot Supersonic Wind Tunnel", EIC paper # 40 from the 1961 Annual General Meeting.

12. Dean, R. C., Ed., "Aerodynamic Measurements", Gas Turbine Laboratory, Massachusetts Institute of Technology, 5th edition, 1958.

13. Pope, A. and Goin, J., "High Speed Wind Tunnel Testing", Pitman, 1958.

14. Paradis, M. A., "Pressure and Velocity Measurements in Subsonic Flow", A Monogram, Department of Mechanical Engineering, Laval University, 1971.

15. Pankhurst, R. C. and Holder, D. W., "Wind Tunnel Technique", Pitman, 1965.

16. Bryer, D. W. and Pankhurst, R. C., "Pressure Probe Methods for Determining Wind Speed and Flow Direction", HMSO, 1971.

17. Schlichting, H., "Boundary Layer Theory", Trans. by J. Kestin, McGraw-Hill, 1968.

18. Fottner, L., "Analytical Approach for the Loss and Deflection Behaviour of Cascades in Transonic Flow Including Axial Mass Flow Variation", Suruge, J. - Ed. AGARD AG-164-1972.

19. Wade, J. H. T., "Visualization of Low Speed Airflows", March 1954, private communication.

20. Kumar, V., "The Design of Three Related Gas Turbines for an Experimental Investigation of the Effect of Blade Loading on Performance", M.Eng. Thesis, Dept. of Mechanical Eng., Carleton University, 1968.

21. Liepmann, H. W. and Roshko, A., "Elements of Gas Dynamics", J. Wiley and Sons, 1956.

22. Private Communication - Professor P. C. Chakravarti, Dept. of Applied Mathematics, McMaster University.

23. Ralston, T., "A First Course in Numerical Analysis", McGraw-Hill, 1965.

24. Pennington, K. G., "Introductory Computational Methods and Numerical Analysis", MacMillan Co., 1965.

APPENDIX I

ERROR ANALYSIS

<u>Effect of Varying Po_1 on M_{IN} During a Run</u>

<u>Assumptions</u>: (1) no dA

(2) no friction

(3) no dT_o

(4) no gas injection

Thus, generally

$$\frac{dM^2}{M^2} = \frac{2(1+\gamma M^2)(1+\frac{\gamma-1}{2} M^2)}{1-M^2} (\frac{dw}{w})_A$$

and

$$\frac{dP_o}{P_o} = -\gamma M^2 (\frac{dw}{w})_B$$

Since, $(\frac{dw}{w})_A = (\frac{dw}{w})_B$, we obtain:

$$\frac{d\ M^2}{M^2} = \frac{d\ P_o}{P_o} (\frac{2(1+\gamma M^2)(1+\frac{\gamma-1}{2} M^2)}{\gamma M^2(M^2-1)} \qquad (8)$$

However, for M is close to 1.0 (two are found in this region); the influence coefficient approaches infinity and the equation is not useable.

Thus we perform the following analysis for M close to 1.0.

Analysis for M Close to 1.0

As before:

$$\frac{1-M^2}{M^2}\, dM^2 = 2(1+\gamma M^2)(1+\frac{\gamma-1}{2} M^2)(\frac{dw}{w})_A$$

Integrating we obtain for M close to 1.0

$$[\ln M^2 - M^2]_{M_1}^{M_2} = \frac{2(1+\gamma)(1+\frac{\gamma-1}{2})}{1} \ln w_A \Big/_{w_1}^{w_2} \qquad (9)$$

Also

$$\frac{dP_o}{P_o} = -\gamma M^2 \left(\frac{dw}{w}\right)_B$$

$$\therefore \ln P_o \Big/_{P_{o_1}}^{P_{o_2}} = -\gamma M^2 \ln w_B \Big/_{w_1}^{w_2}$$

and since $\ln w_A \Big/_{w_1}^{w_2} = \ln w_B \Big/_{w_1}^{w_2}$

and for M = .96; $\ln M^2 \cong 0$ we obtain

$$-M^2 \Big/_{M_1}^{M_2} \left[\frac{1}{2(1+\gamma)(1+\frac{\gamma-1}{2})}\right] = -\frac{1}{\gamma M^2} [\ln P_o]_{P_{o_1}}^{P_{o_2}}$$

- now we substitute $P_{o_2} = P_{o_1} - d\, P_o$

and with $M_1 = M = .96$; we solve for M_2 and obtain $dM \cong M - M_2$

We therefore obtain the following information for typical values of d P_o experienced during an acceptable run:

$\frac{P_{o_1}}{P_{atm}}$	M_{exit}	Design M_{inlet}	P_o psia	$(d\ P_o)$ psi	$(d\ M)_{in}$	$(d\ M)_{exit}$
2.73	1.29	.696	40.2	0.80	0 } *	.015
2.03	1.06	.696	29.9	0.40	0	.010
1.81	0.96	.693	26.6	0.29	0.026	.010
1.41	0.78	.602	22.0	0.27	0.060	.012
1.14	0.44	.392	16.8	0.07	0.016	.005

* For supersonic exit flow the inlet Mach number stays fixed for small variations in P_{o_1}.

APPENDIX II

QUASI-ORTHOGONAL PROGRAM USER'S MANUAL

The following user's manual will outline the purpose of each subroutine and the variables that must be input to the main program. A flow chart is included to further explain the calculation sequence.

The program starts by reading in the coordinates of the blade under investigation and the pitch between adjacent blades. Next, the matrix of coordinates is orthogonalized and a smooth polynomial fitted to the data by a least squares technique. It is important to remark at this point that the McMaster library program LESQ is not recommended as it was found to frequently become ill-conditioned due to matrix representations in the computer. Instead the library program ORLSQ was used which orthogonalizes the data before fitting a curve. Using the polynomial representation of the blade surfaces (which a subroutine automatically selects) and the input orthogonal start point, the technique described in Chapter 7 is carried out. The orthogonals fitted to second order polynomials and their lengths calculated by a simple Simpson's rule numerical integration. Finally, the blade surface curvatures at the orthogonal start and end points are calculated. The same procedure is carried out using a finer grid near the pressure and suction surface leading edges. The location of the quasi-orthogonals, their lengths and the blade surface curvatures are received as punched output from the program. This can be fed directly into the streamline curvature program to allow quick potential flow solutions.

To permit easy verification of the computer orthogonal results, various computer plotting routines have been included in the program. This gives the designer a visual presentation of the quasi-orthogonal grid constructed in the regions of interest: the main passage and the areas of high flow turning near the suction and pressure surface leading edges. A computer plot of the turbine blade is also presented.

Due to limitations on the size of the computer plots available, certain limits should be observed when inputting blade data. Of course, if a computer plot is not desired, the various calls to plotter routine can be removed, and any reasonable blade data can be input. The only major restrictions are that the data must describe the blade in a concave-down position and the specified quasi-orthogonal start points must be on the lower surface. Figures 35, 36, 37, 38. show the plotter output. Polynomial representations were used for all streamlines and quasi-orthogonals plotted except the orthogonals extending from the pressure surface leading edge. Instead, straight lines are drawn (although a second order polynomial was used in the length calculations) since a second order fit to these points yielded poor results.

If a plotted output is desired then the coordinates must be scaled to fit inside the limits shown in Figure 39 for a pitch of 0.6 c or less. For larger pitches, the limits shown in Figure 40 must be observed. The program automatically scales all input data for plotting, provided the data is wholly in the first quadrant and the minimum x-value is approximately zero (data scaled back for output).

The following is a list of subroutines and their descriptions:

Subroutine Name	Description
MAIN	- main controlling subroutine - controls number of repetitions of the quasi-orthogonal generation technique (in QUASI) based on the number of spaces (NUS) into which the passage will be divided. - plots orthogonals and prints and punches out required information.
LOOP	- calls QUASI for each orthogonal - fits curves to and plots out stream-lines. - organizes polynomial coefficients for input to QUASI
QUASI	- main orthogonal generation subroutine - procedure same as that done manually

- draws leading edge stagnation streamline

BLADE - plots out blade under investigation as specified by input coordinates

MARG - draws margins for all plots and scales data

TEST - checks to ensure that the intersection point of the perpendiculars drawn from each surface is within the passage range

ADD - fits a polynomial to the data transferred into the subroutine and then plots the polynomial.

LENGTH - rotates the input data to ensure that the polynomial fit to the quasi orthogonals is a smooth function
- calculates a polynomial's length between limits XMAX and XMIN.

CURV - calculates the curvature of a polynomial (at the desired X-location) defined by the coefficients transferred in the argument list

LEADS - since the suction surface leading edge points do not describe a function, they are rotated through 90° and then fit to a polynomial.

- start point curvatures are calculated.

LEADP - The pressure surface leading edge and main portion of the suction surface are rotated through 180°. This is so that the surface from which the orthogonals start is the lower of the two.

CFIT - automatically fits a smooth polynomial of order 18 or less to the transferred coordinates (uses ORLSQ).

Y1 - function subroutine which calculates the functional value of a polynomial at the specified location.

DY1 - function subroutine for first derivative calculation.

DY2 - function subroutine for second derivative calculation.

SCALE - scales all required output to original dimensions.

It should be noted that although ORLSQ is usually far better than LESQ, ORLSQ will <u>not</u> fit a curve of order N-1 (where N = # of data points input). Hence, if a polynomial of order N-1 is desired, LESQ is used instead (i.e., in LENGTH).

The input variables to which numerical values must be assigned are listed as follows. The numbers in brackets are recommended values to be used if the designer does not wish to change the program accuracies.

Variable Name		Description	Units or Value Recommended
1. NUM	-	number of orthogonals desired	(≤ 40)
2. ZK	-	length of main passage plot desired.	inches (170)
3. ANGI	-	inlet gas angle	radians
4. XC	-	X-coordinate of leading edge circle.	----
5. YC	-	y-coordinate of leading edge circle.	----
6. NS, NP	-	number of coordinates used to describe each blade surface	----
7. MC1, MC2, MC3	-	order of polynomials to be plotted to model streamlines in the main blade range, suction surface leading edge and pressure surface leading edge.	(6,3,3)
8. X(P,1,2)	-	orthogonal start point x-coordinates	----
9. NIS	-	number of suction surface points to be fit to a polynomial (< N)	----
10. NIP	-	number of pressure surface points to be fit to a polynomial (< N)	----

11.	NUS	- number of streamtubes drawn (must be a perfect square, i.e., 4, 16, 64,...)	(4)
12.	LN	- maximum number of guesses in the subroutine QUASI	(≤400)
13.	XSUC(I), YSUC(I)	- suction surface coordinates	----
14.	XPR(I), YPR(I)	- pressure surface coordinates	----
15.	NO, NI	- variable dimensions for subroutines	(20,40)
16.	NUMS	- number of points used to represent the suction surface leading edge	(≥ 10)
17.	ZKK	- length of suction surface leading edge plot desired	inches (12)
18.	KO	- number of orthogonals starting from suction surface leading edge	----
19.	NUMP	- number of points used to represent the pressure surface leading edge	(≥ 6)
20.	KOO	- number of orthogonals starting from pressure surface leading edge	----
21.	ZKZ	- length of pressure surface leading edge plot desired	inches (10)
22.	PITCH	- pitch between blades	scaled to data
23.	YPRM	- Maximum y-value of pressure surface leading edge points read in	----

24.	NFP	-	number of points omitted at beginning of pressure surface for polynomial fit	----
25.	XLS(I), YLS(I)	-	suction surface leading edge coordinates	----
26.	YK(P)	-	suction surface leading edge orthogonal start points - y-coordinates	----
27.	XLP(I), YLP(I)	-	pressure surface leading edge coordinates	----
28.	XK(P)	-	pressure surface leading edge orthogonal start points - x-coordinates	----
29.	DX1, DX2, DX3.	-	intervals between points where polynomial characteristics are evaluated	$\frac{X(max)-X(min)}{30}$
30.	ERROR1, ..., ERROR3	-	acceptable errors for polynomial fits	.01xc
31.	TER1,..., TER3		acceptable total errors for polynomial fits.	$\frac{(.1)N}{21}$ x c
32.	CIS1,..., CIS3		acceptable slope change between intervals DX	-5.
33.	TMIN, TMAX	-	allowable maximum and minimum flow turning angle	degrees
34.	W1(I), W2(I), W3(I),		weights of data points in ORLSQ	

FLOW CHART - Fig.34

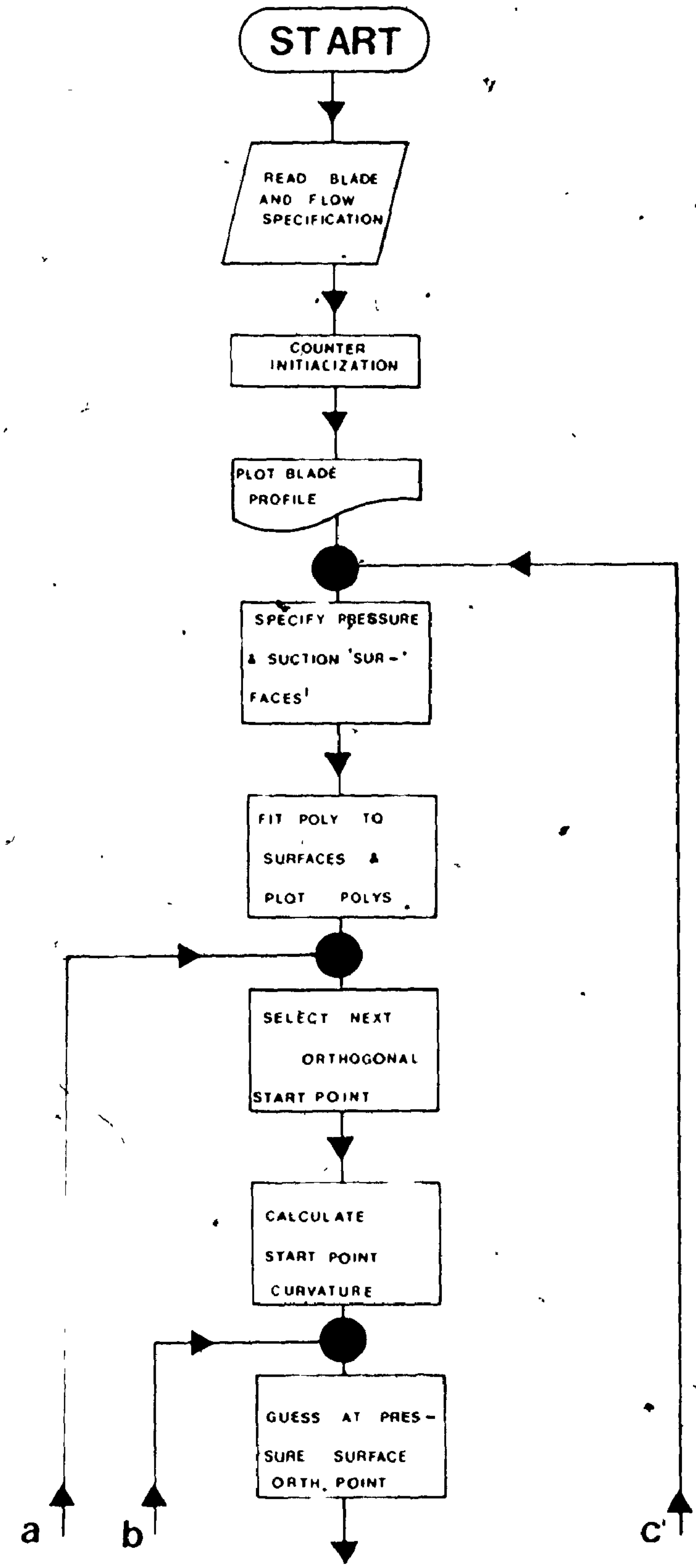

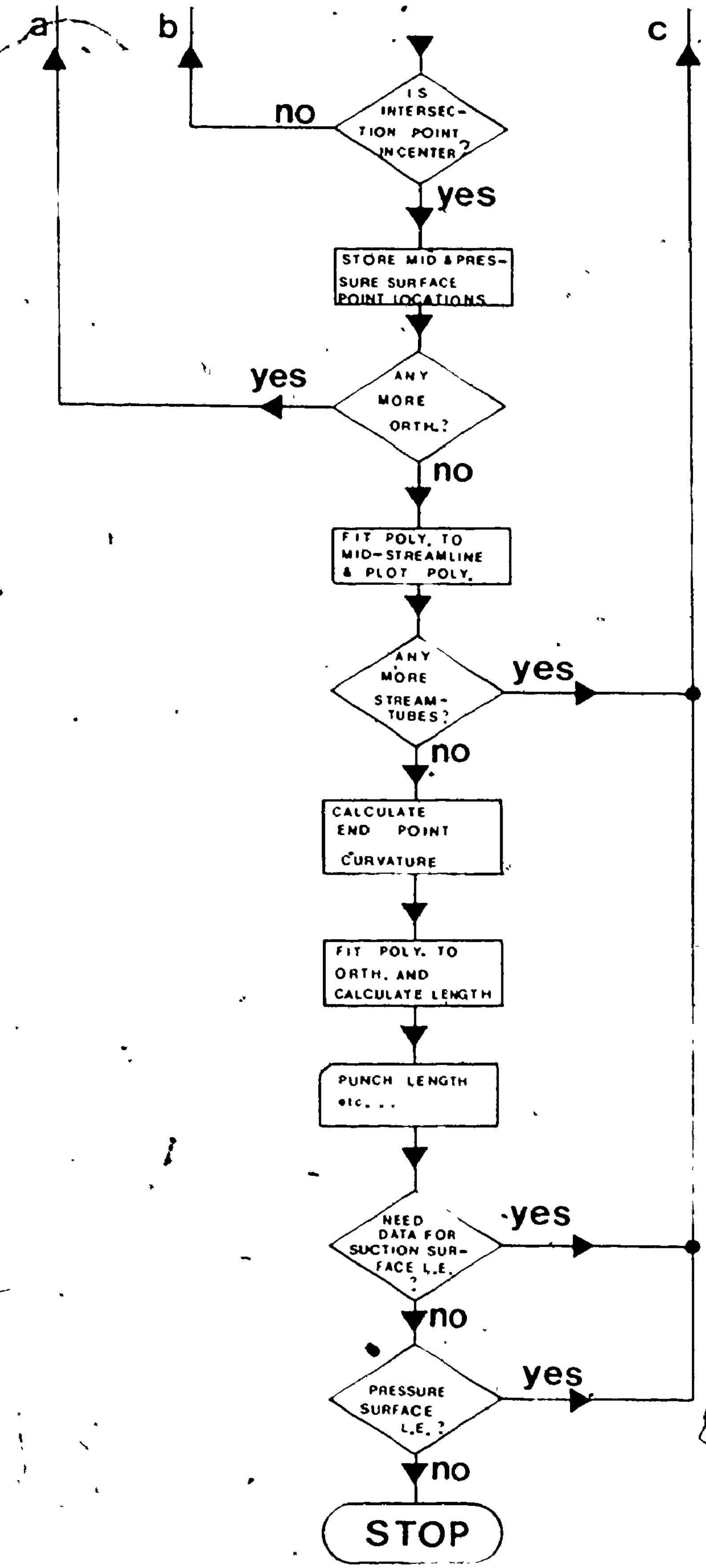
a
b
c
IS INTERSECTION POINT INCENTER?
no
yes
STORE MID & PRESSURE SURFACE POINT LOCATIONS
ANY MORE ORTH.?
yes
no
FIT POLY. TO MID-STREAMLINE & PLOT POLY.
ANY MORE STREAM-TUBES?
yes
no
CALCULATE END POINT CURVATURE
FIT POLY. TO ORTH. AND CALCULATE LENGTH
PUNCH LENGTH etc. . .
NEED DATA FOR SUCTION SURFACE L.E. ?
yes
no
PRESSURE SURFACE L.E. ?
yes
no
STOP

```
      PROGRAM TST(INPUT,OUTPUT,PUNCH,TAPE5=INPUT,TAPE6=OUTPUT,TAPE7=PUNC
     1H)
C
C
C     ******************************************************************
C
C     THIS IS THE ORTHOGONAL GENERATION PROGRAM FOR THE POTENTIAL FLOW
C     SOLUTION
C
C     ******************************************************************
C
C
C
C
C     BLADE DATA MUST BE WHOLLY IN QUANDRANT 1 WITH THE LEADING EDGE
C      LOCATED AT X=0.
C
C
C     NUM IS THE NUMBER OF MAIN BLADE RANGE ORTHOGONAL START POINTS.
C     ZK IS THE LENGTH OF THE PLOT DESIRED FOR THE MAIN BLADE RANGE.
C     ANGI IS THE INLET GAS ANGLE IN RADIANS.
C     XC AND YC ARE THE COORDINATES OF THE LEADING EDGE CIRCLE CENTER.
C     NS AND NP ARE THE NUMBER OF DATA POINTS TO BE READ IN TO MODEL THE
C      SUCTION AND PRESSURE SURFACES RESPECTIVELY.
C     NC1,NC2,NC3 ARE THE ORDER OF THE POLYNOMINALS TO BE PLOTTED FOR TH
C      MAIN BLADE RANGE,THE SUCTION SURFACE LEADING EDGE AND THE PRESSUR
C      SURFACE LEADING EDGE RESPECTIVELY.
C     NFP IS THE NUMBER OF POINTS SKIPPED FOR THE POLY FIT TO THE PRESSU
C      SURFACE MAIN BLADE RANGE.
      DIMENSION NK(20), WK(100), W(40), RA(20)
      DIMENSION XLP(20), YLP(20), XK(20)
      DIMENSION GX(40), GY(40), XSUCP(40), YSUCP(40), XPRP(40), YPRP(40)
      DIMENSION XLS(20), YLS(20).
      DIMENSION XPR(40), YPR(40), XSUC(40), YSUC(40), A(242), BS(20), BP
     1(20)
      DIMENSION XX(40)
      DIMENSION YK(20)
      COMMON XE(40,20),YE(40,20),YP(20),X(40,20,3),Y(40,20,3),C(50,50),A
     1A(20,20),BB(20,20),B(20),NM,N1,N0,N2,BZ(2),NUS,NUM,BMIN,BMAX,TMIN,
     2TMAX,NC1,NC2,NC3,W1(40),W2(40),W3(40),ERROR1,ERROR2,ERROR3,TER1,TE
     3R2,TER3,CIS1,CIS2,CIS3,DX1,DX2,DX3,SCAL1,YDIF,ICR,SCAL3
      INTEGER P,D,E,F
      READ (5,1) NUM,ZK,ANGI,XC,YC,NS,NP,NC1,NC2,NC3,NFP
    1 FORMAT (I5,4F10.4,4I5,2I3)
C
C     NEXT READ IN THE X VALUES FOR THE ORTHOGONAL START POINTS.
C
      READ (5,2) (I,X(P,1,2),P=1,NUM)
    2 FORMAT (I5,F10.4)
C
C     NIS AND NIP ARE THE NUMBER OF POINTS USED TO FIT A POLY TO THE
C      SUCTION AND PRESSURE SURFACES RESPECTIVELY.
C     NUS IS THE NUMBER OF SPACES IN THE ORTHOGONAL GRID.
C     LN IS THE NUMBER OF ITERATIONS THROUGH THE CENTER POINT LOCATION
C      PROCEDURE.
C
      READ (5,3) NIS,NIP,NUS,LN
    3 FORMAT (4I5)
C
C     XSUC AND YSUC ARE THE DATA POINTS FOR THE SUCTION SURFACE.
C     THE W,S ARE THE WEIGHTS APPLIED TO THE VARIOUS DATA POINTS.
C     SUCTION AND PRESSURE SURFACE VALUES SHOULD BE READ IN ORDER OF INC
C      REASING X VALUE.
C
      READ (5,4) (J,XSUC(I),YSUC(I),WT(I),I=1,NS)
    4 FORMAT (I5,3F10.4)
C
C     XPR AND YPR ARE THE DATA POINTS FOR THE PRESSURE SURFACE.
C     IN ANY REGION OF THE BLADE YOU WEIGHT THE SUCTION SURFACE VALUES
C      THE SAME AS THE PRESSURE SURFACE VALUES.
C
      READ (5,5) (J,XPR(I),YPR(I),I=1,NP)
    5 FORMAT (I5,2F10.4)
C
```

```
C     NO AND NI ARE JUST VARIABLE DIMENSIONS WHICH NEED NOT BE CHANGED
C      UNLESS AN EXTREMELY LARGE NUMBER OF DATA POINTS ARE TO BE USED.
C
      READ (5,6) NO,NI
6     FORMAT (2I5)
C
C     NUMS AND NUMP ARE THE NUMBER OF POINTS USED TO MODEL THE SUCTION
C      AND PRESSURE SURFACE LEADING EDGES RESPECTIVELY.
C     ZKK AND ZKZ ARE THE LENGTHS OF THE PLOTS FOR THE SUCTION AND PRES
C      SURE SURFACE LEADING EDGES RESPECTIVELY.
C     KO AND KOO ARE THE NUMBER OF ORTHOGONALS TO BE DRAWN FOR THE SUCTI
C      AND PRESSURE SURFACE LEADING EDGES RESPECTIVELY.
C     PITCH IS THE CASCADE PITCH.
C     YPRM IS THE MAXIMUM Y-VALUE USED TO MODEL THE PRESSURE SURFACE
C      LEADING EDGE.
C
      READ (5,7) NUMS,ZKK,KO,NUMP,KOO,ZKZ,PITCH,YPRM
7     FORMAT (I5,F10.4,3I5,3F10.4)
C
C     XLS AND YLS ARE THE COORDINATES OF THE SUCTION SURFACE LEADING EDG
C
      READ (5,8) (XLS(I),YLS(I),W2(I),I=1,NUMS)
8     FORMAT (3F10.4)
C
C     YK ARE THE Y-VALUES OF THE ORTHOGONAL START POINTS FOR THE
C      SUCTION SURFACE LEADING EDGE
C
      READ (5,9) (YK(P),P=1,KO)
9     FORMAT (F10.4)
C
C     XLP AND YLP ARE THE COORDINATES OF THE PRESSURE SURFACE LEADING ED
C
      READ (5,10) (XLP(I),YLP(I),W3(I),I=1,NUMP)
10    FORMAT (3F10.4)
C
C     XK ARE THE START POINTS FOR THE PRESSURE SURFACE LEADING EDGE
C
      READ (5,11) (XK(P),P=1,KOO)
11    FORMAT (F10.4)
C
C     THE DX,S ARE INTERVALS AT WHICH CALCULATION IS PERFORMED IN CFIT
C
      READ (5,12) DX1,DX2,DX3
12    FORMAT (3F10.4)
C
C     THE ERROR,S ARE THE PERMISSIBLE ERROR ALLOWED IN CFIT FOR THE POLY
C     THE TER,S ARE THE PERMISSIBLE TOTAL ERRORS ALLOWED IN CFIT.
C
      READ (5,13) ERROR1,TER1,ERROR2,TER2,ERROR3,TER3
13    FORMAT (6F10.4)
C
C     THE CIS,S ARE THE PERMISSIBLE CHANGES IN SLOPE ALLOWED BETWEEN
C      DATA POINTS CALCULATED IN CFIT
C
      READ (5,14) CIS1,CIS2,CIS3
14    FORMAT (3F10.4)
C
C     TMAX AND TMIN ARE EXTREMES OF THE TOTAL TURNING ANGLE IN THE BLADE
C
      READ (5,15) TMAX,TMIN
15    FORMAT (2F10.4)
C
C     TO SPECIFY THE POLYNOMINAL ORDERS FOR THE TWO SURFACES(INSTEAD OF
C      LETTING CFIT SELECT IT) ,READ IN IS AND IT RESPECTIVLY EQUAL TO 1
C      OTHERWISE SET THEM TO ZERO.
C
      READ (5,16) IS,IT
16    FORMAT (2I5)
      WRITE (6,17)
17    FORMAT (1X,*UNSCALED INPUT DATA*,///)
      WRITE (6,18) NIS,NIP,NUS,LN
18    FORMAT (1X,4I6)
      WRITE (6,19) ANGI,XC,YC,NS,NP,NC1,NC2,NC3
19    FORMAT (1X,3F10.4,5I5,/)
```

```
      WRITE (6,20) NFP,PITCH,NUMS,NUMP,KO,KOO,YPRM
   20 FORMAT (1X,I5,F10.4,4I5,F10.4,/)
      WRITE (6,21) CIS1,CIS2,CIS3
   21 FORMAT (1X,* CIS1=*,F10.4,* CIS2=*,F10.4,* CIS3=*,F10.4,///)
      SCAL1=1.1/(ABS(XSUC(NS)-XSUC(1)))
      YMIN=YPR(1)
      DO 22 N=2,NP
      IF (YPR(N).GT.YMIN) GO TO 22
      YMIN=YPR(N)
   22 CONTINUE
      YMAX=YSUC(1)
      DO 23 N=2,NS
      IF (YSUC(N).LT.YMAX) GO TO 24
      YMAX=YSUC(N)
   23 CONTINUE
   24 YMAX=YMAX*SCAL1
      YMIN=YMIN*SCAL1
      YDIFP=0.0
      SCAL2=1.0
      YMAXP=YMAX
      YMINP=YMIN
   25 IF (YMAXP.LT.0.985.AND.YMINP.GT.0.07) GO TO 26
      SCAL2=.9/(YMAXP-YMINP)
      YMINP=YMINP*SCAL2
      YDIFP=YMINP-0.075
      YMAXP=YMAXP*SCAL2-YDIFP
      YMINP=YMINP-YDIFP
      GO TO 25
   26 DO 27 I=1,NS
      XSUCP(I)=XSUC(I)*SCAL1*SCAL2
      YSUCP(I)=YSUC(I)*SCAL1*SCAL2-YDIFP
   27 CONTINUE
      DO 28 I=1,NP
      XPRP(I)=XPR(I)*SCAL1*SCAL2
      YPRP(I)=YPR(I)*SCAL1*SCAL2-YDIFP
   28 CONTINUE
      NOT=40
      CALL BLADE (XPRP,YPRP,XSUCP,YSUCP,NOT,NP,NS)
      YMAX=YPR(NFP+1)
      NOP=NIP+NFP
      NFPP=NFP+2
      DO 29 I=NFPP,NOP
      IF (YPR(I).LT.YMAX) GO TO 29
      YMAX=YPR(I)
   29 CONTINUE
      YMIN=YSUC(1)
      DO 30 I=2,NIS
      IF (YSUC(I).GT.YMIN) GO TO 30
      YMIN=YSUC(I)
   30 CONTINUE
      YMIN=YMIN*SCAL1
      YMAX=YMAX*SCAL1
      YDIF=YMIN-0.4
      YMAX=YMAX-YDIF
      RG=1.25-PITCH*SCAL1
      ICR=0
   31 IF (YMAX.LT.RG) GO TO 32
      ICR=ICR+1
      YMAX=YMAX/(1.1)+0.03636
      RG=1.25-PITCH*SCAL1/(1.1**ICR)
      GO TO 31
   32 SCAL3=1./(1.1**ICR)
      DO 33 P=1,NUM
      X(P,1,2)=(X(P,1,2)*SCAL1)*SCAL3
   33 CONTINUE
      WRITE (6,34)
   34 FORMAT (1X,*UNSCALED SUCTION SURFACE VALUES*,//)
      WRITE (6,35) (XSUC(I),YSUC(I),I=1,NS)
   35 FORMAT (1X,2F10.4,///)
      WRITE (6,36)
   36 FORMAT (1X,*UNSCALED PRESSURE SURFACE VALUES*,//)
      WRITE (6,37) (XPR(I),YPR(I),I=1,NP)
   37 FORMAT (1X,2F10.4,/)
      WRITE (6,38)
```

```
38    FORMAT (1X,*UNSCALED SUCTION SURFACE LEADING EDGE VALUES*,//)
      WRITE (6,39) (XLS(I),YLS(I),I=1,NUMS)
39    FORMAT (1X,2F10.4)
      WRITE (6,40)
40    FORMAT (1X,*UNSCALED PRESSURE SURFACE LEADING EDGE VALUES*,//)
      WRITE (6,41) (XLP(I),YLP(I),I=1,NUMP)
41    FORMAT (1X,2F10.4)
      WRITE (6,42) ICR
42    FORMAT (1X,*ICR=*,I5,/)
      DO 44 I=1,NS
      XSUC(I)=(XSUC(I)*SCAL1)*SCAL3
      YSUC(I)=(YSUC(I)*SCAL1-YDIF)*SCAL3
      IF (ICR.EQ.0) GO TO 44
      DO 43 J=1,ICR
      YSUC(I)=YSUC(I)+0.03636/(1.1**(J-1))
43    CONTINUE
44    CONTINUE
      DO 46 I=1,NP
      XPR(I)=(XPR(I)*SCAL1)*SCAL3
      YPR(I)=(YPR(I)*SCAL1-YDIF)*SCAL3
      IF (ICR.EQ.0) GO TO 46
      DO 45 J=1,ICR
      YPR(I)=YPR(I)+0.03636/(1.1**(J-1))
45    CONTINUE
46    CONTINUE
      DO 48 I=1,NUMS
      XLS(I)=(XLS(I)*SCAL1)*SCAL3
      YLS(I)=(YLS(I)*SCAL1-YDIF)*SCAL3
      IF (ICR.EQ.0) GO TO 48
      DO 47 J=1,ICR
      YLS(I)=YLS(I)+0.03636/(1.1**(J-1))
47    CONTINUE
48    CONTINUE
      DO 50 I=1,NUMP
      XLP(I)=(XLP(I)*SCAL1)*SCAL3
      YLP(I)=(YLP(I)*SCAL1-YDIF)*SCAL3
      IF (ICR.EQ.0) GO TO 50
      DO 49 J=1,ICR
      YLP(I)=YLP(I)+0.03636/(1.1**(J-1))
49    CONTINUE
50    CONTINUE
      DO 52 I=1,KO
      YK(I)=(YK(I)*SCAL1-YDIF)*SCAL3
      IF (ICR.EQ.0) GO TO 52
      DO 51 J=1,ICR
      YK(I)=YK(I)+0.03636/(1.1**(J-1))
51    CONTINUE
52    CONTINUE
      DO 53 I=1,KOO
      XK(I)=(XK(I)*SCAL1)*SCAL3
53    CONTINUE
      DX1=(DX1*SCAL1)*SCAL3
      DX2=(DX2*SCAL1)*SCAL3
      DX3=(DX3*SCAL1)*SCAL3
      XC=(XC*SCAL1)*SCAL3
      YC=(YC*SCAL1-YDIF)*SCAL3
      PITCH=(PITCH*SCAL1)*SCAL3
      YPRM=(YPRM*SCAL1-YDIF)*SCAL3
      ERROR1=(ERROR1*SCAL1)*SCAL3
      ERROR2=(ERROR2*SCAL1)*SCAL3
      ERROR3=(ERROR3*SCAL1)*SCAL3
      TER1=(TER1*SCAL1)*SCAL3
      TER2=(TER2*SCAL1)*SCAL3
      TER3=(TER3*SCAL1)*SCAL3
      IF (ICR.EQ.0) GO TO 55
      DO 54 J=1,ICR
      YC=YC+.03636/(1.1**(J-1))
      YPRM=YPRM+0.03636/(1.1**(J-1))
54    CONTINUE
55    YCC=YC+PITCH
      BZ(1)=YCC-TAN(ANG1)*XC
      BZ(2)=TAN(ANG1)
      WRITE (6,56) SCAL1,YDIF,SCAL3,YDIF,ICR
56    FORMAT (1X,*SCAL1=*,F10.4,* YDIF=*,F10.4,*SCAL3=*,F10.4,* YDIF=*,I
```

```
      10.4,*ICR=*,I5,/)
      WRITE (6,57)
57    FORMAT (1X,*SCALED VALUES,*///)
      WRITE (6,58)
58    FORMAT (1X,*ORTHOGONAL START POINT X-VALUES*,/)
      WRITE (6,59) (X(P,1,2),P=1,NUMD)
59    FORMAT (1X,F10.4///)
      WRITE (6,60)
60    FORMAT (1X,*SUCTION SURFACE VALUES*,//)
      WRITE (6,61) (XSUC(I),YSUC(I),W1(I),I=1,NS)
61    FORMAT (1X,3F10.4,/)
      WRITE (6,62)
62    FORMAT (1X,*PRESSURE SURFACE VALUES*,//)
      WRITE (6,63) (XPR(I),YPR(I),I=1,NP)
63    FORMAT (1X,2F10.4,/)
      WRITE (6,64)
64    FORMAT (1X,*SCALED SUCTION SURFACE LEADING EDGE VALUES*,//)
      WRITE (6,65) (XLS(I),YLS(I),I=1,NUMS)
65    FORMAT (1X,2F10.4)
      WRITE (6,66)
66    FORMAT (1X,*SCALED PRESSURE SURFACE LEADING EDGE VALUES*,//)
      WRITE (6,67) (XLP(I),YLP(I),I=1,NUMP)
67    FORMAT (1X,2F10.4)
      WRITE (6,68) PITCH,XC,YC,YPRM
68    FORMAT (1X,*PITCH=*,F10.4,* XC=*,F10.4,* YC=*,F10.4,*YPRM=*,F10.4)
      WRITE (6,69) DX1,DX2,DX3
69    FORMAT (1X,*DX1=*,F10.4,* DX2=*,F10.4,* DX3=*,F10.4)
      WRITE (6,70) ERROR1,TER1,ERROR2,TER2,ERROR3,TER3
70    FORMAT (1X,*ERROR1=*,F10.4,* TER1=*,F10.4,* ERROR2=*,F10.4,* TER2=
     1*,F10.4,* ERROR3=*,F10.4,* TER3=*,F10.4)
      LJL=1
      ND=1
      NE=ND+NUS
      NF=(ND+NE)/2
      LJ=1
      LH=1
      LHI=1
      NON=3
      CALL MARG (ZK)
      CALL NEWPEN (3)
      CALL ARROW (7.9,5.0,6.5,6.12,3)
      CALL ARROW (14.78,2.36,15.4,.96,3)
      CALL ARROW (4.0,1.1,4.65,2.13,3)
      CALL LETTER (10,.15,65.,4.4,0.9,10HFLOW INLET)
      CALL LETTER (9,.15,295.,14.62,2.16,9HDISCHARGE)
      CALL LETTER (12,.25,0.,9.0,1.1,12HFLOW PASSAGE)
      CALL LETTER (21,.15,0.,8.0,4.84,21HQUASI-ORTHOGONAL GRID)
      CALL LETTER (16,.15,0.,8.4,8.46,16HPRESSURE SURFACE)
      CALL LETTER (15,.15,0.,8.38,3.00,15HSUCTION SURFACE)
      CALL LETTER (12,.15,0.,1.0,6.8,12HLEADING EDGE)
      CALL LETTER (21,.15,0.,.6,6.55,21HSTAGNATION STREAMLINE)
      XMIN=XSUC(1)
      XMAX=XSUC(NS)
C
C     NOW WE PLOT A POLY FOR THE SUCTION SURFACE.
C
C     WE FIT THE LOWEST ORDER POLY THAT IS ACCEPTABLE FOR THE SUCTION SU
      IF (IS.EQ.1) GO TO 71
      CALL CFIT (NS,XSUC,YSUC,NS,LH,LHI,ND)
      GO TO 75
71    DO 72 I=1,NS
      W(I)=W1(I)
72    CONTINUE
C
C     READ IN THE DESIRED POLY ORDER FOR THE SUCTION SURFACE.
C
      READ (5,73) MS
73    FORMAT (I5)
      CALL ORLSQ (XSUC,YSUC,W,NS,MS,WK,SIGSQ,BA,IERR)
      MMS=MS+1
      DO 74 I=1,MMS
      B(I)=BA(MMS-I+1)
74    CONTINUE
C
```

```
C     STORE THE SELECTED POLY ORDER.
75    IF (NIS.GT.9) GO TO 76
      CALL ADD (XSUC,YSUC,NIS,XMIN,NIS,XMAX,LHI,LH)
      GO TO 77
76    CALL ADD (XSUC,YSUC,NIS,XMIN,NC1,XMAX,LHI,LH)
77    NK(1)=NIS
      NNS=NIS+1
      DO 78 I=1,NNS
      BS(I)=B(I)
78    CONTINUE
      DO 79 I=1,NUM
      XX(I)=X(I,1,2)
79    CONTINUE
C
C     FIND THE CURVATURE AT THE GO START POINT.
      CALL CURV (XX,BS,NIS,ND,XPS,NL,LHI,LH)
      WRITE (6,80)
80    FORMAT (1X,*AA(ND,L) COEFFICIENTS*///)
C
C     STORE THE POLY COEFICIENTS.
      DO 82 L=1,NNS
      AA(ND,L)=BS(L)
      WRITE (6,81) AA(ND,L)
81    FORMAT (1X,E13.6,/)
82    CONTINUE
      DO 83 I=1,NIP
      GX(I)=XPR(I+NFP)
      GY(I)=YPR(I+NFP)+PITCH
83    CONTINUE
      XPS=GX(1)
      XMIN=GX(1)
      XMAX=GX(NIP)
C
C     DRAW A POLY FOR THE PRESSURE SURFACE.
C
C     FIND THE BEST POLY FIT TO THE PRESSURE SURFACE.
      IF (IT.EQ.1) GO TO 84
      CALL CFIT (NIP,GX,GY,NIP,LH,LHI,NE)
      GO TO 88
84    READ (5,85) NIP
85    FORMAT (I5)
      DO 86 I=1,NIP
      W(I)=W1(I)
86    CONTINUE
      CALL ORLSQ (XPR,YPR,W,NIP,NIP,WX,SIGSQ,BA,IERR)
      NMP=NIP+1
      DO 87 I=1,NMP
      B(I)=BA(NMP-I+1)
87    CONTINUE
C
C     STORE THE SELECTED POLY ORDER.
88    IF (NIP.GT.9) GO TO 89
      CALL ADD (GX,GY,NIP,XMIN,NIP,XMAX,LHI,LH)
      GO TO 90
89    CALL ADD (GX,GY,NIP,XMIN,NC1,XMAX,LHI,LH)
90    NK(NUS+1)=NIP
      NMP=NIP+1
      WRITE (6,91)
91    FORMAT (1X,*BB(NE,L) COEFFICIENTS*,/)
C
C     STORE THE POLY COEFICIENTS.
      DO 93 L=1,NMP
      BP(L)=B(L)
      BB(NE,L)=BP(L)
      WRITE (6,92) BB(NE,L)
92    FORMAT (1X,E13.6,/)
93    CONTINUE
      RMAX=1.
      RRMAX=1.
      WRITE (6,94) NK(1),NK(NUS+1)
94    FORMAT (1X,*NK(1)=*,I5,1X,*NK(NUS+1)=*,I5,/)
C
C     FIRST WE DO THE MAIN BLADE RANGE ANALYSIS.
      CALL MAIN (NK,LH,NNS,XPS,LJ,XC,YCC,LJL,BP,NO,NI,NON,NOT,LHI,LH,RMA
```

```
     1X,RRMAX,XSUC,NS,PITCH)
      LJL=0
      CALL PLOT (20.,0.01,-3)
      LHI=0
      NUM=KO
      ND=1
      NE=ND+NUS
      NF=(ND+NE)/2
C
C     NEXT WE DO THE SUCTION SURFACE LEADING EDGE ANALYSIS.
      CALL LEADS (XC,YC,ANGI,ZKK,NUS,KO,XLS,YLS,NOT,NIP,KO,NI,NON,XPS,L
     1J,LJL,BP,ND,NE,NF,LHI,LH,PITCH,YK,XSUC,NIS,NS)
      CALL PLOT (20.,0.01,-3)
      NUM=K00
      LHI=0
      LJL=0
      LH=0
      XPS=1.
      ND=1
      NE=ND+NUS
      NF=(ND+NE)/2
C
C     FINALLY WE DO THE PRESSURE SURFACE LEADING EDGE ANALYSIS.
      CALL LEAD2 (NUMP,K00,ZKZ,XLP,YLP,NE,XSUC,YSUC,XPS,LJ,XC,YC,LJL,BP,
     1NO,NI,NON,NOT,LHI,LH,XK,PITCH,YPRI,NIS,NIS,NS)
      CALL PLOT (20.,0.01,-3)
      CALL PLOT (20.,0.01,999)
      STOP
      END
```

```
      SUBROUTINE MAIN (NK,LN,NMS,XPS,LJ,XC,YCC,LJL,BP,NO,NI,NON,NOT,LHI,
C     ===================================================================
     1LH,RMAX,RRMAX,XSUC,NS,PITCH)
      DIMENSION REX(20), REY(20), NK(20), BS(20), XSUC(40)
      DIMENSION XEX(20), YEX(20), XX(40), TEX(20), DD(40), BP(20)
      COMMON XE(40,20),YE(40,20),YP(20),X(40,20,3),Y(40,20,3),C(50,50),A
     1A(20,20),BB(20,20),B(20),NM,NI,ND,NE,BZ(2),NUS,NUM,BMIN,BMAX,TMIN,
     2TMAX,NC1,NC2,NC3,W1(40),W2(40),W3(40),ERROR1,ERROR2,ERROR3,TER1,TE
     3R2,TER3,CIS1,CIS2,CIS3,DX1,DX2,DX3,SCAL1,YDIF,ICR,SCAL2
      INTEGER P
      IN=0
      II=1
C
C     FIRST DIVIDE THE PASSAGE IN TWO PARTS.
      CALL LOOP (NK,LN,IN,II,NMS,XPS,LJ,XC,YCC,LJL,NO,NI,NON,NOT,LHI,LH,
     1RMAX,RRMAX,XSUC,NS,PITCH)
      NUS1=(NUS)**0.5-1
C
C     NOW DIVIDE THE PASSAGE INTO THE SPECIFIED NUMBER OF PARTS.
      DO 1 IN=1,NUS1
      CALL LOOP (NK,LN,IN,II,NMS,XPS,LJ,XC,YCC,LJL,NO,NI,NON,NOT,LHI,LH,
     1RMAX,RRMAX,XSUC,NS,PITCH)
 1    CONTINUE
      ND=1
      NE=ND+NUS
      DO 2 I=1,NUM
      XX(I)=X(I,NE,2)
 2    CONTINUE
      NP=NK(5)
      IF (LH.EQ.0) GO TO 3
C
C     CALCULATE THE CURVATURE AT THE FINAL PRESSURE SURFACE QO POINT.
      CALL CURV (XX,BP,NP,NE,XPS,NI,LHI,LH)
      GO TO 5
 3    NS=NK(5)
      NSN=NS+1
      DO 4 KIK=1,NSN
      BS(KIK)=BB(5,KIK)
 4    CONTINUE
      CALL CURV (XX,BS,NS,ND,XPS,NI,LHI,LH)
 5    NNU=NUS-1
      NUN=NNU-1
      IF (LH.EQ.0) GO TO 6
      IF (LHI.EQ.0) GO TO 26
      GO TO 8
 6    WRITE (6,7)
 7    FORMAT (1H1,1X,*PRESSURE SURFACE LEADING EDGE RESULTS*)
      WRITE (6,10)
      GO TO 11
 8    WRITE (6,9)
 9    FORMAT (1H1,1X,*MAIN BLADE RANGE RESULTS*,/)
      WRITE (6,10)
 10   FORMAT (1X,*++++++++++++++++++++++++++++++++++++++++++++++++++++*,/
     1)
 11   WRITE (6,12)
 12   FORMAT (4X,*QO NO.*,3X,*START PT X*,3X,*START PT Y*,3X,*START PT C
     1*,3X,*END PT X*,3X,*END PT Y*,3X,*END PT C*,7X,*LENGTH*,//)
      DO 25 P=1,NUM
C
C     XEX AND YEX ARE THE POINTS ON THE QO.
      XEX(1)=X(P,1,2)
      YEX(1)=Y(P,1,2)
      DO 13 III=2,NNU
      XEX(III)=XE(P,III)
      YEX(III)=YE(P,III)
 13   CONTINUE
      IF (LH.EQ.0) GO TO 15
      AY=ABS(YP(1))
      AYY=ABS(YP(NE))
C
C     FOR SLOPES NEAR 0 JUST DRAW A STRAIGHT LINE ACROSS THE PASSAGE.
C     NOTE THAT THIS IS JUST FOR THE PLOT AND A POLY IS FIT TO DETERMINE
C      LENGTH LATER ON.
      IF (AY.LT.0.1.OR.AYY.LT.0.1) GO TO 20
```

```
      IF (YP(I).GT.0.) GO TO 14
      XMIN=XEX(1)
      XMAX=XEX(NNU)
      GO TO 16
   14 XMIN=XEX(NNU)
      XMAX=XEX(1)
      GO TO 16
C
C     XMIN AND XMAX ARE CALCULATED IN CASE IT IS DESIRED TO PLOT A POLY
C     FOR THE PRESSURE SURFACE L.E. ORTHOGONALS
   15 XMAX=RMAX-XEX(NNU)+0.5
      XMIN=RMAX-XEX(1)+0.5
      GO TO 17
C
C     PLOT QO.S.
   16 CALL ADD (XEX,YEX,NNU,XMIN,NUN,XMAX,LHI,LHD)
      GO TO 23
C
C     ROTATE THE CALCULATED VALUES BACK TO THE ORIGINAL ORIENTATION.
   17 DO 18 K=1,NNU
      REX(K)=RMAX-XEX(K)+0.5
      REY(K)=RMAX-YEX(K)
   18 CONTINUE
      DO 19 K=1,NUN
      CALL PLTLN (REX(K),REY(K),REX(K+1),REY(K+1))
   19 CONTINUE
      GO TO 23
   20 DO 21 I=1,NNU
      TEX(I)=XEX(I)+0.9
   21 CONTINUE
      DO 22 I=1,NUN
      CALL PLTLN (TEX(I),YEX(I),TEX(I+1),YEX(I+1))
   22 CONTINUE
   23 YMAX=YEX(NNU)
      YMIN=YEX(1)
C
C     CALCULATE THE QO LENGTHS.
      CALL LENGTH (YMIN,YMAX,NUN,XEX,YEX,DIS,NI)
      DD(P)=DIS
      IF (LH.EQ.0) GO TO 25
      CALL SCALE (P,NE,DD)
      WRITE (6,24) P,X(P,1,2),Y(P,1,2),C(1,P),X(P,NE,2),Y(P,NE,2),C(NE,P
     1),DD(P)
   24 FORMAT (4X,I5,3X,F10.4,2X,F10.4,2X,F10.4,2X,F10.4,2X,F10.4,2X,F10.
     14,2X,F10.4,/)
   25 CONTINUE
      IF (LH.EQ.0) GO TO 34
      GO TO 37
   26 WRITE (6,27)
   27 FORMAT (1H1,1X,*SUCTION SURFACE LEADING EDGE RESULTS*,/)
      WRITE (6,10)
      WRITE (6,28)
   28 FORMAT (5X,*QO NO.*,3X,*START PT Y*,3X,*START PT X*,3X,*START P C*
     1,3X,*END PT Y*,3X,*END PT X*,3X,*END PT C*,3X,*LENGTH*,//)
C
C     ROTATE THE CALCULATED VALUES BACK TO THE ORIGINAL ORIENTATION.
      DO 31 P=1,NUM
      XEX(1)=RMAX-Y(P,1,2)
      YEX(1)=X(P,1,2)
      DO 29 III=2,NNU
      XEX(III)=RMAX-YE(P,III)
      YEX(III)=XE(P,III)
   29 CONTINUE
      XMIN=XEX(NNU)
      XMAX=XEX(1)
C
C     SINCE THE ORTHOGONALS EASILY DESCRIBES A FUNCTION , WE DON,T HAVE
C      TWIST THEM TO GET THEIR LENGTHS HERE.
      CALL LENGTH (XMIN,XMAX,NUN,YEX,XEX,DIS,NI)
      DD(P)=DIS
      CALL ADD (XEX,YEX,NNU,XMIN,NUN,XMAX,LHI,LHD)
      YI=X(P,1,2)
      YLI=X(P,NE,2)
      X(P,1,2)=RMAX-Y(P,1,2)
```

```
      X(P,NE,2)=RMAX-Y(P,NE,2)
      Y(P,1,2)=YJ
      Y(P,NE,2)=YJJ
C
C     WRITE THE RELEVANT INFORMATION.
      CALL SCALE (P,NE,DD)
      WRITE (6,30) P,Y(P,1,2),X(P,1,2),C(1,P),Y(P,NE,2),X(P,NE,2),C(NE,P
     1),DD(P)
30    FORMAT (4X,I5,3X,F10.4,2X,F10.4,2X,F10.4,2X,F10.4,2X,F10.4,2X,F10.
     14,2X,F10.4,/)
31    CONTINUE
      DO 33 P=1,NUM
      WRITE (7,32) C(NE,P),C(1,P),DD(P),Y(P,1,2),Y(P,NE,2)
32    FORMAT (5F10.4)
33    CONTINUE
      GO TO 40
34    DO 36 P=1,NUM
      X(P,1,2)=RMAX-X(P,1,2)
      X(P,NE,2)=RMAX-X(P,NE,2)
      Y(P,1,2)=RRMAX-Y(P,1,2)
      Y(P,NE,2)=RRMAX-Y(P,NE,2)
      CALL SCALE (P,NE,DD)
      WRITE (6,35) P,X(P,NE,2),Y(P,NE,2),C(1,P),X(P,1,2),Y(P,1,2),C(NE,P
     1),DD(P)
35    FORMAT (4X,I5,3X,F10.4,2X,F10.4,2X,F10.4,2X,F10.4,2X,F10.4,2X,F10.
     14,2X,F10.4,/)
36    CONTINUE
C
C     PUNCH OUT THE INFORMATION REQUIRED FOR INPUT TO THE STREAMLINE CUR
C      ATURE PROGRAM.
37    DO 39 P=1,NUM
      WRITE (7,38) C(NE,P),C(1,P),DD(P),X(P,1,2),X(P,NE,2)
38    FORMAT (5F10.4)
39    CONTINUE
40    RETURN
      END
```

```
      SUBROUTINE LOOP (NK,LN,IN,II,NNS,XPS,LJ,XC,YCC,LJL,NO,NI,NON,NOT,L
C     ------------------------------------------------------------------
     1HI,LH,RMAX,RRMAX,XSUC,NS,PITCH)
      DIMENSION XFI(40), YFI(40), NK(20), GYY(40), XSUC(40)
      DIMENSION XF(40,20), YF(40,20), XFF(40), YFF(40)
      COMMON XE(40,20),YE(40,20),YP(20),X(40,20,3),Y(40,20,3),C(50,50),A
     1A(20,20),BB(20,20),B(20),NI,NI,N0,N2,BX(2),NUS,NUM,BMIN,BMAX,THIN,
     2THAX,NC1,NC2,NC3,W1(40),W2(40),W3(40),ERROR1,ERROR2,ERROR3,TER1,TE
     3R2,TER3,CIS1,CIS2,CIS3,DX1,DX2,DX3,SCAL1,YDIF,ICR,SCAL3
      INTEGER PP
      INTEGER P,D,E,F
C
C     SET UP THE PASSAGE COUNTER.
1     INTER=NUS/(2**IN)
      J=1+(INTER)*((2**IN)-1)
      DO 31 ND=1,J,INTER
      NE=ND+INTER
      NF=(NE+ND)/2
      NS=NK(ND)
      NP=NK(NE)
      WRITE (6,2) NE,NF,ND
2     FORMAT (1X,*NE= *,I3,* NF= *,I3,* ND=*,I3,///)
      WRITE (6,3) NS,NP
3     FORMAT (1X,*NS=*,I5,1X,*NP=*,I5,/)
C
C     CALL THE MAIN CENTER POINT LOCATOR SUBROUTINE.
      DO 5 P=1,NUM
      CALL QUASI (NS,NP,P,ND,NE,NF,LN,NNS,XPS,LJ,XC,YCC,LJL,NO,NI,NON,NO
     1T,LHI,LH,XSUC,NS,PITCH)
C
C     STORE LOCATION OF ORTHOGONAL END POINTS AND MID STREAMLINE POINTS
C
      D=ND
      E=NE
      F=NF
      IF (IN.NE.0) GO TO 4
      XXR=(ABS(XSUC(NS)-XSUC(1)))*1.067
      IF (X(P,NE,2).LT.XXR) GO TO 4
      IP=P-1
      GO TO 6
C
C     STORE THE END POINTS(ON THE PRESSURE SURFACE).
4     XE(P,II)=X(P,NE,2)
      YE(P,II)=Y(P,NE,2)
C
C     STORE THE MID-STREAMLINE POINTS.
      XF(P,II)=X(P,NF,2)
      YF(P,II)=Y(P,NF,2)
5     CONTINUE
      GO TO 7
6     NUM=IP
7     DO 9 P=1,NUM
      XFF(P)=XF(P,II)
      YFF(P)=YF(P,II)
      WRITE (6,8) XFF(P),YFF(P)
8     FORMAT (1X,*XFF(P)= *,F10.4,6X,*YFF(P)=*,F10.4,/)
9     CONTINUE
C
C     SELECT THE ORDER FOR THE STREAMLINE POLY REPRESENTATIONS.
      IF (LHI.NE.0) GO TO 11
      IF (IH.NE.0) GO TO 10
      NC=NC3
      GO TO 12
10    NC=NC2
      GO TO 12
11    NC=NC1
12    IF (LH.LQ.0) GO TO 14
      IF (LHI.LQ.0) GO TO 17
      DO 13 P=1,NUM
      XFI(P)=XFF(P)
      YFI(P)=YFF(P)
13    CONTINUE
      XMIN=XFF(1)
      XMAX=XFF(NUM)
```

```
      GO TO 21
14    XMIN=RMAX-XFF(1)
      XMAX=RMAX-YFF(NUM)
      DO 16 P=1,NUM
      XFI(P)=RMAX-XFF(P)
      YFI(P)=RMAX-YFF(P)
      WRITE (6,15) XFI(P),YFI(P)
15    FORMAT (1X,F10.4,2X,F10.4,/)
16    CONTINUE
      GO TO 21
17    DO 19 P=1,NUM
      XFI(P)=(RMAX-YFF(P))+0.9
      YFI(P)=XFF(P)+0.27
      WRITE (6,18) XFI(P),YFI(P)
18    FORMAT (1X,F10.4,2X,F10.4,/)
19    CONTINUE
      PP=NUM-1
C     THE STREAMLINES ARE NOT DRAWN BY A CURVE HERE AS THEY ARE NOT NECE
C      ARILY REPRESENTABLE BY A'FUNCTION.
C
      DO 20 P=1,PP
      CALL PLTLN (XFI(P),YFI(P),XFI(P+1),YFI(P+1))
20    CONTINUE
21    NN=NUM
C
C     FIT A CURVE TO THE MID-STREAMLINE POINTS.
      CALL CFIT (NN,XFF,YFF,NO,LN,LNN,NF)
      IF (LN.EQ.0) GO TO 22
      IF (LNN.EQ.0) GO TO 24
22    IF (NO.GT.9) GO TO 23
C
C     DRAW A POLY FOR THE MIDSTREAMLINES ON THE PLOT.
      CALL ADD (XFI,YFI,NUM,XMIN,NO,XMAX,LNN,LND)
      GO TO 24
23    CALL ADD (XFI,YFI,NUM,XMIN,NC,XMAX,LNN,LND)
C
C     STORE THE MID-STREAMLINE ORDER.
24    NK(NF)=NO
      N1=NO-1
      N2=NO-2
      NN=NO+1
      DO 26 KI=1,NUM
      GYY(KI)=YY(XFF(KI))
      WRITE (6,25) XFF(KI),GYY(KI)
25    FORMAT (1X,*GX(I)=*,F10.4,*GYY(I)=*,F10.4,*IN LOOP*,/)
26    CONTINUE
C
C     STORE THE MID-STREAMLINE POLY COEFFICIENTS.
      WRITE (6,27)
27    FORMAT (1X,*BB(NF,L) COEFFICIENTS*,/)
      DO 29 L=1,NN
      BB(NF,L)=B(L)
      WRITE (6,28) BB(NF,L)
28    FORMAT (1X,*BB(NF,L)= *,E13.6,/)
29    CONTINUE
      II=II+1
      IF (ND.EQ.J) GO TO 32
      NMS=NK(ND)+1
C
C     EXCHANGE POLY COEFFICIENTS.
      DO 30 L=1,NMS
      AA(NF,L)=BB(NS,L)
30    CONTINUE
31    CONTINUE
32    RETURN
      END
```

```
      SUBROUTINE QUASI (NS,NP,P,ND,NE,NF,LN,NMS,XPS,LJ,XC,YCC,LJL,NO,NI,
C     ===================================================================
     1NON,NOT,LNI,LH,XSUC,NS,PITCH)
      DIMENSION THETA(20), ALFA(20), M(20), DI(20), Z(40,20,3), R(20), R
     1R(20), A(242), XSUC(40)
      COMMON XE(40,20),YE(40,20),YP(20),X(40,20,3),Y(40,20,3),C(50,50),A
     1A(20,20),BB(20,20),B(20),NN,N1,NO,N2,BZ(2),NUS,NUM,BMIN,BMAX,TMIN,
     2TMAX,NC1,NC2,NC3,V1(40),V2(40),V3(40),ERROR1,ERROR2,ERROR3,TER1,TE
     3R2,TER3,CIS1,CIS2,CIS3,DX1,DX2,DX3,SCAL1,YDIF,ICR,SCAL3
      REAL M
      INTEGER P
      INTEGER D,E,F
      JJ=0
      KK=0
      JJJ=0
      KKK=0
      Q=1.
      Q2=1.
      TX=X(P,ND,2)
C
C     Y VALUE AT START POINT
      NMS=NS+1
      NO=NS
      N1=NO-1
      N2=NO-2
      NN=NO+1
      DO 1 L=1,NMS
      B(L)=AA(ND,L)
1     CONTINUE
C
      Y(P,ND,2)=Y1(TX)
C
C     SLOPE AT START POINT
C
      YP(ND)=DY1(TX)
C
C     ANGLE OF CURVE AT START POINT
C
      THETA(ND)=ATAN(YP(ND))
C
C     ANGLE OF PERPENDICULAR AT START POINT
C
      ALFA(ND)=3.14159/2.-ABS(THETA(ND))
      IF (YP(ND).GT.0.) GO TO 2
      GO TO 3
2     ALFA(ND)=-ALFA(ND)
C
C     SLOPE OF PERPENDICULAR AT START POINT
C
3     M(ND)=TAN(ALFA(ND))
      DO 99 I=1,LN
      NO=NP
      N1=NO-1
      N2=NO-2
      NN=NO+1
      NMP=NP+1
      DO 4 L=1,NMP
      B(L) BB(NE,L)
4     CONTINUE
      IF (I.NE.1) GO TO 5
      X(P,NE,2)-X(P,ND,2)
5     TX=X(P,NE,2)
      IF (NE.NE.5) GO TO 10
      IF (JHI.NE.1) GO TO 10
      IF (X(P,NE,2).GT.XPS) GO TO 10
      YPS Y1(XPS)
      B(1)-YPS-DY1(XPS)*XPS
      B(2) DY1(XPS)
      XI=(BZ(1)-B(1))/(B(2)-BZ(2))
      DO 6 K=3,NMP
      B(K)=0.
6     CONTINUE
C
C     IF LJ EQ 1,THE SEGMENT BETWEEN XI AND XPS HAS NOT BEEN DRAWN YET.
```

```
      IF (LJ.NE.1) GO TO 7
      YI=Y1(XI)
      TTX=XI+0.9
      XPSS=XPS+0.9
      CALL PLTLN (TTX,YI,XPSS,YPS)
C
C     Y VALUE AT GUESSED PRESSURE POINT
C
      LJ=0
7     IF (X(P,NE,2).LT.XI) GO TO 8
      GO TO 10
8     B(1)=BZ(1)
      B(2)=BZ(2)
      DO 9 K=3,NNP
      B(K)=0.
9     CONTINUE
C
C     IF LJL =1. THE SEGMENT FROM XC AT ANGI HAS NOT BEEN DRAWN YET.
      IF (LJL.NE.1) GO TO 10
      ZTX=-.21*(XSUC(NS)-XSUC(1))/1.05
      ZY=Y1(ZTX)
      TTX=ZTX+0.9
      XPCC=XC+0.9
      CALL PLTLN (TTX,ZY,XPCC,YCC)
      LJL=0
10    Y(P,NE,2)=Y1(TX)
C
C     SLOPE VALUE AT GUESSED PRESSURE SURFACE POINT
C
      YP(NE)=DY1(TX)
      THETA(NE)=ATAN(YP(NE))
      ALFA(NE)=3.14159/2.-ABS(THETA(NE))
      IF (YP(NE).GT.0.) GO TO 11
      GO TO 12
11    ALFA(NE)=-ALFA(NE)
12    M(NE)=TAN(ALFA(NE))
C
C     NOW INTERSECTION POINT IS CALCULATED
C
      X(P,NF,2)=(Y(P,ND,2)-Y(P,NE,2)-M(ND)*X(P,ND,2)+M(NE)*X(P,NE,2))/(M
     1(NE)-M(ND))
      Y(P,NF,2)=Y(P,ND,2)+M(ND)*(X(P,NF,2)-X(P,ND,2))
C
C     NOW THE LENGTHS OF THE LINES TO THE INTERSECTION POINTS ARE CAL-
C     CULATED
      DI(ND)=SQRT((X(P,ND,2)-X(P,NF,2))**2.+(Y(P,ND,2)-Y(P,NF,2))**2.)
      DI(NE)=SQRT((X(P,NE,2)-X(P,NF,2))**2.+(Y(P,NE,2)-Y(P,NF,2))**2.)
C
C     Z IS THE ERROR FUNCTION
C
      Z(P,ND,2)=(DI(ND)-DI(NE))/(DI(NE))
      ZZ=ABS(Z(P,ND,2))
      IF (DI(NE).GT.PITCH.OR.DI(ND).GT.PITCH) GO TO 14
      IF (ZZ.GT.0.001) GO TO 14
      IF (I.NE.1) GO TO 13
      IF (X(P,NF,2).GT.1.5.OR.X(P,NF,2).LT.-1.) GO TO 14
      GO TO 40
13    IF (X(P,NF,1).GT.1.5.OR.X(P,NF,1).LT.-1..AND.X(P,NF,2).GT.1.5.OR.X
     1(P,NF,2).LT.-1.) GO TO 14
      CALL TTST (W,WW,T,TT,V,VV,NF,P,NS,N9)
      IF (W.GT.T.OR.W.LT.V.AND.WW.GT.TT.OR.WW.LT.VV) GO TO 14
      GO TO 40
14    IF (I.EQ.LN) GO TO 40
C
C     TEST FOR SIGN OF SLOPE AT ORIGINAL POINT
C
      PYP=YP(ND)
      IF (PYP.LE.0.) GO TO 26
      IF (I.EQ.1) GO TO 17
C
C     PRODUCT OF THIS AND LAST ERROR FUNCTION
C
      R(ND)=Z(P,ND,2)*Z(P,ND,1)
      IF (X(P,NF,1).GT.1.5.OR.X(P,NF,1).LT.-1..AND.X(P,NF,2).GT.1.5.OR.X
```

```
     1(P,NF,2).LT.-1.) GO TO 15
C
C     IF R IS LESS THAT 0 WE HAVE STRADDLED THE DESIRED POINT
C
      IF (R(ND).GT.0.) GO TO 16
      CALL TEST (W,WW,T,TT,V,VV,NF,P,NS,ND)
      IF (W.GT.T.OR.W.LT.V.AND.WW.GT.TT.OR.WW.LT.VV) GO TO 15
      LL=1
      GO TO 23
C
C     TEST TO SEE WHICH SIDE OF THE DESIRED POINT WE ARE ON
C
15    L=1
16    MI=(Y(P,NE,1)-Y(P,NE,2))/(X(P,NE,1)-X(P,NE,2))
      XI=(Y(P,NE,2)-Y(P,ND,2)+M(ND)*X(P,ND,2)-MI*X(P,NE,2))/(M(ND)-MI)
      IF (XI.GT.X(P,NE,2).AND.XI.LT.X(P,NE,1).OR.XI.GT.X(P,NE,1).AND.XI.
     1LT.X(P,NE,2)) GO TO 23
17    IF (Z(P,ND,2).LT.0.) GO TO 19
      IF (YP(NE).GT.YP(ND)) GO TO 20
C
C     AS THE SLOPE IS +VE AND Z IS STILL +VE,WE INCREASE XPRE SO THAT Z
C     WILL DECREASE FURTHER
C
18    X(P,NE,3)=X(P,NE,2)+0.01/Q
      L=0
      LL=0
      K=0
      GO TO 38
C
C     SINCE BOTH Z,S ARE -VE WITH +VE ORIGINAL SLOPE PUSH TO LEFT
C
19    IF (YP(NE).GT.YP(ND)) GO TO 22
20    IF (JJ.NE.1.AND.KK.NE.0) GO TO 21
      IF (JJ.EQ.0.AND.KK.EQ.0) GO TO 21
      Q=Q*10.
21    X(P,NE,3)=X(P,NE,2)-0.01/Q
      L=0
      LL=0
      K=0
      JJ=0
      KK=1
      GO TO 38
22    IF (JJ.EQ.1) GO TO 18
      Q=Q*10.
      JJ=1
      KK=0
      GO TO 18
23    IF (L.EQ.1) GO TO 24
      IF (LL.EQ.1) GO TO 24
      GO TO 17
24    IF (K.EQ.1) GO TO 25
      Q=Q*10.
C
C     WE,VE STRADDLED THE DESIRED POINT THUS TAKE THE AVERAGE OF THE LAS
C     T TWO POINTS
25    X(P,NE,3)=(X(P,NE,2)+X(P,NE,1))/2.
      K=1
      KK=0
      JJ=0
      L=0
      LL=0
      GO TO 38
C
C     THIS PART IS FOR -VE ORIGINAL SLOPE
C
26    IF (L.EQ.1) GO TO 29
      IF (X(P,NF,1).GT.1.5.OR.X(P,NF,1).LT.-1..AND.X(P,NF,2).GT.1.5.OR.X
     1(P,NF,2).LT.-1.) GO TO 27
      RR(ND)=Z(P,ND,2)-Z(P,ND,1)
      IF (RR(ND).GT.0.) GO TO 28
      CALL TEST (W,WW,T,TT,V,VV,NF,P,NS,ND)
      IF (W.GT.T.OR.W.LT.V.AND.WW.GT.TT.OR.WW.LT.VV) GO TO 27
      LLX=1
      GO TO 35
```

```
27    LX=1
28    MI=(Y(P,NE,1)-Y(P,NE,2))/(X(P,NE,1)-X(P,NE,2))
      XI=(Y(P,NE,2)-Y(P,ND,2)+M(ND)*X(P,ND,2)-MI*X(P,NE,2))/(M(ND)-MI)
      IF (XI.GT.X(P,NE,2).AND.XI.LT.X(P,NE,1).OR.XI.GT.X(P,NE,1).AND.XI.
     1LT.X(P,NE,2)) GO TO 35
29    IF (Z(P,ND,2).LT.0.) GO TO 31
      IF (YP(NE).LT.YP(ND)) GO TO 32
30    X(P,NE,3)=X(P,NE,2)-0.01/QQ
      LX=0
      LLX=0
      K=0
      GO TO 38
31    IF (YP(NE).LT.YP(ND)) GO TO 34
32    IF (JJJ.NE.1.AND.KKK.NE.0) GO TO 33
      IF (JJJ.EQ.0.AND.KKK.EQ.0) GO TO 33
      QQ=QQ*10.
33    X(P,NE,3)=X(P,NE,2)+0.01/QQ
      JJJ=0
      KKK=1
      LX=0
      LLX=0
      K=0
      GO TO 38
34    IF (JJJ.EQ.1) GO TO 30
      QQ=QQ*10.
      JJJ=1
      KKK=0
      GO TO 30
35    IF (LX.EQ.1) GO TO 36
      IF (LLX.EQ.1) GO TO 36
      GO TO 29
36    IF (K.EQ.1) GO TO 37
      QQ=QQ*10.
37    X(P,NE,3)=(X(P,NE,2)+X(P,NE,1))/2.
      K=1
      KKK=0
      JJJ=0
      LX=0
      LLX=0
C     STACK TO KEEP LAST AND PRESENT AND FUTURE GUESSES
38    X(P,NE,1)=X(P,NE,2)
      X(P,NE,2)=X(P,NE,3)
      X(P,NF,1)=X(P,NF,2)
      Z(P,ND,1)=Z(P,ND,2)
      Y(P,NF,1)=Y(P,NF,2)
      Y(P,NE,1)=Y(P,NE,2)
39    CONTINUE
40    RETURN
      END
```

```
      SUBROUTINE BLADE (XPR,YPR,XSUC,YSUC,NOF,NP,NS)
C     ==========================================
      DIMENSION GX(40), GY(40), XPR(NOF), YPR(NOF), YSUC(NOF), XSUC(NOF)
      DIMENSION GYY(40)
      COMMON XE(40,20),YE(40,20),YP(20),X(40,20,3),Y(40,20,3),C(50,50),A
     1A(20,20),BB(20,20),B(20),NEI,NI,NO,N2,BZ(2),NUS,NUM,BMIN,BMAX,TMIN,
     2TMAX,NC1,NC2,NC3,W1(40),W2(40),W3(40),ERROR1,ERROR2,ERROR3,TER1,TE
     3R2,TER3,CIS1,CIS2,CIS3,DX1,DX2,DX3,SCAL1,YDIF,ICR,SCAL3
C
C     THIS SUBROUTINE PLOTS THE SPECIFIED BLADE PROFILE.
C
      ZK=13.
      CALL MARG (ZK)
      CALL LETTER (21,.25,0.,2.8,1.0,21HTURBINE BLADE PROFILE)
      CALL NEWPEN (1)
C
C     VALUES ARE ADDED TO CENTER THE PLOT.
      DO 1 I=1,NP
      GX(I)=XPR(I)+.45
      GY(I)=YPR(I)+0.3
    1 CONTINUE
      NNIP=NP-1
      CALL NEWPEN (3)
      DO 2 I=1,NNIP
      CALL PLTLN (GX(I),GY(I),GX(I+1),GY(I+1))
    2 CONTINUE
      DO 3 I=1,NS
      GX(I)=XSUC(I)+.45
      GY(I)=YSUC(I)+0.3
    3 CONTINUE
      NNIS=NS-1
C
C     A SERIES OF STRAIGHT LINES ARE PLOTTED.
      DO 4 I=1,NNIS
      CALL PLTLN (GX(I),GY(I),GX(I+1),GY(I+1))
    4 CONTINUE
      CALL PLOT (14.0,0.01,-3)
      RETURN
      END


      SUBROUTINE MARG (A)
C     ==================
C
C     THIS SUBROUTINE PLOTS MARGINES AND SCALES THE DATA.
    1 CALL NEWPEN (9)
      AL=A/10.+1.
      CALL PLTIN (0.10,0.10,0.353,0.30,0.00,AL,0.00,3.0)
      AM=A-0.5
      CALL PLOT (0.1,0.02,3)
      CALL PLOT (0.,10.4,2)
      CALL PLOT (A,10.4,2)
      CALL PLOT (A,0.02,2)
      CALL PLOT (0.1,0.02,2)
      CALL INCHTO (0.5,0.5,XMN,YMN)
      CALL INCHTO (AM,10.0,XMX,YMX)
      CALL NEWPEN (3)
      CALL PLTLN (XMN,YMN,XMN,YMX)
      CALL PLTLN (XMN,YMX,XMX,YMX)
      CALL PLTLN (XMX,YMX,XMX,YMN)
      CALL PLTLN (XMX,YMN,XMN,YMN)
      RETURN
      END
```

```
      SUBROUTINE TEST (W,WW,T,TT,V,VV,NF,P,NS,ND)
C     ==========================================
      DIMENSION YYP(2), YYS(2)
      COMMON XE(40,20),YE(40,20),YP(20),X(40,20,3),Y(40,20,3),C(50,50),A
     1A(20,20),BB(20,20),B(20),NM,N1,NO,N2,BZ(2),NUS,NUM,BMIN,BMAX,TMIN,
     2TMAX,NC1,NC2,NC3,W1(40),W2(40),W3(40),ERROR1,ERROR2,ERROR3,TER1,TE
     3R2,TER3,CIS1,CIS2,CIS3,DX1,DX2,DX3,SCAL1,YDIF,ICR,SCAL3
C
C     THIS SUBROUTINE TESTS TO SEE IF THE CALCULATED MID POINT IS WITHIN
C      BLADE RANGE.
      INTEGER P
      TX=X(P,NF,2)
      YYP(2)=Y1(TX)
      TXX=X(P,NF,1)
      YYP(1)=Y1(TXX)
      N0=NS
      N1=N0-1
      N2=N0-2
      NM=N0+1
      DO 1 I=1,NM
      B(I)=AA(ND,I)
    1 CONTINUE
      YYS(2)=Y1(TX)
      YYS(1)=Y1(TXX).
      W=Y(P,NF,2)
      WW=Y(P,NF,1)
      T=YYP(2)
      TT=YYP(1)
      V=YYS(2)
      VV=YYS(1)
      RETURN
      END


      SUBROUTINE ADD (XL,YL,NN,XMIN,N,XMAX,LHI,LH)
C     ==========================================
      DIMENSION W(40), WK(100), BA(20), BK(20)
      DIMENSION XL(40), YL(40), GX(40), GY(40), A(242)
      COMMON XE(40,20),YE(40,20),YP(20),X(40,20,3),Y(40,20,3),C(50,50),A
     1A(20,20),BB(20,20),B(20),NM,N1,N0,N2,BZ(2),NUS,NUM,BMIN,BMAX,TMIN,
     2TMAX,NC1,NC2,NC3,W1(40),W2(40),W3(40),ERROR1,ERROR2,ERROR3,TER1,TE
     3R2,TER3,CIS1,CIS2,CIS3,DX1,DX2,DX3,SCAL1,YDIF,ICR,SCAL3
C
C     THIS SUBROUTINE PLOTS A POLYNOMINAL FOR THE INPUT DATA(ORDER SPECI
      DO 3 I=1,NN
      W(I)=1.000
      IF (LH.EQ.0) GO TO 2
      GX(I)=XL(I)+0.9
      IF (LHI.EQ.0) GO TO 1
      GY(I)=YL(I)
      GO TO 3
    1 GY(I)=YL(I)+0.27
      GO TO 3
    2 GX(I)=XL(I)+0.5
      GY(I)=YL(I)
    3 CONTINUE
      IF (LH.EQ.0) GO TO 4
      XMIN=XMIN+0.9
      XMAX=XMAX+0.9
      GO TO 5
    4 XMIN=XMIN+0.5
      XMAX=XMAX+0.5
    5 M0=N
      NM=N+1
      M1=N-1
      M2=N-2
      NNN=NN-1
C
C     ORLSQ IS USED FOR ALL POLY ORDER LESS THAN NN-1.
C     OTHERWISE LESQ IS USED.
      IF (N.EQ.NNN) GO TO 7
      CALL ORLSQ (GX,GY,W,NN,N,WK,SIGSQ,BA,IERR)
      DO 6 I=1,NM
      BK(I)=BA(NM-I+1)
    6 CONTINUE
      GO TO 8
    7 CALL LESQ (A,BK,GX,GY,N,NN)
C
C     CUVPLT IS A MACLIB PROGRAM USED TO PLOT POLYNOMINALS.
    8 CALL CUVPLT (XMIN,XMAX,0.02,BK,N,0)
      RETURN
      END
```

```
      E LENGTH (XMIN,XMAX,H,YY,XX,D,NI)
C     =========================================
      DIMENSION XX(NI), YY(NI), A(242)
      COMMON XE(40,20),YE(40,20),YP(20),X(40,20,3),Y(40,20,3),C(50,50),A
     1A(20,20),BB(20,20),B(20),MM,M1,MO,M2,BZ(2),NUS,NUM,BMIN,BMAX,TMIN,
     2TMAX,NC1,NC2,NC3,W1(40),W2(40),W3(40),ERROR1,ERROR2,ERROR3,TER1,TE
     3R2,TER3,CIS1,CIS2,CIS3,DX1,DX2,DX3,SCAL1,YDIF,ICR,SCAL3
C
C     THIS SUBROUTINE IS USED TO CALCULATE QO LENGTHS.
      WO(F)=SQRT(1+(DY1(F))**2.)
      SI(X)=(H/3.)*(WO(X+H)+4.*WO(X)+WO(X-H))
      NNU=NUS-1
C     ORLSQ CAN BE USED WHERE M.LT.(NNU-1).
C
C     MACLIB SUBROUTINE ORLSQ CAN BE USED WHERE M.LT.(NNU-1).
      CALL LESQ (A,B,XX,YY,M,NNU)
      MO=M
      MM=M+1
      M1=M-1
      M2=M-2
      H=(XMAX-XMIN)/50.
      D=0.0
C
C     NOW A SIMPLE SIMPSON,S RULE NUMERICAL INTEGRATION IS USED TO EVALU
C      ATE THE INTEGRAL WHICH DESCRIBES THE LENGTH OF A LINE.
      DO 1 K=1,49,2
      RK=FLOAT(K)
      XR=RK*H+XMIN
      D=D+SI(XR)
    1 CONTINUE
      RETURN
      END
```

```
      SUBROUTINE CURV (XX,SB,M,N,XPS,NI,LHI,LH)
C     =========================================
      DIMENSION XX(NI), SB(20)
      COMMON XE(40,20),YE(40,20),YP(20),X(40,20,3),Y(40,20,3),C(50,50),A
     1A(20,20),BB(20,20),B(20),MM,M1,MO,M2,BZ(2),NUS,NUM,BMIN,BMAX,TMIN,
     2TMAX,NC1,NC2,NC3,W1(40),W2(40),W3(40),ERROR1,ERROR2,ERROR3,TER1,TE
     3R2,TER3,CIS1,CIS2,CIS3,DX1,DX2,DX3,SCAL1,YDIF,ICR,SCAL3
C
C     THIS SUBROUTINE CALCULATES THE CURVATURE AT THE DESIRED POINTS FOR
C      NOMINAL WHOSE COEFFICIENTS ARE INPUT IN THE VARIABLE LIST.
      WRITE (6,1)
    1 FORMAT (1X,'SECOND DERIVATIVES EVALUATED IN CURV',//)
      DO 7 I=1,NUM
      IF (N.NE.5) GO TO 3
      IF (LH.EQ.0) GO TO 3
      IF (LHI.EQ.0) GO TO 2
      IF (XX(I).GT.XPS) GO TO 3
C
C     THE CURVATURE OF A STRAIGHT LINE IS GIVEN AS A SMALL NUMBER TO ALL
C      CALCULATIONS(0 WOULD NOT WORK IN THE STREAMLINE CURVATURE PROGRAM
    2 C(N,I)=0.0020
      GO TO 7
    3 MA=M-1
      MO=MA
      MM=MA+1
      M1=MA-1
      M2=MA-2
      MMM=MM+1
      DO 4 J=1,MMM
      B(J)=SB(J)
    4 CONTINUE
      TX=XX(I)
C
C     SEC IS THE SECOND DERIVATIVE EVALUATED AT EACH INPUT POINT.
      SEC=DY2(TX)
      WRITE (6,5) SEC
    5 FORMAT (1X,E18.6,/)
      MO=M
      MM=M+1
      M1=M-1
      M2=M-2
      DO 6 K=1,MM
      B(K)=SB(K)
    6 CONTINUE
      C(N,I)=ABS(SEC)/((1.+(DY1(TX))**2.)**1.5)
    7 CONTINUE
      RETURN
      END
```

```
      SUBROUTINE LEADS (XC,YC,ANGI,ZKK,NUMS,KO,XLS,YLS,NOT,NP,NO,NI,NON,
C     ==================================================================
     1XPS,LJ,LJL,BP,ND,NE,NF,LNI,LN,PITCH,YK,XSUC,NIS,NS)
      DIMENSION XLS(NO), YLS(NO), XLSS(20), YLSS(20), XLL(20), YLL(20),
     1YK(20), NK(20), YYL(40), DSB(20), XSUC(40)
      COMMON XE(40,20),YE(40,20),YP(20),X(40,20,3),Y(40,20,3),C(50,50),A
     1A(20,20),BB(20,20),B(20),NM,N1,N0,N2,BZ(2),NUS,NUM,BMIN,BMAX,TMIN,
     2TMAX,NC1,NC2,NC3,W1(40),W2(40),W3(40),ERROR1,ERROR2,ERROR3,TER1,TE
     3R2,TER3,CIS1,CIS2,CIS3,DX1,DX2,DX3,SCAL1,YDIF,ICR,SCAL3
C
C     THIS SUBROUTINE STARTS THE ANALYSIS FOR THE SUCTION SURFACE LEADIN
      INTEGER P
      RMAX=XLS(NUMS)+XLS(NUMS)/10.
      KK=NUMS-1
C
C     FIRST THE WHOLE COORDINATE SET IS TWISTED 90 DEGREES SO THAT THE S
C      SURFACE LEADING EDGE IS REPRESENTABLE BY A FUNCTION.
      DO 2 I=1,NUMS
      X(I,1,2)=YK(I)
C
C     VALUES ARE ALSO ADDED ON TO THE INPUT DATA TO CENTER THE PLOT.
      XLSS(I)=XLS(I)+0.9
      XLL(I)=YLS(I)
      YLL(I)=RMAX-XLS(I)
      YLSS(I)=YLS(I)+0.27
      WRITE (6,1) XLL(I),YLL(I)
1     FORMAT (1X,*XLL(I)=*,F10.4,* YLL(I)=*,F10.4,/)
2     CONTINUE
C
C     BMAX AND BMIN ARE CALCULATED BASED ON THE INPUT DATA.
      BMAX=XLL(1)+(ABS(XLL(NUMS)-XLL(1)))/3.
      BMIN=XLL(NUMS)-(ABS(XLL(NUMS)-XLL(1)))/3.
      WRITE (6,3) BMAX,BMIN
3     FORMAT (1X,*BMAX=*,F10.4,*BMIN=*,F10.4,/)
      CALL NARG (Z,X)
      DO 4 I=1,KK
      CALL PLTLN (XLSS(I),YLSS(I),XLSS(I+1),YLSS(I+1))
4     CONTINUE
      CALL ARROW (3.8,2.4,4.4,3.85,8)
      CALL LETTER (10,.15,67.,4.1,2.35,10HFLOW INLET)
      CALL LETTER (37,.25,0.,1.4,1.5,37HSUCTION SURFACE LEADING EDGE C-O
     1 GRID)
      CALL LETTER (15,.15,0.,5.7,5.1,15HSUCTION SURFACE)
      CALL LETTER (34,.15,0.,1.0,8.6,34HLEADING EDGE STAGNATION STREAMLI
     1NE)
      NK(NE)=NP
      N0=NP
      NN=NP+1
      N1=NP-1
      N2=NP-2
      NNP=NP+1
C
C     THE LEADING EDGE STAGNATION STREAMLINE IS NOW CALCULATED AND PLOTT
      B(1)=BZ(1)
      B(2)=BZ(2)
      DO 5 K=3,NNP
      B(K)=0.
5     CONTINUE
      ZTX=(-.275)*(XSUC(NS)-XSUC(1))/1.05
6     ZY=Y1(ZTX)+0.27
      IF (ZY.LT.0.5) GO TO 7
      IF (ZY.LT.0.7) GO TO 8
      ZTX=ZTX-0.01*(XSUC(NS)-XSUC(1))/1.05
      IF (ZTX.GT.-.475) GO TO 6
      GO TO 8
7     ZTX=ZTX+0.01*(XSUC(NS)-XSUC(1))/1.05
      GO TO 6
8     XCR=YC
      XZY=ZTX+0.9
      YCC=YC+0.27+PITCH
9     IF (YCC.LT.1.069) GO TO 10
      XCR=XCR-0.01*((XSUC(NS)-XSUC(1))/1.05)
      YCC=Y1(XCR)+0.27
      GO TO 9
```

```
10    XCC=XCR+0.9
      CALL PLTLN (XZY,ZY,XCC,YCC)
C
C     A POLY IS FIT TO THE LEADING EDGE SUCTION SURFACE.
      CALL CFIT (NUMS,XLL,YLL,NL,LN,LNI,ND)
      WRITE (6,11) NUMS,NL
11    FORMAT (1X,*NUMS=*,I5,* NL=*,I5,/)
      NK(I)=NL
      NLL=NL+1
      NN=NLL
      N1=NL-1
      N2=NL-2
      N0=NL
C
C     THE COEFFICIENTS ARE INITIALIZED.
      DO 13 I=1,NLL
      AA(1,I)=B(I)
      BSB(I)=B(I)
      WRITE (6,12) I,B(I)
12    FORMAT (1X,I5,E18.6,/)
13    CONTINUE
      DO 15 I=1,NUMS
      YYL(I)=YI(XLL(I))
      WRITE (6,14) XLL(I),YYL(I)
14    FORMAT (1X,*XLL(I)=*,F10.4,*YYL(I)=*,F10.4,/)
15    CONTINUE
C
C     THE CURVATURE IS CALCULATED AT EACH QO START POINT.
      CALL CURV (XLL,BSB,NL,ND,XPS,N1,LNI,LN)
C
C     THE COEFFICIENTS ARE INITIALIZED.
      BB(NE,1)=(RMAX-XC)*TAN(3.14159/2.-ANG1) (YC+PITCH)
      BB(NE,2)=-TAN(3.14159/2.-ANG1)
      DO 17 K=3,NNP
      BB(NE,K)=0.
      WRITE (6,16) NE,K,BB(NE,K)
16    FORMAT (1X,2I5,E18.6,/)
17    CONTINUE
      LJ=0
      LJL=0
      RMAX=1.
C
C     THE MAIN CALCULATION PROCEDURE IS RETURNED TO.
      CALL MAIN (NK,400,NLL,XPS,LJ,XC,YC,LJL,BP,NO,N1,NON,NOT,LNI,LN,RMA
     1X,PRMAX,XSUC,LS,PITCH)
      RETURN
      END
```

```
      SUBROUTINE LEADP (NUMP,K00,ZKZ,XLP,YLP,NE,XSUC,YSUC,XPS,LJ,XC,YC,L
C     ==================================================================
     1JL,PP,NO,NI,NON,NOT,LHI,LH,XK,PITCH,YPRM,NIS,NIS,NS)
      DIMENSION XLPP(20), YLPP(20), XSUK(40), XSUC(NI), YSUK(40), YSUC(N
     1I)
      DIMENSION BP(NI), XK(40), WY(20), DS(20), NK(20), XLP(NO), YLP(NO)
     1, ZXLP(40), ZYLP(40), ZXSU(40), ZYSU(40), W(40), WK(100), BA(20)
      COMMON XE(40,20),YE(40,20),YP(20),X(40,20,3),Y(40,20,3),C(50,50),A
     1A(20,20),BB(20,20),B(20),NM,N1,NQ,N2,BZ(2),NUS,NUN,BMIN,BMAX,TMIN,
     2TMAX,NC1,NC2,NC3,W1(40),W2(40),W3(40),ERROR1,ERROR2,ERROR3,TER1,TE
     3R2,TER3,CIS1,CIS2,CIS3,DX1,DX2,DX3,SCAL1,YDIF,ICR,SCAL3
C
C     THIS PART STARTS THE ANALYSIS FOR THE PRESSURE SURFACE LEADING EDG
      INTEGER P
      KK=NUMP-1
      CALL NARG (ZKZ)
      CALL LETTER (16,.25,0.,1.3,1.23,16HPRESSURE SURFACE)
      CALL LETTER (21,.25,0.,.95,.8,21HLEADING EDGE Q-O GRID)
      CALL LETTER (15,.15,0.,3.5,2.5,15HSUCTION SURFACE)
      CALL LETTER (29,.15,0.,1.2,8.3,29HPRESSURE SURFACE LEADING EDGE)
      CALL ARROW (.0,2.5,1.4,3.5,3)
      CALL LETTER (10,.15,62.,1.0,2.2,10HFLOW INLET)
C
C     YPRM IS MOVED UP TO THE OTHER SIDE OF THE PASSAGE.
      YPRM2=YPRM+PITCH
      RMAX=YPRM+YPRM/1000.
      RMAX=0.2*(ABS(XSUC(NS)-XSUC(1)))
      DO 1 P=1,K00
      X(P,1,2)=RMAX-XK(P)
    1 CONTINUE
C
C     HERE THE WHOLE PLOTTED INPUT VALUES ARE TWISTED 180 DEGREES.
      DO 2 I=1,NIS
      W(I)=1.0
      XSUK(I)=RMAX-XSUC(I)
      YSUK(I)=RMAX-YSUC(I)
      ZXSU(I)=XSUC(I)+0.5
      ZYSU(I)=YSUC(I)
    2 CONTINUE
      DO 3 I=1,NIS
      IF (ZYSU(I).GT..8.OR.ZYSU(I).LT..475) GO TO 3
      IF (ZXSU(I+1).GT.1.05.OR.ZXSU(I).LT..45) GO TO 3
      IF (ZYSU(I+1).GT..8 OR ZYSU(I+1).LT..475) GO TO
      CALL PLTLN (ZXSU(I),ZYSU(I),ZXSU(I+1),ZYSU(I+1))
    3 CONTINUE
      NO=NIS
      NK(NE)=NIS
      N1=NO-1
      N2=NO-2
      NM=NO+1
C
C     A POLY IS FIT TO THE SUCTION SURFACE VALUES ONCE THEY ARE ROTATED
C      DEGREES(NOTE THAT THE THE SAME POLY ORDER IS USED AS WAS IN THE F
C      PART OF THE PROGRAM FOR THE SUCTION SURFACE).
      CALL ORLSQ (XSUK,YSUK,W,NIS,NIS,WK,SIGSQ,BA,IERR)
      NK(5)=NIS
      DO 4 JK=1,NM
      B(JK)=BA(NM-JK+1)
    4 CONTINUE
      DO 6 I=1,NSUC
      WY(I)=Y1(XSUK(I))
      WRITE (6,5) XSUK(I),WY(I)
    5 FORMAT (1X,*XSUK(I)=*,F10.4,*YSUK(I)=*,F10.4,/)
    6 CONTINUE
C
C     THE POLY COEFFICIENTS ARE NOW STORED.
      DO 7 I=1,NM
      BB(NE,I)=B(I)
    7 CONTINUE
      DO 8 I=1,NUMP
      YLP(I)=YLP(I)+PITCH
      XLPP(I)=RMAX-XLP(I)
      YLPP(I)=RMAX-YLP(I)
      ZXLP(I)=XLP(I)+0.5
```

```
      ZYLP(I)=YLB(I)
8     CONTINUE
      BMIN=XLPP(NUMP)-(ABS(XLPP(NUMP)-XLPP(1)))/3.
      BMAX=XLPP(1)+(ABS(XLPP(NUMP)-XLPP(1)))/3.
      WRITE (6,9) BMAX,BMIN
9     FORMAT (1X,*BMAX=*,F10.4,*BMIN=*,F10.4,/)
      DO 10 I=1,KK
      CALL PLTLN (ZXLP(I),ZYLP(I),ZXLP(I+1),ZYLP(I+1))
10    CONTINUE
C
C     NOW A BEST FIT POLY IS FOUND FOR THE PRESSURE SURFACE LEADING EDGE
      ND=1
      CALL CFIT (NUMP,XLPP,YLPP,MLN,LN,LNI,ND)
      MLP=MLN+1
      MK(1)=MLN
      M0=MLN
      M1=M0-1
      M2=M0-2
      MM=M0+1
C
C     THE COEFFICIENTS ARE STORED.
      DO 12 I=1,MLP
      AA(1,I)=B(I)
      BS(I)=B(I)
      WRITE (6,11) M1,M0,MLP,AA(1,I)
11    FORMAT (1X,*M1= *,I5,* M0= *,I5,* MLP= *,I5,* AA(1,I)= *,E18.6,/)
12    CONTINUE
      ND=1
      DO 14 I=1,NUMP
      WY(I)=Y1(XLPP(I))
      WRITE (6,13) XLPP(I),WY(I)
13    FORMAT (1X,*XLPP(I)= *,F10.4,* YLPP(I)= *,F10.4,/)
14    CONTINUE
C
C     THE CURVATURE IS FOUND AT THE QO START POINTS.
      CALL CURV (XLPP,BS,MLN,NE,XPS,N1,LNI,LN)
C
C     WE RETURN TO THE MAIN CALCULATION SUBROUTINE.
      CALL MAIN (NK,400,MLP,XPS,LJ,XC,YC,LJL,BP,NO,NI,NON,NOT,LNI,LN,RMA
     1X,RRMAX,XSUC,NS,PITCH)
      RETURN
      END
```

```
      SUBROUTINE CFIT (N,GX,GY,M,LH,LHI,IF)
C     ===================================
C
C     **** POLY SELECTION SUBROUTINE ****
C
C
C     THE FOLLOWING PROGRAM IS USED TO EXAMINE THE BEST POLYNOMINAL FIT
C     FOR THE COORDINATES SPECIFIED
C
C
C  M  POLYNOMIAL  DECREE
C  N  NUMBER OF DATA POINTS
C  DX  X INCREMENT
C  DY1  FIRST DERIVATIVE
C  S  SLOPE IN DEGREE
C     CH(I) = CHANGE IN THE VALUE OF SLOPE BETWEEN LAST TWO DATA POINTS
C     CHS(I) = SLOPE OF SLOPE CURVE USING LAST TWO DATA POINTS
C     CSS(I) = CHANGE IN VALUE OF SLOPE OF SLOPE CURVE BETWEEN LAST TWO
C     DATA POINTS
C     ATE(M)= THE NULL HYPOTHESIS ERROR**2 FOR POLY ORDER M
C     DATE(M) = THE PERCENT DECREASE OF THE NULL HYPOTHESIS ERROR**2
C     SINCE THE LAST POLY ORDER
C
      DIMENSION XD(200), XX(40), YD(40), YY(40), YIP(40), S(200), APD(20
     10), E(50), GX(40), GY(40), CH(200), PR(40), ZEROR(20), ZEROI(20),
     2XID(40)
      DIMENSION TE(20), ATE(20), DATE(20), BIB(20), F(40)
      DIMENSION W(40), WK(100), BA(20), A(242), FY(50), BATE(20), PE(40)
      COMMON XE(40,20),YE(40,20),YP(20),X(40,20,3),Y(40,20,3),C(50,50),A
     1A(20,20),BB(20,20),B(20),MM,M1,M0,M2,BZ(2),NUS,NUM,BMIN,BMAX,TMIN,
     2TMAX,MC1,MC2,MC3,W1(40),W2(40),W3(40),ERROR1,ERROR2,ERROR3,TER1,TE
     3R2,TER3,CIS1,CIS2,CIS3,DX1,DX2,DX3,SCAL1,YDIF,ICR,SCAL3
      WRITE (6,1) IF
    1 FORMAT (1X,*NOW THE BEST POLY FIT FOR STREAMLINE NO.*,I3,* IS FOUN
     1D*,/)
      IF (LH.EQ.1.AND.LHI.EQ.1) GO TO 3
C
C     FIRST THE CORRECT ALLOWABLE ERRORS ARE SELECTED.
C
      IF (LH.EQ.1.AND.LHI.EQ.0) GO TO 5
      TER=TER3
      ERROR=ERROR3
      CIS=CIS3
      DX=DX3
      DO 2 I=1,N
      W(I)=W3(I)
    2 CONTINUE
      GO TO 7
    3 TER=TER1
      ERROR=ERROR1
      CIS=CIS1
      DX=DX1
C
C     THE WEIGHTS FOR THE STREAMLINE POINTS ARE THE SAME AS A WEIGHT ON
C      THE BLADE SURFACE.
C
      DO 4 I=1,N
      W(I)=W1(13)
    4 CONTINUE
      GO TO 7
    5 TER=TER2
      ERROR=ERROR2
      CIS=CIS2
      DX=DX2
      DO 6 I=1,N
      W(I)=W2(I)
    6 CONTINUE
    7 CONTINUE
C
C     THE NUMBER OF INTERVALS AT WHICH THE FUNCTION IS TO BE EVALUATED A
C      DETERMINED.
      NUMY=(ABS(GX(1)-GX(N)))/DX
      NU1S=N-1
C
```

```
C       READ DATA AND CALCULATE POLYNOMIAL  EFFICIENTS
C
        DO 50 ICOUNT=1,14
C       THE NA VARIABLES ARE JUST COUNTERS TO INDICATE THE ACCEPTABILITY O
C       F A SPECIFIC POLYNOMINAL ORDER
        IF (ICOUNT.EQ.NUTS) GO TO 53
        NA1=0
        NA2=0
        NA3=0
        NA4=0
        NA5=0
        DO 9 I=1,N
        IF (I.GT.15) GO TO 8
        B(I)=0.000
 8      XID(I)=GX(I)
        YD(I)=GY(I)
 9      CONTINUE
        M=ICOUNT+1
        WRITE (6,10) M
 10     FORMAT (1X,*THE ACCEPTABILITY OF POLY ORDER*,I3,* IS DETERMINED*,/
       1)
C
C       INITIALIZATION.
        TE(M)=0.0
        ATE(M)=0.0
        DATE(M)=0.0
        NO=M
        MN=M+1
        M1=M-1
        M2=M-2
        IF (M.EQ.NUTS) GO TO 12
C
C       ORLSQ IS USED EXCEPT WHERE M.EQ. N-1.
        CALL ORLSQ (XID,YD,W,N,M,WK,SIGSQ,BA,IERR)
        DO 11 LL=1,MN
        B(LL)=BA(MN-LL+1)
 11     CONTINUE
        GO TO 13
 12     CALL LESQ (A,B,XID,YD,M,N)
C
C       CALCULATE NEW Y(YP) AND ERROR(E)
C
 13     ZZ=FLOAT(N)
        WW=FLOAT(M)
        ARR=ZZ-WW-1.
        DO 14 I=1,N
        TX=XID(I)
C
C       YIP IS THE CALCULATED ORDINATE VALUE.
        YIP(I)=YI(TX)
        E(I)=(YIP(I)-YD(I))
C
C       THE PERCENTAGE ERROR IS CALCULATED.
        PE(I)=(YIP(I)-YD(I))*100.0/YIP(I)
C
C       THE TOTAL ERROR FOR THIS POLYNOMINAL ORDER IS CALCULATED.
        TE(M)=ABS(ABS(E(I)))+TE(M)
 14     CONTINUE
        DO 15 I=1,N
        IF (ABS(E(I)).GT.ERROR) GO TO 17
 15     CONTINUE
        NA1=1
        WRITE (6,16)
 16     FORMAT (1X,*THE ABSOLUTE ERROR IS WITHIN SPECIFIED LIMITS*)
        GO TO 19
C
C       ATE IS THE NULL HYPOTHESIS ERROR.
 17     WRITE (6,18)
 18     FORMAT (1X,*THE ABSOLUTE ERROR IS TOO LARGE*)
 19     IF (ARR.EQ.0.) GO TO 20
        ATE(M)=(TE(M))**2./(ZZ-WW-1.)
 20     IF (TE(M).GT.TER) GO TO 22
        NA2=1
        WRITE (6,21)
```

```
21    FORMAT (1X,*THE TOTAL ABSOLUTE ERROR IS WITHIN SPECIFIED LIMITS*)
      GO TO 24
22    WRITE (6,23)
23    FORMAT (2X,*THE TOTAL ABSOLUTE ERROR IS TOO LARGE*)
24    IF (M.EQ.2) GO TO 27
C
C
C     BATE IS THE DECREASE IN ATE SINCE THE LAST POLY ORDER.
C     DATE IS THE PERCENTAGE DECREASE IN ATE SINCE THE LAST POLY ORDER.
C     DATE AND BATE CAN BE READ OUT IF DESIRED
      IF (ARR.EQ.0.) GO TO 25
      BATE(M)=ATE(M-1)-ATE(M)
      DATE(M)=((ATE(M-1)-ATE(M))/(ATE(M-1)))*100.
C
C     DEFINE NEW X AND COMPUTE Y,DY1 AND S
C
25    F(1)=0.
      DO 26 J=2,M
      F(J)=F(J-1)+2.*FLOAT(J-1)
C
C     THE BIB VALUES ARE THE SECOND DERIVATIVE COEFFICIENTS.
      BIB(J-1)=B(J+1)*F(J)
26    CONTINUE
27    DO 29 I=1,NUMY
      K=I-1
      XD(I)=DX*FLOAT(K)
      TX=XD(I)
C
C     NOW Y VALUES ARE CALCULATED WITH A SMALLER DX
C
      S(I)=(ATAN(DY1(TX)))*180.0/3.14159
      IF (I.NE.1) GO TO 28
      CH(I)=0.000
      GO TO 29
C
C     NOW THE CHANGE IN SLOPE IS CALCULATED BETWEEN THE LAST TWO DATA
C     POINTS
C
28    CH(I)=S(I)-S(I-1)
C
C     NOW THE SECOND DERIVATIVE IS CALCULATED
C
29    IF (M.EQ.2) GO TO 30
      IF (I.GE.M) GO TO 30
C
C     PR(I) ARE THE SECOND DERIVATIVE COEFFICIENTS LISTED IN REVERSE
C     ORDER FOR INPUT TO THE MACLTB SUBPROGRAM RPOLY
C
      PR(I)=BIB(M-I)
30    CONTINUE
      DO 31 I=1,NUMY
      IF (CH(I).LT.CIS) GO TO 33
31    CONTINUE
      WRITE (6,32)
32    FORMAT (1X,*THE CHANGE IN SLOPE IS NOT TO LARGE*)
      NA3=1
      GO TO 35
C
C     NOW THE ZEROS OF THE SECOND DERIVATIVE ARE DETERMINED
C
33    WRITE (6,34)
34    FORMAT (1X,*THE CHANGE IN SLOPE IS TOO HIGH*)
35    IF (M.EQ.2) GO TO 42
      CALL RPOLY (PR,M2,ZEROR,ZEROI,FAIL)
C
C     F INDICATES THAT RPOLY FUNCTIONED PROPERLY, A T INDICATES THAT IT
C     DID NOT
C
      EMAX=XID(N)
      EMIN=XID(1)
      IF (LHL.EQ.1) GO TO 36
      EMIN=XID(N)
      EMAX=XID(1)
36    DO 38 J=1,M2
```

```
      IF (ZEROI(J).EQ.0.) GO TO 37
      GO TO 38
 37   IF (ZEROR(J).GT.BMAX) GO TO 38
      IF (ZEROR(J).LT.BMIN) GO TO 38
      NA4=3
 38   CONTINUE
      IF (NA4.EQ.3) GO TO 40
      WRITE (6,39)
 39   FORMAT (1X,*THERE ARE NO ZEROS TO THE SECOND DERIVATIVE WITHIN THE
     1 BLADE RANGE*)
      NA4=1
      GO TO 43
 40   WRITE (6,41)
 41   FORMAT (1X,*THERE ARE ZEROS TO THE SECOND DERIVATIVE WITHIN THE BL
     1ADE RANGE*)
      NA4=0
      GO TO 43
C
C     COMPUTE THE TOTAL TURNING ANGLE
C
 42   NA4=1
 43   IF (LHI.EQ.0.OR.LH.EQ.0) GO TO 46
      TTA=0.0
      NN=NUMY-1
      DO 44 I=1,NN
      APD(I)=S(I+1)-S(I)
      TTA=TTA+APD(I)
 44   CONTINUE
      IF (TTA.LT.TMIN) GO TO 46
      IF (TTA.GT.TMAX) GO TO 46
      WRITE (6,45)
 45   FORMAT (1X,*THE TOTAL TURNING ANGLE IS WITHIN THE SPECIFIED RANGE*
     1,////)
      NA5=1
      GO TO 48
 46   IF (LHI.EQ.0.OR.LH.EQ.0) GO TO 48
      WRITE (6,47)
 47   FORMAT (1X,*THE TOTAL TURNING ANGLE IS OUTSIDE THE SPECIFIED RANGE
     1*,////)
 48   NA=NA1+NA2+NA3+NA4+NA5
      IF (LH.EQ.0.OR.LHI.EQ.0) GO TO 49
      IF (NA.EQ.5) GO TO 51
      GO TO 50
 49   IF (NA.EQ.4) GO TO 51
 50   CONTINUE
      GO TO 53
 51   WRITE (6,52) IF,N
 52   FORMAT (1X,*STREAMLINE NO.*,I3,* WILL BE MODELLED BY POLY ORDER*,I
     13,//////)
      GO TO 55
 53   WRITE (6,54)
 54   FORMAT (1H1,1X,*NO POLYNOMINAL ORDER ,15 OR LESS, COULD PROPERLY F
     1 IT THE DATA TO THE ACCURACY SPECIFIED BY THE INPUT VALUES*,//////
     2)
 55   RETURN
      END
```

```
      SUBROUTINE SCALE (P,NE,DD)
C     ==========================
      DIMENSION DD(40)
      COMMON XE(40,20),YE(40,20),YP(20),X(40,20,3),Y(40,20,3),C(50,50),A
     1A(20,20),BB(20,20),B(20),NM,N1,N0,N2,BZ(2),NUS,NUM,BMIN,BMAX,TMIN,
     2TMAX,NC1,NC2,NC3,W1(40),W2(40),W3(40),ERROR1,ERROR2,ERROR3,TER1,TE
     3R2,TER3,CIS1,CIS2,CIS3,DX1,DX2,DX3,SCAL1,YDIF,ICR,SCAL3
C
C     THIS SUBROUTINE SCALES ALL THE DATA BACK TO THE ORIGINAL INPUT
C      SCALE.
C
      INTEGER P
      C(1,P)=(C(1,P)*SCAL1)*SCAL3
      C(NE,P)=(C(NE,P)*SCAL1)*SCAL3
      DD(P)=DD(P)/(SCAL1*SCAL3)
      X(P,1,2)=X(P,1,2)/(SCAL1*SCAL3)
      X(P,NE,2)=X(P,NE,2)/(SCAL1*SCAL3)
      DO 1 I=1,ICR
      Y(P,1,2)=Y(P,1,2)-0.03636/(1.1**(I-1))
      Y(P,NE,2)=Y(P,NE,2)-0.03636/(1.1**(I-1))
    1 CONTINUE
      Y(P,1,2)=(Y(P,1,2)/SCAL3+YDIF)/SCAL1
      Y(P,NE,2)=(Y(P,NE,2)/SCAL3+YDIF)/SCAL1
      RETURN
      END
```

```
      FUNCTION Y1 (Z)
C     ===============
      COMMON XE(40,20),YE(40,20),YP(20),X(40,20,3),Y(40,20,3),C(50,50),A
     1A(20,20),BB(20,20),B(20),NM,N1,N0,N2,BZ(2),NUS,NUM,BMIN,BMAX,TMIN,
     2TMAX,NC1,NC2,NC3,W1(40),W2(40),W3(40),ERROR1,ERROR2,ERROR3,TER1,TE
     3R2,TER3,CIS1,CIS2,CIS3,DX1,DX2,DX3,SCAL1,YDIF,ICR,SCAL3
C
C     THIS FUNCTION SUBROUTINE CALCULATES THE FUNCTIONAL VALUE AT Z.
      Y1=B(NM)*Z
      DO 1 J=1,N1
      Y1=(Y1+B(NM-J))*Z
    1 CONTINUE
      Y1=B(1)+Y1
      RETURN
      END
```

```
      FUNCTION DY1 (Z)
C     ================
      COMMON XE(40,20),YE(40,20),YP(20),X(40,20,3),Y(40,20,3),C(50,50),A
     1A(20,20),BB(20,20),B(20),NM,N1,N0,N2,BZ(2),NUS,NUM,BMIN,BMAX,TMIN,
     2TMAX,NC1,NC2,NC3,W1(40),W2(40),W3(40),ERROR1,ERROR2,ERROR3,TER1,TE
     3R2,TER3,CIS1,CIS2,CIS3,DX1,DX2,DX3,SCAL1,YDIF,ICR,SCAL3
C
C     THIS FUNCTION SUBROUTINE CALCULATES THE VALUE OF THE FIRST DERIVAT
      DY1=FLOAT(N0)*B(NM)*Z
      IF (N0.EQ.2) GO TO 2
      DO 1 J=1,N2
      DY1=(DY1+FLOAT(N0-J)*B(NM-J))*Z
    1 CONTINUE
    2 DY1=DY1+B(2)
      RETURN
      END
```

```
      FUNCTION DY2 (Z)
C     ================
      COMMON XE(40,20),YE(40,20),YP(20),X(40,20,3),Y(40,20,3),C(50,50),A
     1A(20,20),BB(20,20),B(20),NM,N1,N0,N2,DZ(2),NUS,NUT,BMIN,BMAX,TMIN,
     2TMAX,NC1,NC2,NC3,W1(40),W2(40),W3(40),ERROR1,ERROR2,ERROR3,TER1,TE
     3R2,TER3,CIS1,CIS2,CIS3,DX1,DX2,DX3,SCAL1,YDIF,ICR,SCAL3
C
C      THIS FUNCTION SUBROUTINE CALCULATES THE VALUE OF THE SECOND DERIVA
C       AT Z.
      B(1)=B(2)
      DO 1  I=2,NM
      AI=FLOAT(I)
      B(I)=AI*B(I+1)
1     CONTINUE
      DY2=DY1(Z)
      RETURN
      END
```

MAIN BLADE RANGE RESULTS

++

OO NO.	START PT X	START PT Y	START PT C	END PT X	END PT Y	END PT C	LENGTH
1	.0100	.4036	.7375	-.2007	.5045	.0021	.2322
2	.0200	.4340	.8352	-.1825	.5349	.0021	.2247
3	.0300	.4621	.9399	-.1654	.5636	.0021	.2184
4	.0400	.4881	1.0503	-.1495	.5902	.0021	.2133
5	.0500	.5122	1.1648	-.1341	.6161	.0021	.2092
6	.0600	.5346	1.2815	-.1195	.6403	.0021	.2061
7	.0700	.5553	1.3930	-.1059	.6633	.0021	.2039
8	.0800	.5746	1.5118	-.0928	.6853	.0021	.2025
9	.0900	.5926	1.6204	-.0802	.7053	.0021	.2019
10	.1000	.6093	1.7215	-.0631	.7265	.0021	.2020
11	.1200	.6395	1.8937	-.0453	.7648	.0021	.2041
12	.1400	.6659	2.0199	-.0109	.8140	.0021	.2070
13	.1600	.6892	2.1025	.0139	.8394	.0021	.2013
14	.1800	.7098	2.1535	.0476	.8640	1.3565	.1960
15	.2200	.7444	2.2344	.1083	.9096	1.5180	.1933
16	.2600	.7718	2.4001	.1703	.9462	1.6638	.1891
17	.3000	.7930	2.7229	.2337	.9740	1.7892	.1851
18	.3400	.8082	3.1814	.2980	.9930	1.8971	.1814
19	.3800	.8173	3.5554	.3628	1.0032	1.9947	.1753
20	.4200	.8202	3.9525	.4275	1.0046	2.3747	.1752
21	.4600	.8164	3.9107	.4918	.9968	2.1159	.1752
22	.5000	.8058	3.5257	.5551	.9798	2.0687	.1750
23	.5200	.7979	3.2496	.5862	.9677	2.0424	.1751
24	.5400	.7882	2.9509	.6167	.9533	1.9740	.1752
25	.5600	.7769	2.5518	.6466	.9366	1.8654	.1754
26	.5800	.7638	2.3692	.6757	.9175	1.7807	.1754
27	.6000	.7490	2.1142	.7041	.8959	1.6647	.1753

SUCTION SURFACE LEADING EDGE RESULTS

++

QO NO.	START PT Y	START PT X	START P C	END PT Y	END PT X	END PT C	LENGTH
1	.3729	.0014	45.3568	.4927	-.2077	.0021	.2395
2	.3636	-.0004	68.8105	.4398	-.2393	.0021	.2537
3	.3541	.0026	70.1637	.3789	-.2756	.0021	.2937
4	.3488	.0065	60.6932	.3476	-.2943	.0021	.3225
5	.3457	.0095	51.8447	.3310	-.3042	.0021	.3397

PRESSURE SURFACE LEADING EDGE RESULTS

++

QO NO.	START PT X	START PT Y	START PT C	END PT X	END PT Y	END PT C	LENGTH
1	.1118	.6276	1.8287	.0150	.8472	55.4099	.2463
2	.1233	.6441	1.9178	.0185	.8467	59.6394	.2295
3	.1312	.6547	1.9701	.0210	.8467	61.0002	.2231
4	.1458	.6729	2.0479	.0260	.8479	60.3946	.2377
5	.1599	.6891	2.1023	.0315	.8509	56.4956	.2012

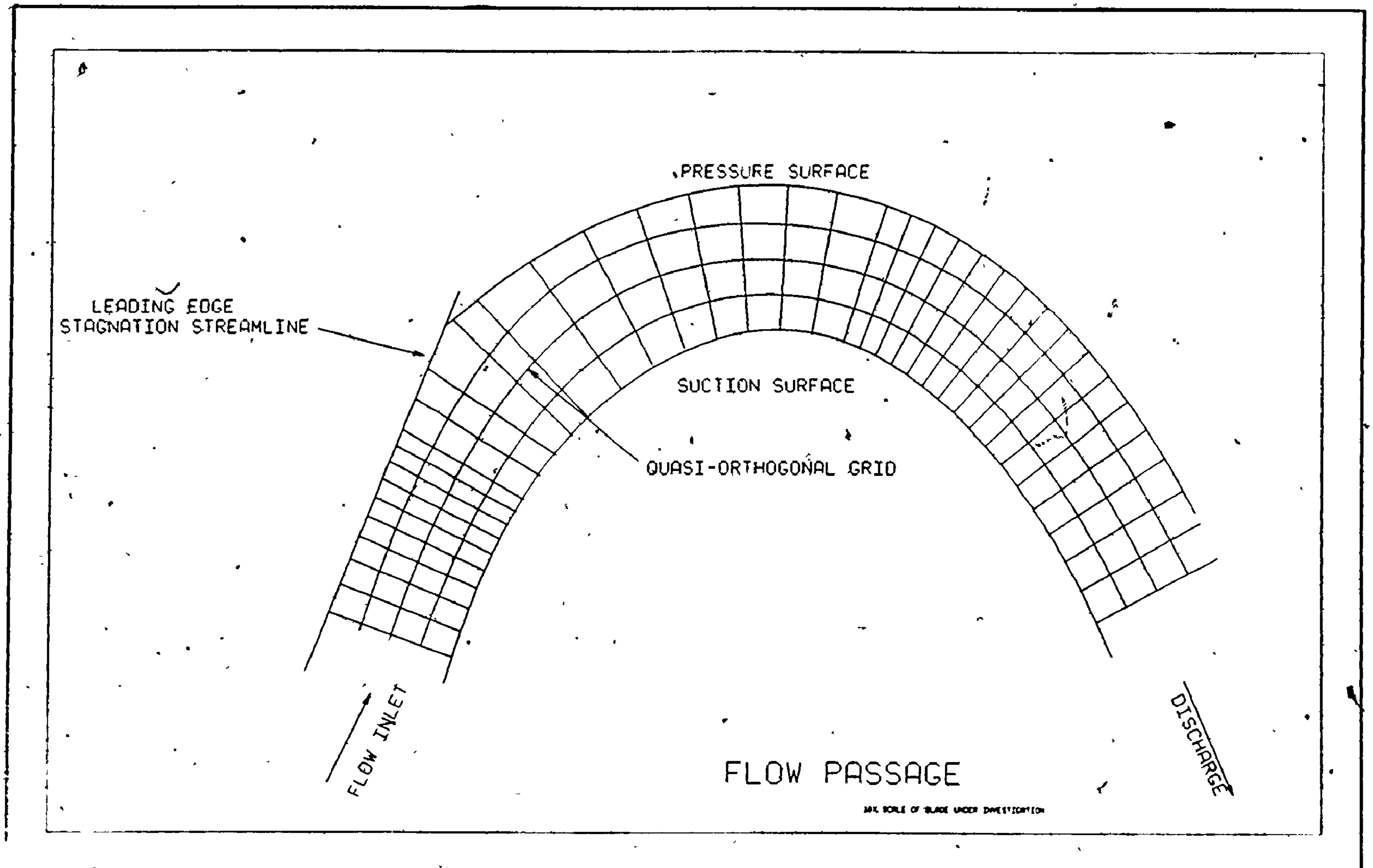

Figure 35 Plotter Output for Main Blade Range
($\beta' = 67.5^{\circ}$; dense grid near leading edge)

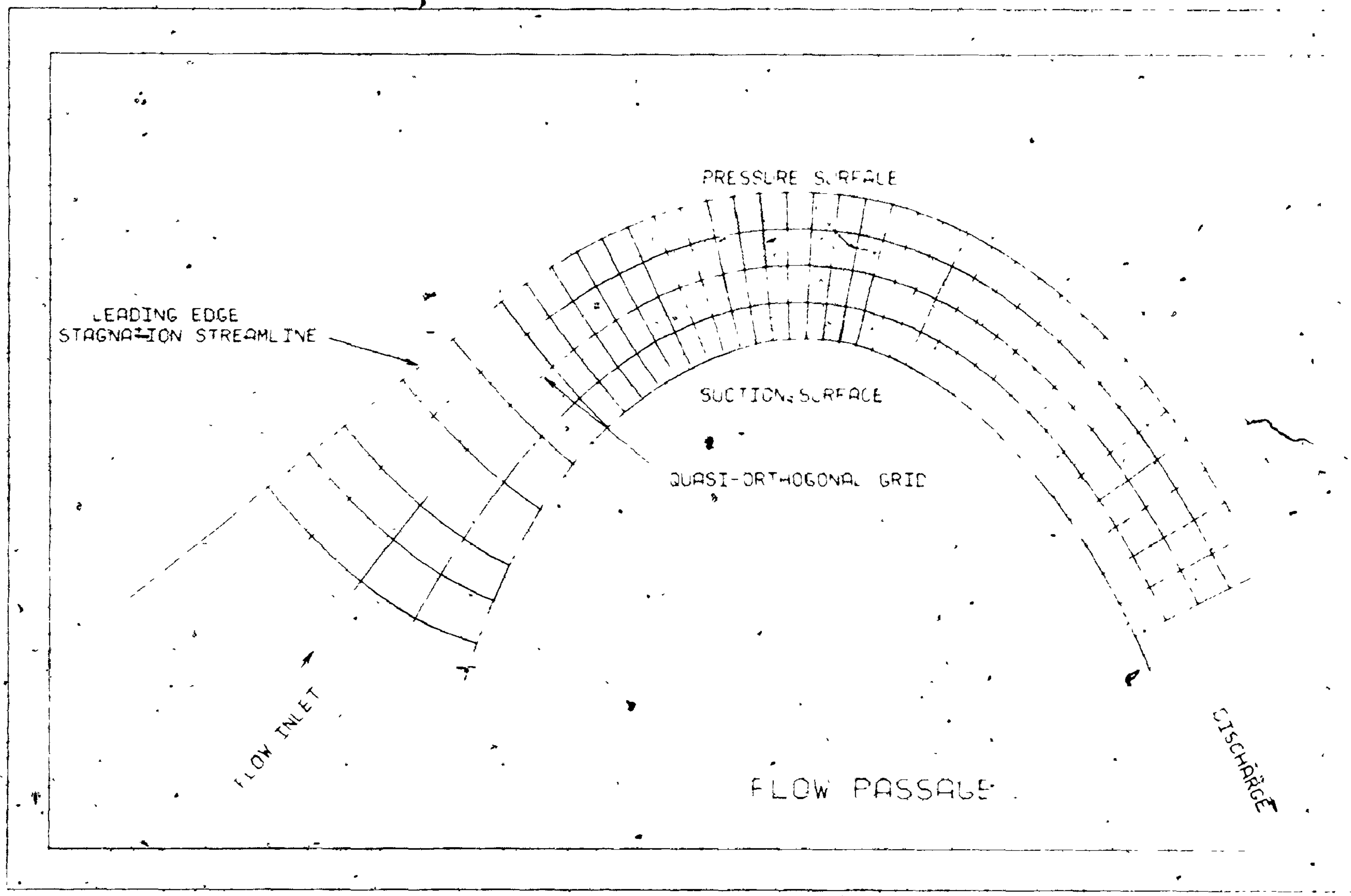

Figure 36 Plotter Output for Main Blade Range
(β = 38^o ; dense grid at mid chord)

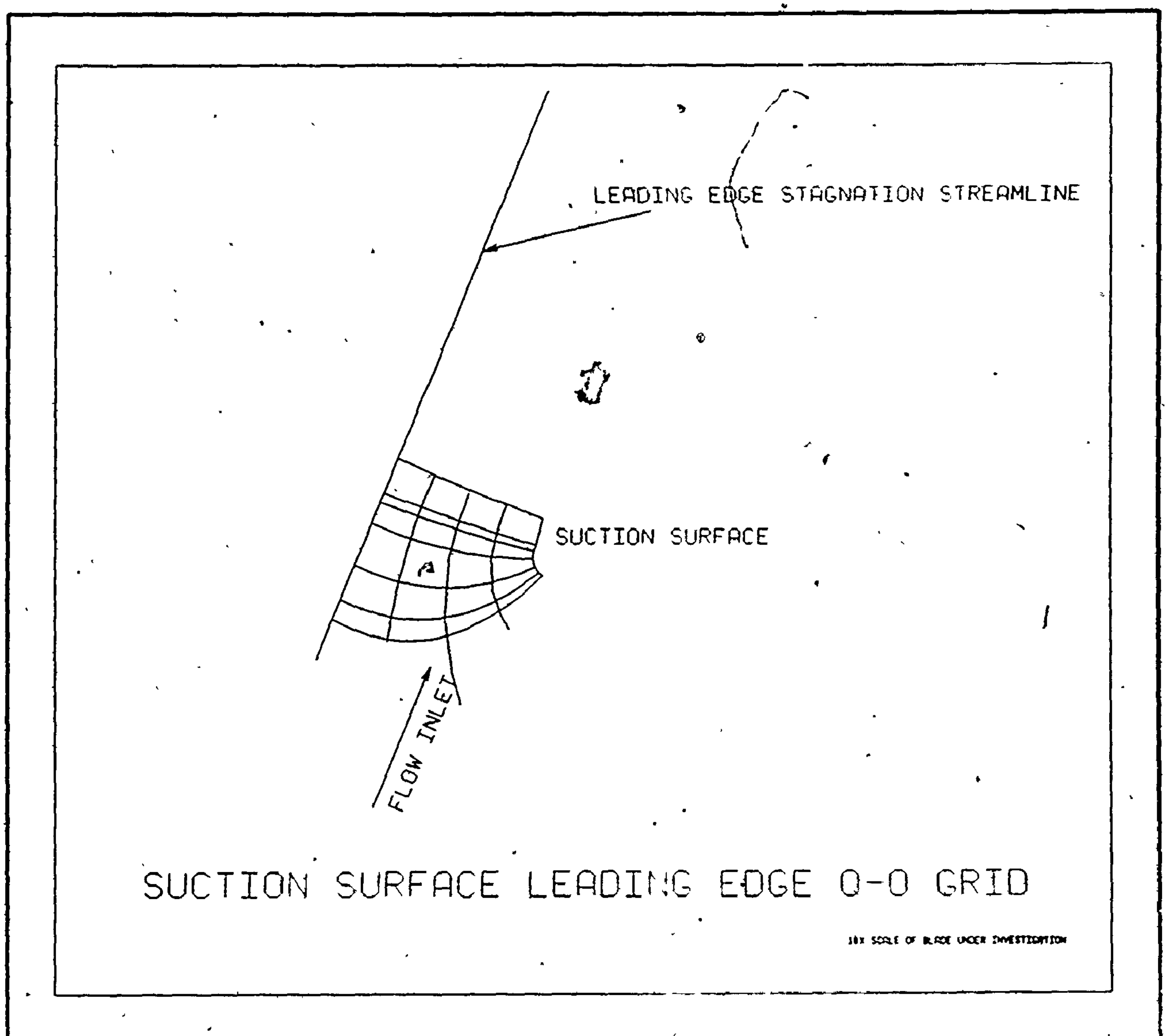

Figure 37 Plotter Output for Suction Surface Side of Leading Edge ($\beta = 67.5^{o}$)

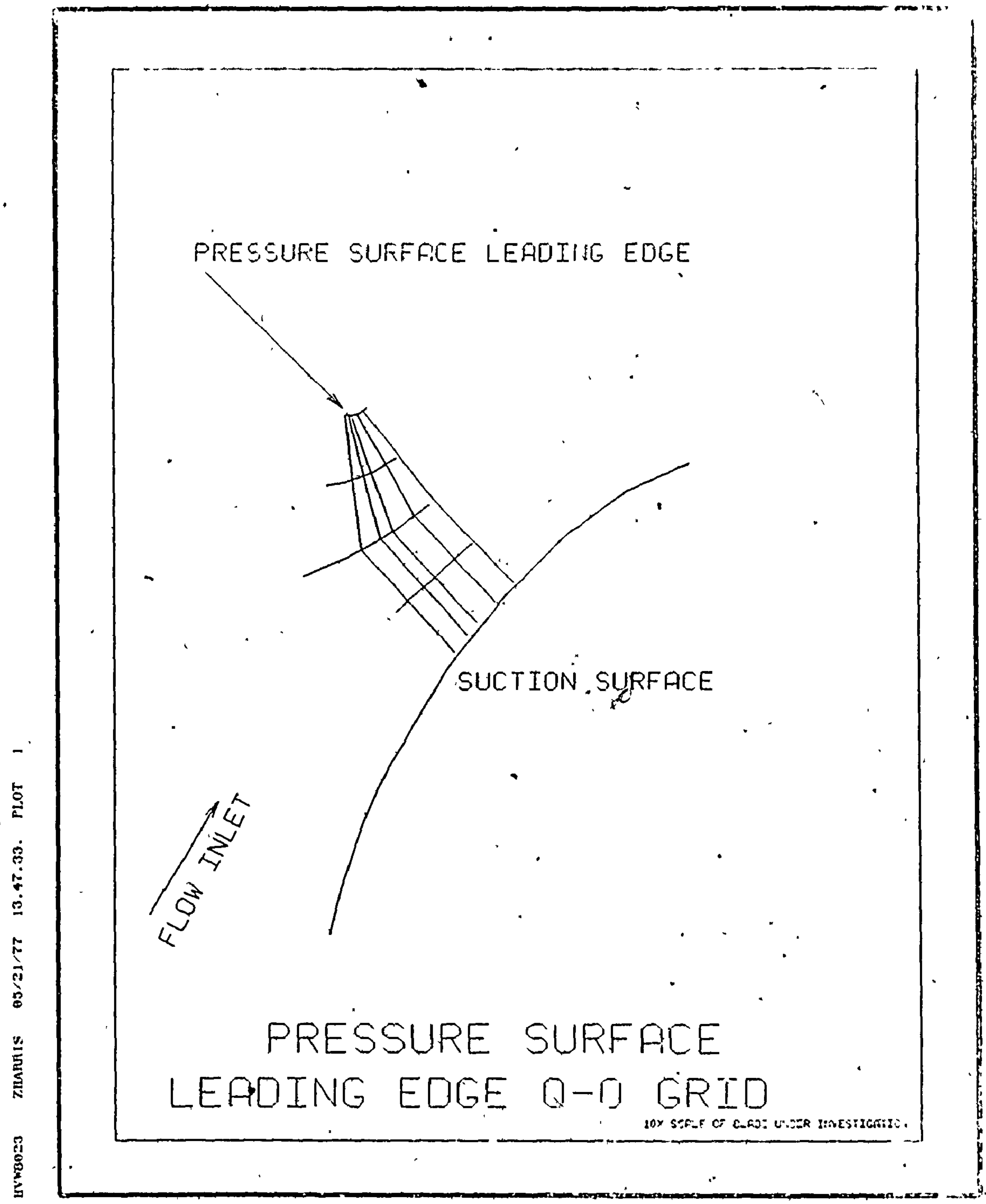

Figure 38 Plotter Output for Pressure Surface of Leading Edge

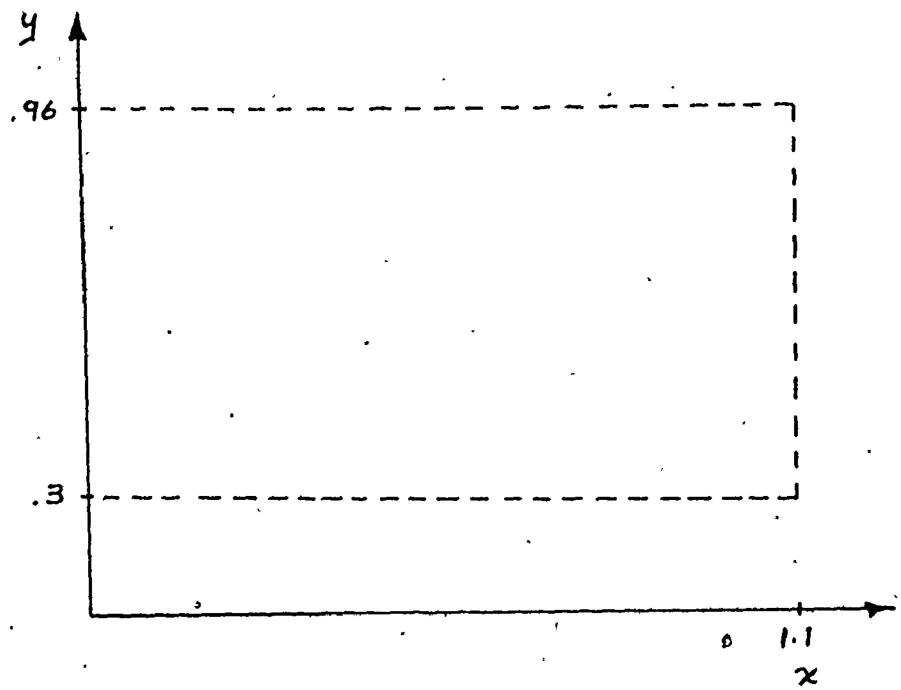

Figure 39 Range of Data for Small Pitches

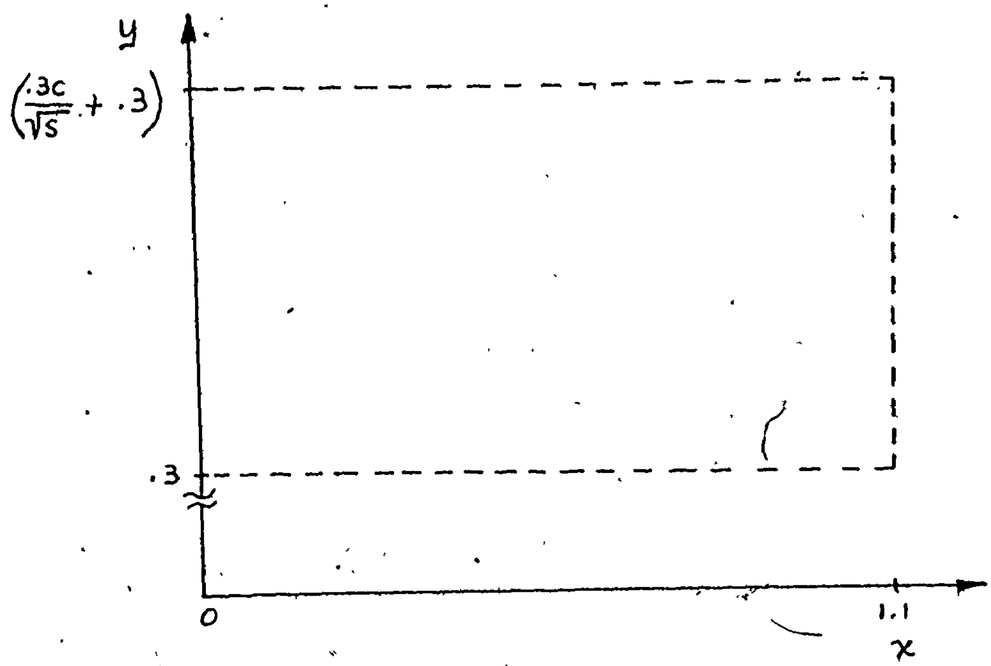

Figure 40 Range of Data for Large Pitches

APPENDIX III

REMAINDER OF EXPERIMENTAL DATA

Remainder of Pressure Drop Coefficient Data

INLET GAS ANGLE	ϕ_N^2	ϕ_N^2
	m = .43	m = .74
62.0^{o}	.049	.194
66.0^{o}	.042	.195
69.0^{o}	.032	.216

PRESSURE DISTRIBUTION DATA NOT GRAPHED

$P_{o_1}/P_{atm} = 1.29$

$M_{EXIT} \cong 2.73$

Pressure Port	Location % Axial Chord	P_s/P_{o_1}		
		$\beta=62^{\circ}$	$\beta=66^{\circ}$	$\beta=69^{\circ}$
P_1	4.8	.773	.785	.787
P_2	11.6	.787	.792	.787
P_3	18.6	.757	.766	.758
P_4	25.6	.796	.795	.792
P_5	33.9	.796	.800	.802
P_6	48.7	.666	.663	.656
P_7	61.3	.639	.640	.646
P_8	73.2	.743	.741	.748
P_9	81.8	.655	.641	.639
S_1	3.1	.746	.641	.580
S_2	6.8	.698	.578	.521
S_3	10.2	.712	.641	.616
S_4	14.0	.669	.646	.631
S_5	40.4	.465	.457	.466
S_6	68.5	.564	.557	.557
S_7	74.2	.552	.579	.582
S_8	84.5	.467	.465	.464

PRESSURE DISTRIBUTION DATA NOT GRAPHED

$P_{o_1}/P_{atm} = 2.03$

$M_{EXIT} = 1.06$

Pressure Port	Location % Axial Chord	P_s/P_{o_1}		
		$\beta=62^o$	$\beta=66^o$	$\beta=69^o$
P_1	4.8	.745	.772	.786
P_2	11.6	.792	.783	.791
P_3	18.6	.781	.778	.772
P_4	25.6	.762	.764	.652
P_5	33.9	.774	.778	.777
P_6	48.7	.722	.723	.722
P_7	61.3	.684	.686	.690
P_8	73.2	.705	.709	.702
P_9	81.8	.654	.656	.652
S_1	3.1	.743	.687	.553
S_2	6.8	.680	.579	.516
S_3	10.2	.702	.625	.586
S_4	14.0	.679	.632	.622
S_5	40.4	.440	.441	.442
S_6	68.5	.549	.546	.545
S_7	74.2	.567	.564	.560
S_8	84.5	.506	.499	.482

PRESSURE DISTRIBUTION DATA NOT GRAPHED

$P_{o_1}/P_{atm} = 1.81$

$M_{EXIT} \cong 0.96$

Pressure Port	Location % Axial Chord	P_s/P_{o_1}		
		$\beta=62^{o}$	$\beta=66^{o}$	$\beta=69^{o}$
P_1	4.8	.750	.775	.784
P_2	11.6	.774	.783	.782
P_3	18.6	.785	.784	.782
P_4	25.6	.776	.768	.773
P_5	33.9	.780	.780	.783
P_6	48.7	.743	.747	.743
P_7	61.3	.710	.724	.727
P_8	73.2	.726	.725	.724
P_9	81.8	.678	.673	.668
S_1	3.1	.743	.634	.544
S_2	6.8	.689	.602	.535
S_3	10.2	.699	.630	.589
S_4	14.0	.681	.645	.634
S_5	40.4	.458	.456	.463
S_6	68.5	.567	.565	.564
S_7	74.2	.582	.580	.575
S_8	84.5	.577	.573	.572

PRESSURE DISTRIBUTION DATA NOT GRAPHED

$P_{o_1}/P_{atm} = 1.50$

$M_{EXIT} \cong 0.78$

Pressure Port	Location % Axial Chord	P_s/P_{o_1}		
		$\beta=62^o$	$\beta=66^o$	$\beta=68.5^o$
P_1	4.8	.782	.806	.827
P_2	11.6	.805	.813	.823
P_3	18.6	.805	.812	.820
P_4	25.6	.796	.800	.808
P_5	33.9	.802	.809	.818
P_6	48.7	.791	.795	.805
P_7	61.3	.762	.770	.777
P_8	73.2	.766	.767	.774
P_9	81.8	.727	.727	.773
S_1	3.1	.753	.616	.601
S_2	6.8	.708	.616	.608
S_3	10.2	.715	.637	.634
S_4	14.0	.707	.668	.671
S_5	40.4	.539	.544	.553
S_6	68.5	.671	.636	.642
S_7	74.2	.657	.653	.699
S_8	84.5	.664	.659	.664

PRESSURE DISTRIBUTON DATA NOT GRAPHED

$P_{o_1}/P_{atm} = 1.14$

$M_{EXIT} \cong .43$

Pressure Port	Location % Axial Chord	P_s/P_{o_1}		
		$\beta=62^o$	$\beta=66^o$	$\beta=69^o$
P_1	4.8	.926	.941	.947
P_2	11.6	.931	.935	.934
P_3	18.6	.930	.933	.934
P_4	25.6	.930	.934	.932
P_5	33.9	.933	.935	.943
P_6	48.7	.930	.931	.947
P_7	61.3	.920	.924	.948
P_8	73.2	.919	.922	.958
P_9	81.8	.906	.906	.943
S_1	3.1	.891	.855	.826
S_2	6.8	.882	.854	.837
S_3	10.2	.878	.857	.844
S_4	14.0	.876	.863	.857
S_5	40.4	.820	.824	.826
S_6	68.5	.865	.865	.862
S_7	74.2	.850	.875	.870
S_8	84.5	.879	.877	.874

APPENDIX IV

POLYNOMIAL SELECTION CRITERIA

After unsuccessful attempts at fitting several overlapping polynomials to the set of blade surface data points (it was difficult to ensure a smooth change of slope between the curves), it was decided to use one polynomial for the whole range. However, it was found that the use of high order polynomial fits was not usually acceptable due to "ripples" between data points caused by a change in sign of the function's second derivative. Also the calculation of the higher order coefficients sometimes led to ill-conditioned Hermitian matrices which are not properly represented in the computer (tends to "blow up" as numbers greater than 10^{12} are encountered). This is especially true for LESQ. The library program ORLSQ allows higher order selection before the above problems become serious. It is unfortunate that high orders are not usable as Reference [24] states that "Although no completely general rule can be given it is frequently desirable to conduct polynomial fits using "an order" 1/2 to 3/4 that of the number of points to be fitted". Thus a 15^{th} order would originally have seemed desirable.

Due to the above limitations the following five general criteria were used in polynomial selection:

(1) the absolute error at any calculated point must be less than a specified value

(2) the sum of all of the absolute errors must be less than a specified amount

(3) the "null hypothesis" variable, as defined in Reference [23], should change by only a "small" amount when the polynomial order is increased by one

(4) no real zeros to the polynomial's second derivative should exist within the blade range. Imaginary zeros very close to the real plane also should be avoided as these may cause ripples to appear in the polynomial

(5) the change in slope between two consecutive interpolated polynomial points should be less than a specified amount.

For polynomial fits to "streamlines" within the flow passage, an additional constraint was that the total turning angle of the "streamline" should be between those of the passage boundaries. The subroutine CFIT uses these criteria in the selection of the polynomial order.

```
*** [illegible] ANGLE COMPUTATION ***
C THE [illegible] PROGRAM IS [illegible] THE BEST POLYNOMIAL FIT
C N POLYNOMIAL DEGREE
C N NUMBER OF DATA POINT
C CHS(I) = CHANGE IN THE VALUE OF SLOPE [illegible] LAST TWO DATA POINTS
C [illegible] SLOPE OF SLOPE CURVE USING LAST TWO DATA POINTS
C [illegible] CHANGE IN VALUE OF SLOPE OF SLOPE CURVE BETWEEN LAST TWO
C DATA POINTS
C [illegible] THE NULL HYPOTHESIS [illegible]
C [illegible] DECREASE OF THE NULL HYPOTHESIS [illegible]
C SINCE THE LAST POLY [illegible]
[illegible]
C READ DATA AND CALCULATE POLYNOMIALS COEFFICIENT
[illegible]
   80 FORMAT(///,1X,*THIS IS THE EVALUATION OF POLYNOMINAL ORDER *,I3)
[illegible]
      FORMAT(///,1X,*POLYNOMIAL COEFFICIENT*,[illegible])
[illegible]
   76 FORMAT([illegible] NO [illegible] COEFFICIENTS[illegible])
C CALCULATE NEW [illegible]
[illegible]
```

```
PROGRAM TST [illegible] 03/18/77 [illegible] PAGE 3

      FORMAT(1X,'[illegible] FOR THIS POLYNOMIAL [illegible] ARE SMALL ENOUGH'
     1/)
      MA=1
      GO TO [illegible]
   97 WRITE(6,99)
   99 FORMAT(1X,'THE [illegible] POLYNOMIAL ORDER ARE TOO LARGE'///)
  100 AT=[illegible]
      WRITE(6,[illegible])
   [illegible] FORMAT(1X,'THE TOTAL ABSOLUTE ERROR FOR THIS ORDER [illegible]
     1/)
      IF ([illegible].0.06) GO TO [illegible]
      WRITE(6,[illegible])
  101 FORMAT(1X,'THE TOTAL ERROR FOR THIS POLYNOMIAL [illegible] SMALL ENO
     1UGH'/)
      MA=1
      GO TO [illegible]
  [illegible] WRITE(6,[illegible])
  [illegible] FORMAT(1X,'THE TOTAL ERROR FOR THIS POLYNOMIAL ORDER IS TOO LARGE
     1'/)
  104 WRITE(6,[illegible])AT(M)
   [illegible] FORMAT(1X,'THE NULL HYPOTHESIS [illegible] SQUARE [illegible]
      IF (M.[illegible]) GO TO [illegible]
      [illegible]
    6 [illegible]
      WRITE (6,[illegible])
   [illegible] FORMAT(1X,'THE NULL HYPOTHESIS [illegible] SQUARE [illegible] BY [illegible]
     1[illegible] PER CENT'///////)
      WRITE(6,69)
   69 FORMAT(///)
   67 WRITE(6,34)
   34 FORMAT(1X,'THE FOLLOWING GRAPH PLOTS THE DEPENDENT DATA VARIABLE
     1AND THE [illegible] CALCULATED VALUE [illegible] THE INDEPENDENT VARIABLE')
      CALL [illegible]
      WRITE(6,35)
   35 FORMAT(1H1)
C
C     DEFINE NEW [illegible] AND COMPUTE [illegible]
C
      WRITE(6,[illegible])
   [illegible] FORMAT([illegible])
      DO [illegible]
      [illegible]
C
C     NOW Y VALUES ARE CALCULATED WITH A SMALLER [illegible]
C
      WRITE(6,[illegible])
  [illegible] FORMAT([illegible])
      [illegible]
      IF [illegible]
      DO [illegible]
      [illegible]
   [illegible] CONTINUE
   [illegible] [illegible]
      [illegible]


PROGRAM TST [illegible] 03/18/77 [illegible] PAGE 4

      IF [illegible] GO TO 57
      [illegible]
      GO TO [illegible]
C
C     NOW THE CHANGE IN SLOPE IS CALCULATED [illegible] THE LAST TWO DATA
C     POINTS
C
   [illegible] [illegible]
C
C     NOW THE SECOND DERIVATIVE [illegible] CALCULATED
C
   [illegible] [illegible]
     1[illegible]
     1[illegible]
     1[illegible]
      IF ([illegible]) GO TO 71
      IF ([illegible]) GO TO 71
C
C     [illegible] ARE THE [illegible] DERIVATIVE COEFFICIENTS [illegible]
C     [illegible] FOR INPUT TO THE [illegible] SUBPROGRAM PROLY
C
      [illegible]
   71 [illegible]
      [illegible]
      CALL [illegible]
   57 CONTINUE
      WRITE(6,[illegible])
   [illegible] FORMAT(////,[illegible])
      DO [illegible]
      WRITE(6,[illegible])
   [illegible] FORMAT([illegible]///)
   55 CONTINUE
      WRITE(6,[illegible])
   [illegible] FORMAT(///[illegible]'THE [illegible]
      CALL [illegible]
      WRITE [illegible]
   [illegible] FORMAT([illegible]'THE [illegible] CHANGE IN SLOPE [illegible]
     1[illegible] DATA POINT'////)
      WRITE(6,[illegible])
   [illegible] FORMAT([illegible]
     1[illegible]////)
      DO [illegible]
      [illegible]
      [illegible]
      WRITE [illegible]
   [illegible] FORMAT([illegible])
      CONTINUE
      IF [illegible] GO TO 116
   [illegible] CONTINUE
      WRITE(6,[illegible])
  [illegible] FORMAT(///[illegible]'THE CHANGE IN SLOPE IS [illegible] ENOUGH FOR THE [illegible]
     1[illegible]')
      MA=1
      [illegible]
  116 [illegible]
```

```
PROGRAM TST        73/73    OPT=1 ROUND=+-*/        FTN 4.6+452        05/18/77  13.51.39        PAGE    5

  114   FORMAT(//,1X,*THE [illegible] OF THE [illegible] THAT OCCUR IS [illegible]
       1[illegible] ACCEPTABLE *//)
C     FOR THE ZEROS OF THE SECOND DERIVATIVE ARE DETERMINED
  118 IF (M.[illegible]) GO TO 113
      CALL ZPOLY(P,M,[illegible],ZERO,ZEROI,FAIL)
      WRITE (6,72)(ZERO(J),J=1,M2)
   72 FORMAT(1H5,2X,*THE REAL PARTS OF THE ZEROS OF THE SECOND DERIVATIV
     1E ARE *///,3(E16.5///),2X//////)
      WRITE (6,73)(ZEROI(J),J=1,M2)
   73 FORMAT(///1X,*THE IMAGINARY PARTS OF THE ZEROS OF THE SECOND DERI
     1VATIVE ARE *///,3(E16.5///),2X,//////)
      WRITE(6,74)FAIL
   74 FORMAT(1X,L3////)
C     INDICATES THAT ZPOLY FUNCTIONS PROPERLY, AND [illegible] THAT IT
C     DID NOT
      J=0
  145 J=J+1
      IF(ZEROI(J).[illegible]) GO TO 127
      IF (J.LT.M2)GO TO 145
      GO TO 90
  127 IF(ZERO(J).GT.[illegible])GO TO 130
      IF(ZERO(J).LT.0.)GO TO 130
      MAN=1
  130 IF (J.LT.M2)GO TO 145
   90 IF(MAN.EQ.1)GO TO 905
      WRITE(6,137)
  137 FORMAT(///,1X,*THERE ARE NO ZEROS TO THE SECOND DERIVATIVE WITHIN
     1 THE PLACE RANGE FOR THIS POLYNOMINAL APPROXIMATION*///)
      MAN=1
      GO TO 915
  905 WRITE(6,125)
  125 FORMAT(///,1X,*THERE IS A ZERO TO THE SECOND DERIVATIVE WITHIN TH
     1E PLACE RANGE FOR THIS POLYNOMINAL APPROXIMATION*//)
      MAN=3
  915 WRITE(6,44)
   44 FORMAT(///1X,*THE FOLLOWING GRAPH SHOWS THE VARIATION OF ABSOLUTE
     1 SLOPE VS THE INDEPENDENT VARIABLE*)
      CALL OUTPLT
C     COMPUTE INCREMENTAL TURNING ANGLE AND RADIUS OF CURVATURE AT XX
C
      TTA=0.
      [illegible]=1
      WRITE(6,64)
   64 FORMAT(1H1,1X,*R(I) IS THE RADIUS OF CURVATURE*////)
      WRITE(6,52)
   52 FORMAT(5X,*I*,6X,*X(I)*,5X,*R(I)*////)
      DO 40 I=1,NM
      K=I-1
      XX(I)=(DX/2.0)+DX*FLOAT(K)
      [illegible]=XX(I)
      YY(I)=Y1(TY)
      APD(I)=S(I+1)-S(I)

PROGRAM TST        73/73    OPT=1 ROUND=+-*/        FTN 4.6+452        05/18/77  13.51.39        PAGE    6

      APR(I)=ABS(APD(I))*3.14159/180.0
      R(I)=(SQRT((X(I+1)-X(I))**2+(YY(I+1)-YY(I))**2))/(2*TAN(APR(I)/2))
      WRITE(6,46)I,X(I),R(I)
   46 FORMAT(5X,I3,2F10.4)
      C(I)=1.0/R(I)
      TTA=TTA+APD(I)
      XPLT=XX(I)
      YPLT=C(I)
      CALL PLOTPT(XPLT,YPLT,8)
   40 CONTINUE
      WRITE(6,66)
   66 FORMAT(1X,*THE FOLLOWING GRAPH SHOWS THE VARIATION OF RADIUS OF
     1 CURVATURE VS THE INDEPENDENT VARIABLE*)
      CALL OUTPLT
      WRITE(6,70) TTA
   70 FORMAT(1X///,5X,*TOTAL TURNING ANGLE =*,F13.4/)
      IF (TTA.LT.-35.) GO TO 136
      IF (TTA.GT.+35.)GO TO 136
      WRITE(6,140)
  140 FORMAT(///,1X,*THE TOTAL TURNING ANGLE IS WITHIN THE ACCEPTABLE RA
     1NGE FOR THIS POLYNOMINAL ORDER APPROXIMATION*//)
      MAS=1
      GO TO 430
  136 WRITE(6,150)
  150 FORMAT(///,1X,*THE TOTAL TURNING ANGLE FOR THIS POLYNOMINAL APPROX
     1IMATION IS OUT OF THE ACCEPTABLE RANGE*//)
  430 MAAPAS=MAS+MAS+MAN+MAS
      IF (MA.[illegible]) GO TO 420
      WRITE(6,400)
  400 FORMAT(///,1X,*THE POLYNOMINAL ORDER APPROXIMATION IS ACCEPTA
     1BLE [illegible]*//////)
      GO TO [illegible]
  420 WRITE(6,425)
  425 FORMAT(///,1X,*THE POLYNOMINAL ORDER APPROXIMATION IS NOT ACCEPTA
     1BLE*//)
   45 RETURN
      STOP
      END
```

THE [illegible] VARIATION OF POLYNOMIAL [illegible]

POLYNOMIAL COEFFICIENT

.[illegible] .[illegible] -.[illegible] -.[illegible] .17866[illegible]

-.[illegible] .[illegible]

SECOND DERIVATIVE COEFFICIENT

-.[illegible] -.[illegible] .[illegible] -.[illegible] .[illegible]

YF(I) IS THE CALCULATED Y COORDINATE, E(I) IS THE ERROR OF THE CALCULATED POINT AWAY FROM THE DATA POINT

I	X(I)	Y(I)	YF(I)	E(I)	PERCENT E(I)
1	.1339	.9664	.[illegible]	.[illegible]	.0047
2	.1598	.9663	.9663	-.[illegible]	-.3037
3	.1860	.9815	.9815	.[illegible]	.0024
4	.2124	.9971	.[illegible]	-.0001	-.0136
5	.2390	1.0165	1.[illegible]	.[illegible]	.0015
6	.2656	1.0215	1.[illegible]	.[illegible]	.0027
7	.2921	1.0366	1.[illegible]	.[illegible]	.0042
8	.3186	1.0377	1.[illegible]	.[illegible]	.0070
9	.3449	1.0679	1.[illegible]	.[illegible]	.0036
10	.37[illegible]	1.06[illegible]	1.[illegible]	.[illegible]	.0017
11	.3973	1.0677	1.[illegible]	.[illegible]	.0017
12	.4236	1.0676	1.[illegible]	-.[illegible]	-.[illegible]
13	.4495	1.06[illegible]	1.06[illegible]	-.[illegible]	-.3013
14	.4756	1.[illegible]	1.0[illegible]	-.[illegible]	-.0079
15	.5017	1.[illegible]	1.[illegible]	-.[illegible]	-.0036
16	.5268	1.02[illegible]	1.[illegible]	-.[illegible]	-.0049
17	.5521	1.0141	1.[illegible]	.[illegible]	.0015
18	.5772	1.0061	1.0051	.[illegible]	.0024
19	.6020	.99[illegible]	.[illegible]	.0000	.0001
20	.6264	.9806	.[illegible]	.[illegible]	.3105
21	.6505	.9641	.9642	.0001	.3141
22	.6743	.[illegible]	.[illegible]	.[illegible]	.0056
23	.6974	.92[illegible]	.9256	.[illegible]	.0049
24	.7212	.9071	.9330	-.[illegible]	-.0131
25	.7442	.87[illegible]	.8736	-.[illegible]	-.3062
26	.7663	.8519	.[illegible]	-.[illegible]	-.[illegible]
27	.7[illegible]	.[illegible]	.[illegible]	-.[illegible]	-.[illegible]
28	.9116	.7913	.7[illegible]	-.[illegible]	-.[illegible]
29	.8[illegible]	.7[illegible]	.7[illegible]	.[illegible]	.0059
30	.8565	.7[illegible]	.7[illegible]	.[illegible]	.[illegible]
31	.[illegible]	.[illegible]	.[illegible]	.[illegible]	.015[illegible]
32	.9966	.[illegible]	.[illegible]	-.[illegible]	-.0025
33	.9176	.[illegible]	.[illegible]	-.[illegible]	-.[illegible]
34	.[illegible]	.[illegible]	.[illegible]	.[illegible]	.0057

THE ERRORS FOR THIS POLYNOMIAL [illegible] ARE SMALL ENOUGH

THE TOTAL ABSOLUTE ERROR FOR THIS POLYNOMIAL IS .[illegible]

THE TOTAL ERROR FOR THIS POLYNOMIAL [illegible] IS SMALL ENOUGH

THE NULL HYPOTHESIS [illegible] SQUARE IS .[illegible]

THE NULL HYPOTHESIS [illegible] SQUARE HAS DECREASED BY .[illegible] [illegible] PERCENT

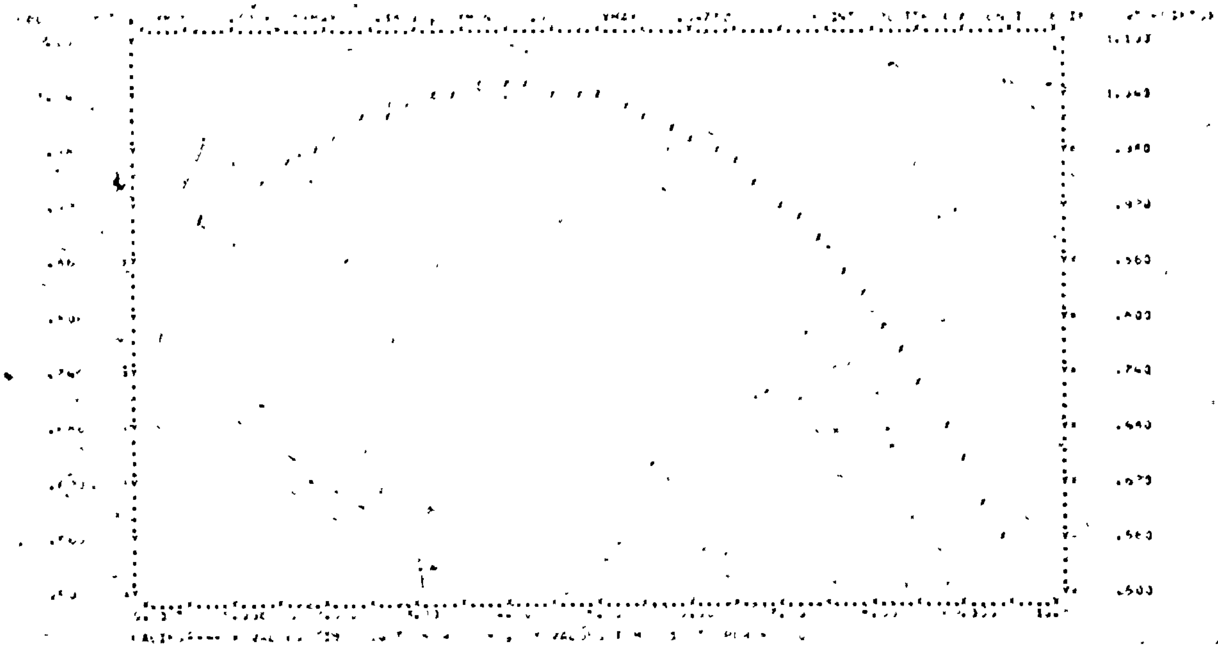

[illegible]

I	X(I)	Y(I)	Y'(I)	Y''(I)	Y'''(I)
1	.0000	[illegible]	1.[illegible]	[illegible]	-3.[illegible]
2	.0200	[illegible]	1.[illegible]	-1.67[illegible]	-3.[illegible]
3	.0400	49.[illegible]	1.0411	-1.[illegible]	-3.[illegible]
4	.0600	[illegible]	1.[illegible]	-1.9177	-3.[illegible]
5	.0800	[illegible]	.9055	[illegible]	-3.[illegible]
6	.1000	[illegible]	.[illegible]	-2.1615	-3.[illegible]
7	.1200	40.[illegible]	.[illegible]	-2.2771	-3.5111
8	.1400	37.[illegible]	.7[illegible]	-2.[illegible]	-3.[illegible]
9	.1600	[illegible]	.7310	[illegible]	-3.[illegible]
10	.1800	[illegible]	.[illegible]	[illegible]	-3.[illegible]
11	.2000	30.20[illegible]	[illegible]	[illegible]	-3.[illegible]
12	.2200	27.[illegible]	[illegible]	-2.7618	-3.[illegible]
13	.2400	[illegible]	[illegible]	-2.[illegible]	-3.[illegible]
14	.2600	21.73[illegible]	.[illegible]	-2.[illegible]	-2.9[illegible]
15	.2800	18.[illegible]	.3606	[illegible]	-2.[illegible]
16	.3000	15.[illegible]	.[illegible]	[illegible]	-2.5[illegible]
17	.3200	12.[illegible]	.[illegible]	[illegible]	-2.7457
18	.3400	[illegible]	.[illegible]	[illegible]	-2.[illegible]
19	.3600	[illegible]	.1[illegible]	-3.0036	-2.6606
20	.3800	5.[illegible]	.0675	-3.[illegible]	-2.6[illegible]
21	.4000	.[illegible]	.[illegible]	-3.[illegible]	-2.6215
22	.4200	-2.[illegible]	-.0375	-3.[illegible]	-2.[illegible]
23	.4400	-5.[illegible]	-.[illegible]	-2.9971	-2.6345
24	.4600	-9.1363	-.1629	[illegible]	-2.[illegible]
25	.4800	-11.[illegible]	-.1966	-2.[illegible]	-2.[illegible]
26	.5000	-14.1091	-.[illegible]	-2.[illegible]	-2.7633
27	[illegible]	-17.[illegible]	[illegible]	[illegible]	[illegible]
28	[illegible]	[illegible]	[illegible]	[illegible]	[illegible]
29	[illegible]	[illegible]	[illegible]	[illegible]	[illegible]
30	[illegible]	[illegible]	[illegible]	[illegible]	[illegible]
31	[illegible]	[illegible]	[illegible]	[illegible]	[illegible]
32	[illegible]	[illegible]	[illegible]	[illegible]	[illegible]
33	[illegible]	[illegible]	[illegible]	[illegible]	-3.[illegible]
34	[illegible]	[illegible]	[illegible]	[illegible]	-3.7[illegible]
35	[illegible]	[illegible]	[illegible]	[illegible]	[illegible]
36	[illegible]	[illegible]	[illegible]	[illegible]	[illegible]
37	[illegible]	[illegible]	[illegible]	[illegible]	[illegible]
38	[illegible]	[illegible]	[illegible]	[illegible]	[illegible]
39	[illegible]	[illegible]	[illegible]	[illegible]	[illegible]
40	[illegible]	[illegible]	[illegible]	[illegible]	[illegible]
41	[illegible]	[illegible]	[illegible]	[illegible]	-5.[illegible]
42	[illegible]	[illegible]	[illegible]	[illegible]	-5.7[illegible]
43	[illegible]	[illegible]	[illegible]	[illegible]	-6.[illegible]
44	[illegible]	[illegible]	[illegible]	[illegible]	[illegible]
45	[illegible]	[illegible]	[illegible]	[illegible]	[illegible]
46	[illegible]	-63.7[illegible]	[illegible]	1.[illegible]	-6.9[illegible]
47	[illegible]	[illegible]	[illegible]	1.[illegible]	-7.2515
48	[illegible]	[illegible]	[illegible]	1.[illegible]	-7.[illegible]
49	[illegible]	[illegible]	[illegible]	1.[illegible]	-7.8660
50	[illegible]	[illegible]	[illegible]	1.[illegible]	-8.16[illegible]

* THE CHANGE IN SLOPE [illegible] ACTUAL [illegible] THE POLYNOMIAL TO BE ACCEPTABLE

THE REAL PARTS OF THE ZEROS OF THE SECOND DERIVATIVE ARE

[illegible]   [illegible]   [illegible]   [illegible]

THE IMAGINARY PARTS OF THE ZEROS OF THE SECOND DERIVATIVE ARE

0.   .15[illegible]   -.15[illegible]   0.

THERE ARE NO ZEROS TO THE SECOND DERIVATIVE WITHIN THE [illegible] OF THIS POLYNOMIAL APPROXIMATION

THE FOLLOWING GRAPH SHOWS THE [illegible] VS THE INDEPENDENT VARIABLE

SCALED LIMITS, XMIN= [illegible] XMAX= [illegible] YMIN= [illegible] YMAX= [illegible] 50 POINTS PLOTTED [illegible] DENOTES COINCIDENT POINTS)

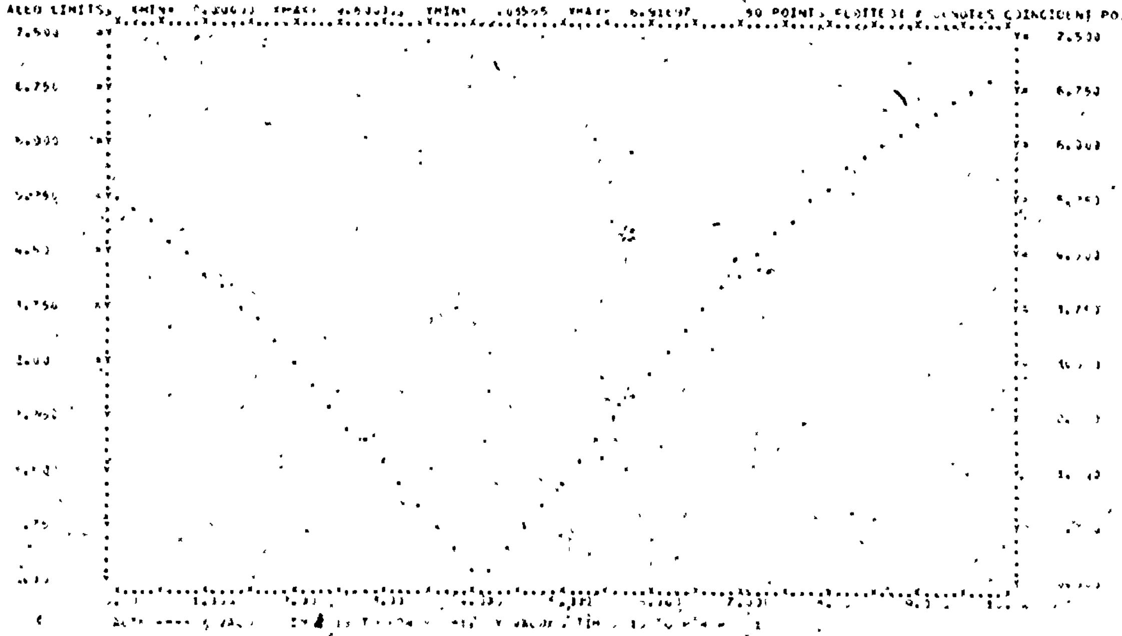

[illegible]

I	X(I)	Y(I)
1	.0100	1.[illegible]
2	.0300	[illegible]
3	.0500	[illegible]
4	.0700	[illegible]
5	.0900	.7[illegible]
6	.1100	[illegible]
7	.1300	[illegible]
8	.1500	[illegible]
9	.1700	[illegible]
10	.1900	.5023
11	.2100	.47[illegible]
12	.2300	.45[illegible]
13	.2500	.4[illegible]
14	.2700	.417[illegible]
15	.2900	.40[illegible]6
16	.3100	.3965
17	.3300	.3903
18	.3500	.3865
19	.3700	.38[illegible]
20	.3900	.3816
21	.4100	.3817
22	.4300	.383[illegible]
23	.4500	.3865
24	.4700	.3890
25	.4900	.39[illegible]
26	.5100	.3995
27	.5300	.4075
28	[illegible]	.4171
29	[illegible]	[illegible]
30	[illegible]	[illegible]
31	[illegible]	[illegible]
32	[illegible]	[illegible]
33	[illegible]	[illegible]
34	[illegible]	[illegible]
35	[illegible]	[illegible]
36	[illegible]	[illegible]
37	[illegible]	[illegible]
38	[illegible]	[illegible]
39	[illegible]	[illegible]
40	[illegible]	[illegible]
41	[illegible]	[illegible]
42	[illegible]	1.161[illegible]
43	[illegible]	1.[illegible]
44	[illegible]	1.[illegible]
45	[illegible]	1.[illegible]
46	[illegible]	1.7[illegible]
47	[illegible]	1.[illegible]
48	[illegible]	2.[illegible]
49	[illegible]	[illegible]

THE FOLLOWING GRAPH SHOWS THE VARIATION [illegible] VS. THE INDEPENDENT VARIABLE

SCALED LIMITS, XMIN= .10000, XMAX= 9.7[illegible], YMIN= .[illegible], YMAX= [illegible] 49 POINTS PLOTTED # DENOTES COINCIDENT POINTS)

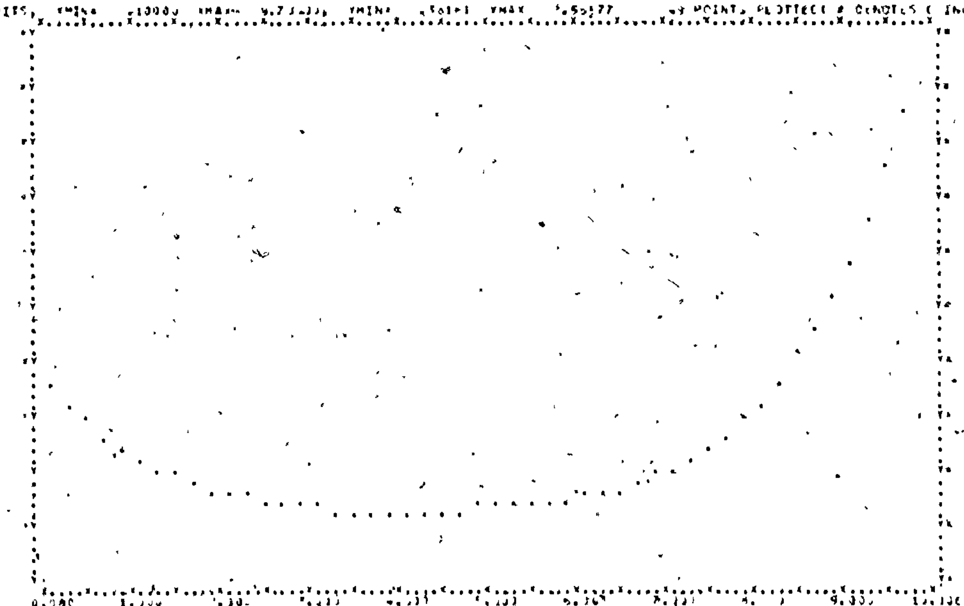

SCALING--- X VALUES TIMES 10 TO POWER [illegible] Y VALUES TIMES 10 TO POWER [illegible]

TOTAL TURNING ANGLE [illegible]

THE TOTAL TURNING ANGLE IS WITHIN [illegible] THIS POLYNOMIAL [illegible] APPROXIMATION

THIS POLYNOMIAL [illegible] APPROXIMATION [illegible]

```
      PROGRAM TST (INPUT,OUTPUT,TAPE5=INPUT,TAPE6=OUTPUT)
      DIMENSION W(3),EPS(9),T(9),AMACH(9),PREP(9),
     1RO(50),CS(50),CAU,C(50),RT(9),A(9),RO(9)
      DIMENSION AMACE(50),AMACS(50)
      DIMENSION Y(50),PRS(50),CSS(50),XX(50),XY(50)
      DIMENSION XS(50),XP(50)
      READ (5,15)RETORT,PEXIT,AMACHIN,RELTOT,DELTA
      READ (5,16) GASC,G,GAMMA,SPACE,JX
      READ(5,17)ACC,GAGE,THROAT,RATIO,AMCRIT,NDATA
15    FORMAT(5F8.4)
16    FORMAT(4F8.4,I2)
17    FORMAT(5F8.4,I4)
C
C
C     USEFUL CONSTANTS AND CHOKING MASS FLOW ARE CALCULATED
C
C
      C1=2.0*GAMMA*GASC*G
      C3=GAMMA-1.0
      C2=GAMMA/C3
      C4=GAMMA+1.0
      CMAS=(((GAMMA*G)/(GASC*RELTOT))**0.5)*THROAT*RETORT*12.0/1.728
      WRITE(6,21)   CMAS
      WRITE(6,999)
      WRITE(6,999)
      WRITE(6,22)RETORT,PEXIT,AMACHIN,RELTOT,DELTA
      WRITE(6,999)
      WRITE(6,23) GASC,G,GAMMA,SPACE,JX
      WRITE(6,999)
      WRITE(6,25)ACC,GAGE,THROAT,RATIO,AMCRIT,NDATA
      WRITE(6,999)
C
C
C     THE DESIGN MASS FLOW IS CALCULATED AND THE SURFACE CURVATURES AND
C     QUASI-ORTHOGONAL LENGTH READ IN
C
C
      AT=RELTOT/(1+(C3*(AMACHIN**2.0))/2.0)
      AP=RETORT*(AT/RELTOT)**C2
      RO=AP/GASC/AT*144
      AV=AMACHIN*((GAMMA*GASC*G*AT)**0.5)
      AMAS=RO*AV*GAGE/12.0
      WRITE(6,24)AMAS
      WRITE(6,999)
      DO 500 K=1,NDATA
      READ(5,240)CP(K),CS(K),GAUGE(K),XS(K),XP(K)
      WRITE(6,999)
      WRITE(6,999)
      WRITE(6,999)
      WRITE(6,999)
      WRITE(6,26)
      WRITE(6,999)
      WRITE(6,241)CP(K),CS(K),GAUGE(K)
      WRITE(6,999)
      WRITE(6,999)
      IF(GAUGE(K)-THROAT) 63,63,62
63    IF(AMCRIT-AMACHIN) 64,64,62
C
C
62    W(5)=AV*GAGE/GAUGE(K)
51    IF(((W(5)**2)*C3/C1).LT.(RELTOT)) GOTO 52
      W(5)=W(5)/2.0
      GOTO 51
52    CONTINUE
55    W(5)=W(5)*RATIO
C
C
C
C
      DO 335 I=1,9
53    J=I
      DELG=(J-1.0)*GAUGE(K)/8.0
      IF(JX.EQ.2) GOTO 57
54    POW=GAUGE(K)*((CS(K)*(1.0/8.0-DELG/GAUGE(K))+.125*CP(K)-.5*
     *(CP(K)-CS(K))*(DELG/GAUGE(K))**2.0)
49    W(I)=W(5)*EXP(POW)
      GOTO 60
57    IF(CP(K)-CS(K))58,59,58
58    W(I)=W(5)*(2.0*(CP(K)+(CS(K)-CP(K))*DELG/GAUGE(K))/(CP(K)+
     *CS(K)))**(GAUGE(K)*CS(K)*CP(K)/(CP(K)-CS(K)))
      GOTO 60
59    POW=GAUGE(K)*(.5-DELG/GAUGE(K))*CS(K)
      GOTO 49
60    DELT(F=RETORT
      RT(I)=RELTOT-(W(I)**2)*C3/C1
      A(I)=(GAMMA*GASC*G*RT(I))**0.5
      AMACH(I)=W(I)/A(I)
      PRE(I)=RELTOP/(RELTOT/RT(I))**C2
      PREP(I)=PRE(I)/RELTOP
      RO(I)=144.0*PRE(I)/(GASC*RT(I))
      Z(I)=RO(I)*W(I)
335   CMAS(K)=((Z(1)+Z(9))*0.29760+(Z(2)+Z(8))-0.03274*(Z(3)+
     *Z(7))+.1012)*(Z(4)+Z(6))-0.16.14*Z(5))*GAUGE(K)/12.0
C
C
      RATIO=2.0-(CMAS/AMAS)
      IF(ABS(AMAS-CMAS).GT.ACC) GOTO 61
      GOTO 66
C
C
64    DO 345 I=1,9
      RT(5)=RELTOT*2.0/(GAMMA+1.0)
      A(5)=(GAMMA*GASC*G*RT(5))**0.5
      J=I
      DELG=(J-1.0)/8.0
      POW=GAUGE(K)*((CP(K)+CS(K)-2.0*CS(K)*DELG-(CP(K)-CS(K))*(DELG**2))
      W(I)=W(5)*EXP(POW)
      DELTOP=RETORT
      RT(I)=RELTOT-(W(I)**2.0)*C3/C1
      A(I)=(GAMMA*GASC*G*RT(I))**0.5
      AMACH(I)=W(I)/A(I)
      PRE(I)=RELTOP/(RELTOT/RT(I))**C2
```

```
      DRPR(I)=RPR(I)/PLLTCP
      RC(I)=144.0*RPR(I)/(GASC*RT(I))
 245  Z(I)=RO(I)*W(I)
      THAS=(.03499*(Z(1)+Z(9))+.20769*(Z(2)+Z(8))-.02273*(Z(3)+Z(7))
     *+.37C2**(Z(4)+Z(6))-.16014*(Z(5)))*GAUGE(K)/12.0
C
C
 61   WRITE(6,22)THAS
      WRITE(6,999)
      WRITE(6,999)
      WRITE(6,30)
      WRITE(6,999)
      DO 26 I=1,9
 21   FORMAT(1H1,40X,10HINPUT DATA/40X,10H----------//*
     *CHOKING MASS FLOW RATE =*,F10.3)
 22   FORMAT(5F8.3)
 23   FORMAT(4F8.4,I2)
 24   FORMAT(1H1,40X,11HOUTPUT DATA/40X,11H-----------//*
     *DESIGN MASS FLOW RATE =*,F10.3)
 25   FORMAT(5F8.4,I8)
 26   WRITE(6,29)RPR(I),AMACH(I),W(I),DRPR(I),RT(I),RO(I)
 27   FORMAT(1H0,20X,*CALCULATED MASS FLOW RATE =*,F10.3)
 28   FORMAT(1H0,20X,*CP(K)          CS(K)          GAUGE(K)*)
 29   FORMAT(1H0,12X,F10.3,1X,F10.3,3X,F10.3,1X,F6.3,3X,F10.3,3X,
     1F6.3)
 30   FORMAT(1H0,*                          RPR(I)       AMACH(I)       W(I)       DRPR(
     *I)         RT(I)         RO(I)*)
 240  FORMAT(5F10.4)
 241  FORMAT(16X,3F10.4)
 999  FORMAT(10X,*   *)
      HI=FLOAT(K)-1.
      AMACP(K)=AMACH(9)+0.6
      AMACS(K)=AMACH(1)+0.6
      XS(K)=XS(K)+0.5
      XP(K)=XP(K)+0.5
      RSS(K)=RPR(1)+15.
      RPS(K)=RPR(9)+15.
 980  CONTINUE
      ZK=5.
      CALL MARG(ZK)
      CALL PLTLN(0.5,15.,11.55,15.)
      CALL PLTLN(0.5,15.,0.5,45.)
      AREA=0.
      NDAT=NDATA-1.
      DO 1 K=1,NDAT
      IF(XP(K).LT.0.5)GO TO 1
      CALL PLTLN(XP(K),RPS(K),XP(K+1),RPS(K+1))
      AREA=(XP(K+1)-XP(K))*((RPS(K)-15.)+(RPS(K+1)-15.))/2.+AREA
 1    CONTINUE
      CALL NEWPEN(1)
      DO 2 K=1,NDAT
      CALL PLTLN(XS(K),RSS(K),XS(K+1),RSS(K+1))
      AREA=AREA-(XS(K+1)-XS(K))*((RSS(K)-15.)+(RSS(K+1)-15.))/2.
 2    CONTINUE
      WRITE(6,5)AREA
 5    FORMAT(1X,///,5X,*THE LIFT FORCE PER INCH BLADE LENGTH IS *,E12.6,
     1* POUNDS FORCE*,/)
      DO 3 N=1,10
      RN=FLOAT(N)
      YY(N)=15.
      XX(N)=RN/10.+0.5
 3    CONTINUE
      CALL NEWPEN(3)
      CALL PLTMSP(XX,YY,.15,1H-,90.,10)
      DO 4 N=1,6
      RN=FLOAT(N)
      YY(N)=(RN/6.)*30.+15.
      XX(N)=0.5
 4    CONTINUE
      CALL PLTMSP(XX,YY,.15,1H-,0.,6)
      CALL LETTER(30,.15,0.,4.,2.5,30HNON DIMENSIONAL AXIAL DISTANCE)
      CALL LETTER(14,.15,90.,.9,4.45,14HPRESSURE(PSIG))
      CALL LETTER(3,.1,0.,6.4,2.75,3H0.5)
      CALL LETTER(3,.1,0.,11.4,2.75,3H1.0)
      CALL LETTER(3,.15,0.,1.0,2.8,3H0.0)
      CALL LETTER(2,0.1,90.,1.3,4.9,2H10)
      CALL LETTER(2,0.1,90.,1.3,6.9,2H20)
      CALL LETTER(42,.2,0.,2.05,9.3,42HPRESSURE DISTRIBUTION ALONG BLADE
     1 SURFACES)
      CALL LETTER(35,.15,0.,6.6,8.60,35HUPPER CURVE IS FOR PRESSURE SURF
     1ACE)
      CALL NEWPEN(1)
      CALL LETTER(34,.15,0.,6.6,8.25,34HLOWER CURVE IS FOR SUCTION SURFA
     1CE)
      CALL PLOT(14.,0.,-3)
      ZK=0.2
      CALL MARG(ZK)
      CALL PLTLN(0.5,0.6,1.55,0.6)
      CALL PLTLN(0.5,0.6,0.5,1.8)
      DO 6 K=1,NDAT
      IF(XP(K).LT.0.5)GO TO 6
      CALL PLTLN(XP(K),AMACP(K),XP(K+1),AMACP(K+1))
 6    CONTINUE
      CALL NEWPEN(1)
      DO 7 K=1,NDAT
      CALL PLTLN(XS(K),AMACS(K),XS(K+1),AMACS(K+1))
 7    CONTINUE
      DO 8 N=1,10
      RN=FLOAT(N)
      YY(N)=0.6
      XX(N)=RN/10.+0.5
      CALL NEWPEN(3)
 8    CONTINUE
      CALL PLTMSP(XX,YY,.15,1H-,90.,10)
      DO 9 N=1,6
      RN=FLOAT(N)
      YY(N)=(RN/6.)*1.2+0.6
      XX(N)=0.5
 9    CONTINUE
      CALL PLTMSP(XX,YY,.15,1H-,0.,6)
      CALL LETTER(30,.15,0.,4.,2.5,30HNON DIMENSIONAL AXIAL DISTANCE)
      CALL LETTER(8,.15,90.,.9,4.45,8HMACH NO.)
      CALL LETTER(3,.1,0.,6.4,2.75,3H0.5)
      CALL LETTER(3,.1,0.,11.4,2.75,3H1.0)
      CALL LETTER(3,.15,0.,1.0,2.8,3H0.0)
      CALL LETTER(3,0.1,90.,1.3,4.9,3H0.4)
      CALL LETTER(3,0.1,90.,1.3,6.9,3H0.8)
      CALL LETTER(3,0.1,90.,1.3,8.9,3H1.2)
      CALL LETTER(42,.2,0.,2.05,9.3,42HMACH NO. DISTRIBUTION ALONG BLADE
     1 SURFACES)
      CALL PLOT(14.,0.,-3)
      CALL PLOT(14.,0.,999)
      STOP
      END
```

```
SUBROUTINE MARG(A)
CALL NEWPEN(3)
CALL PLOT(0.,0.0?,3)
CALL PLOT(0.,10.5?,2)
CALL PLOT(13.0,10.5?,2)
CALL PLOT(13.0,0.0?,2)
CALL PLOT(0.,0.0?,2)
IA=12.*A
CALL PLTIN(0.1?,A,0.??,0.,?.?0,1.70,0.,IA)
CALL INCHTO(?.?,0.?,XMN,YMN)
CALL INCHTO(12.?,10.0,XMX,YMX)
CALL NEWPEN(1)
CALL PLTLN(XMN,YMN,XMN,YMX)
CALL PLTLN(XMN,YMX,XMX,YMX)
CALL PLTLN(XMX,YMX,XMX,YMN)
CALL PLTLN(XMX,YMN,XMN,YMN)
RETURN
END
```

INPUT DATA

CHOKING MASS FLOW RAT = 1.385

29.830 14.690 .??0 510.0?? ?.010

53.3530 32.1600 1.4000 .480? 1

.0810 .2106 .1675 1.0000 .5450 19

OUTPUT DATA

DESIGN MASS FLOW RATE = 1.38?

CP(K)	CF(K)	GAUCE(K)
.0070	1.163?	.169?

CALCULATED MASS FLOW RATE = 1.38?

RPR(I)	AMACH(I)	W(I)	CRPR(I)	RT(I)	RO(I)
21.33?	.709	76?.31?	.715	481.617	.120
21.72?	.6?9	74?.?03	.72?	484.099	.121
22.04?	.672	72?.742	.735	486.148	.122
22.313	.65?	711.?52	.748	48?.810	.123
22.524	.646	70?.?90	.755	489.124	.124
22.68?	.6??	692.10?	.760	490.119	.125
22.79?	.612	685.034	.764	490.?15	.125
22.86?	.62?	68?.495	.767	491.229	.126
22.8??	.62?	6?1.17?	.767	491.360	.126

CP(K)	CF(K)	GAUCE(K)
.0820	1.400?	.1?4?

CALCULATEC MASS FLOW RATE = 1.3?7

RPR(I)	AMACH(I)	W(I)	CRPR(I)	RT(I)	RO(I)
20.31?	.762	?1?.?05	.6?1	474.?7?	.115
20.799	.73?	7??.?5?	.697	47?.110	.117
21.20?	.716	769.?1?	.711	4?0.762	.119
21.537	.69?	752.1??	.722	482.901	.120
21.881	.6??	73?.59?	.731	484.?82	.121
22.001	.674	72?.21?	.738	485.?49	.122
22.141	.667	72?.?4?	.742	486.713	.123
22.22?	.6?2	716.50?	.745	48?.257	.123
22.25?	.6?1	715.034	.746	48?.41?	.123

CP(K)	CF(K)	GAUGE(K)
.?11?	.?4??	.1?1?

CALCULATEC MASS FLOW RATE = 1.3?6

RPR(I)	AMACH(I)	W(I)	CRPR(I)	RT(I)	RO(I)
17.?51	.?3?	?3?.9??	.599	45?.?92	.105
1?.12?	.?7?	?1?.14?	.60?	459.?61	.106
1?.???	.8?1	50?.??3	.616	461.???	.10?
1?.?4?	.???	?9?.?5?	.625	463.419	.109
1?.?99	.?35	???.19?	.634	465.201	.110
19.1??	.???	?7?.???	.642	466.926	.111
19.3??	.?09	?5?.?12	.650	468.?3?	.112
19.?19	.???	?4?.?7?	.658	47?.?1?	.113
19.???	.7?6	???.???	.665	471.759	.114

THE LIFT FORCE PER INCH BLADE LENGTH IS .?86?54E+01 POUNDS FORCE

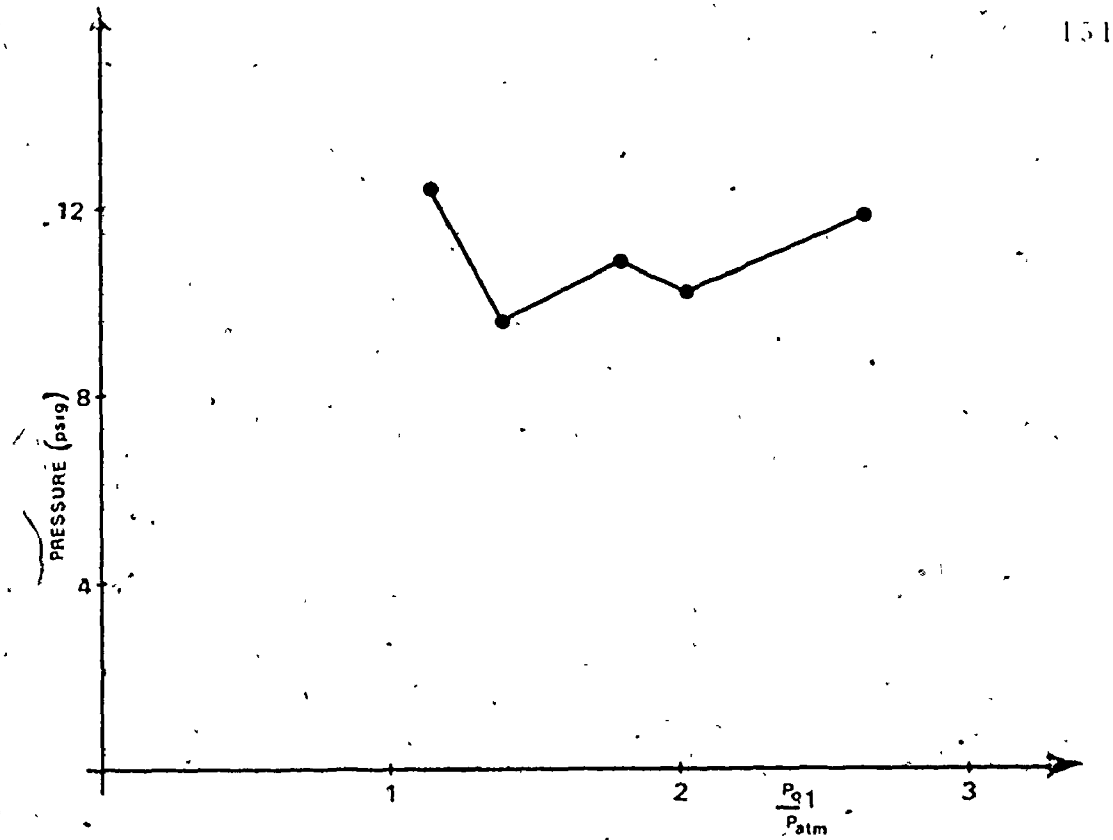

FIGURE 41a PRESSURE DISTRIBUTION
suction surface side of leading edge (X = 0.14 % chord)

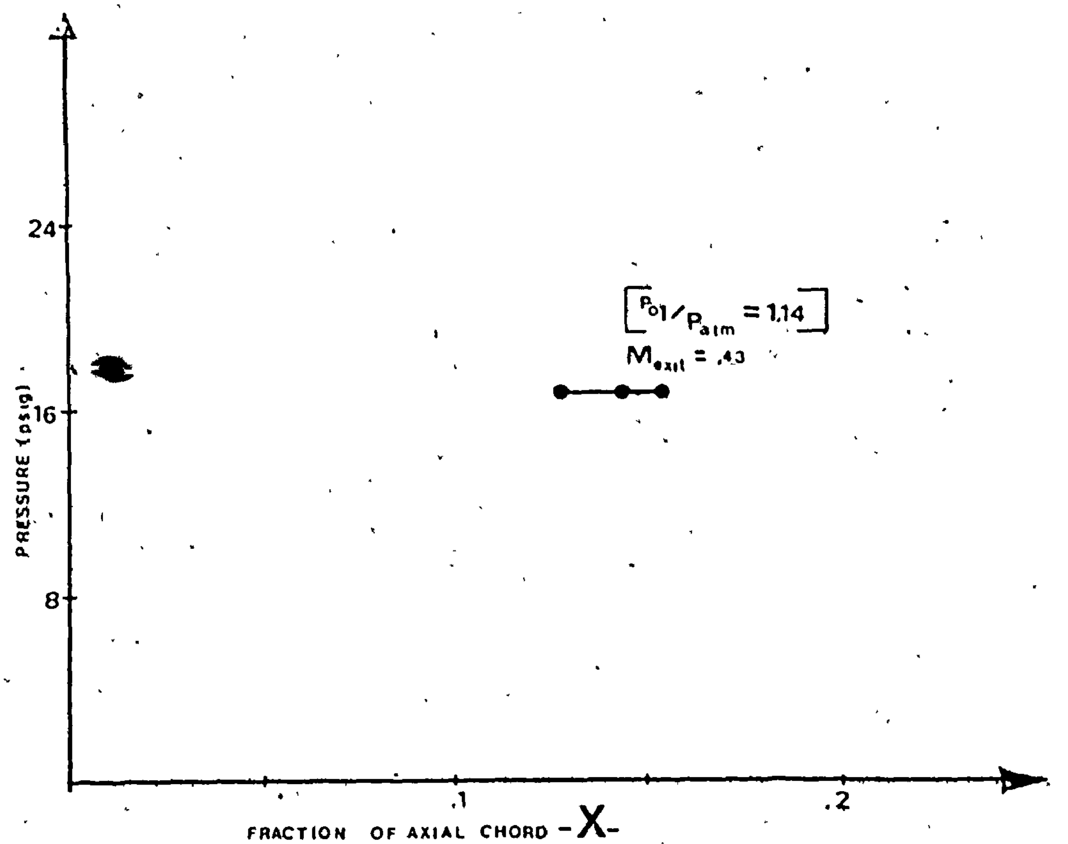

FIGURE 41b PRESSURE DISTRIBUTION
pressure surface side of leading edge

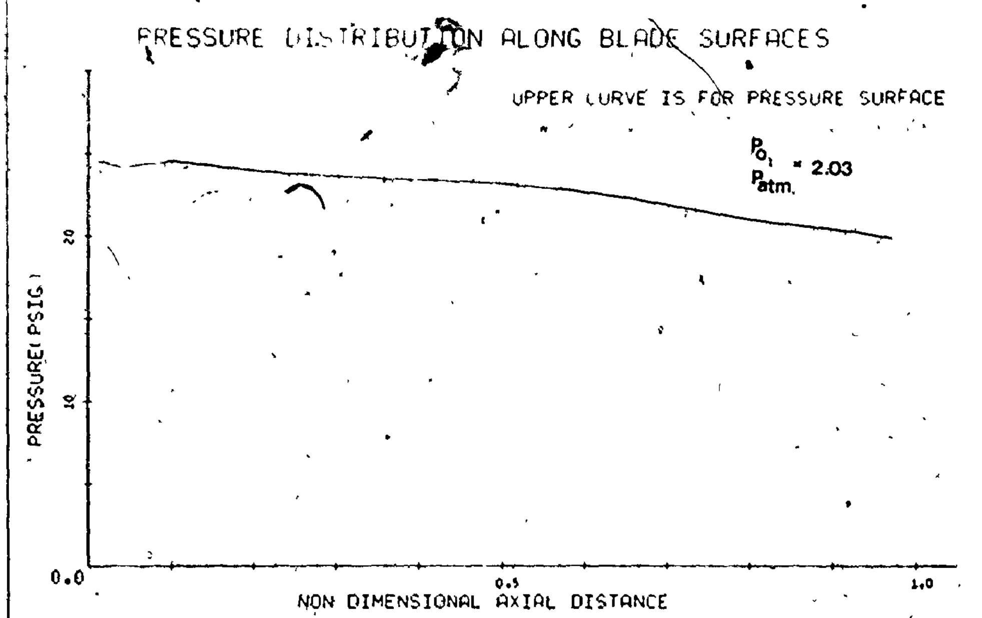

Figure 42 Plotter Output

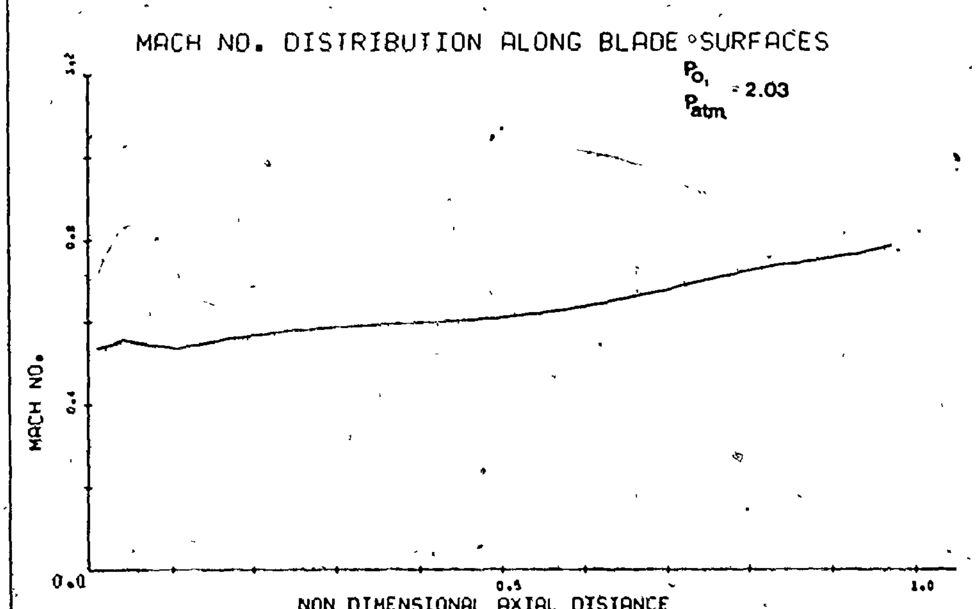

Upper surface is for suction surface
Lower curve is for pressure surface

Figure 43 Plotter Output

APPENDIX VII

DISCUSSION OF LEADING EDGE THEORETICAL RESULTS

Figures 41a and 41b demonstrate a fundamental limitation to the streamline curvature technique when used in regions where a very high change in curvature occurs along an orthogonal. In any gas stream, the maximum possible velocity is a function of the total temperature as follows:

$$U_{max} = \sqrt{2C_pT_o} \qquad (10)$$

where C_p = specific heat at constant pressure

T_o = gas stream's total temperature.

Examination of equation (6) (page 69) will show that when $C_s' >> C_p'$ or when $C_p' >> C_s'$ (curvature differences of 10 in.$^{-1}$ or more), the calculation technique will yield excessively high velocities causing calculated local static temperatures to be less than absolute zero. This impossible result prevents the determination of a local speed of sound and a programming mode error results.

In the derivation of equation (6), a linear variation of curvature across the channel was assumed. This approximation diverges considerably from reality in regions of high curvature change. This fact is easily seen when one realizes that the potential flow technique predicts extreme supersonic patches on each side of the leading edge. A linear variation of curvature across the channel would result in a large portion of the inlet being supersonic. Besides being an unrealistic prediction of the flow characteristics, correct inlet mass flows cannot be obtained as this parameter reaches a maximum at sonic velocities.

To allow the streamline curvature technique to predict a velocity distribution requires abandoning the assumption of linear variation of curvature along an orthogonal. Instead, some kind of power function is required which would yield the highest rate of curvature change close to the most curved surface. This would allow highly supersonic patches in the regions of high curvature while maintaining the subsonic velocities over most of the channel width necessary to obtain the correct mass flow. Two possible equations expressing this relationship are:

$$C = C_s' + (C_p' - C_s')\left(\frac{N}{N_o}\right)^x \qquad (11)$$

$$C = C_s' + (C_p' - C_s')\{\sin[(\frac{N}{N_o})\frac{\pi}{2}]\}^x \qquad (12)$$

where x would be a function of the ratio of the orthogonal end point curvatures and would be of the following form:

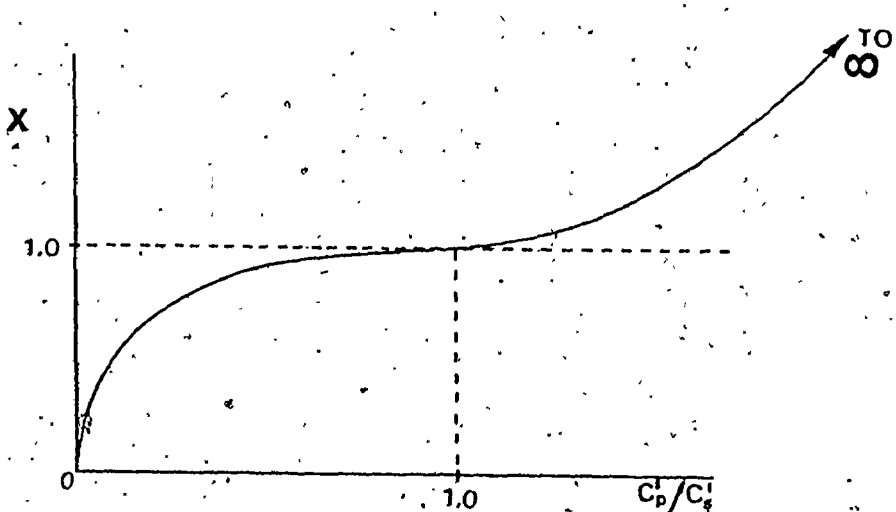

The velocity for equation (11), for example, can be shown to be expressed by the relation:

$$V = e^{\left[\frac{-N_o}{(C_p' - C_s')^{1/x}} (C - C_s')^{1/x} \left\{\frac{(C - C_s')^{x+1}}{x+1} + C_s'\right\}\right]} \qquad (13)$$

From this point the calculation procedure would follow that outlined in Reference (2).

Although the above technique will allow the generation of potential flow results, it is likely to be purely an academic exercise as several inherent assumptions become invalid near the leading edge. Since the radius of curvature is now of the same order of magnitude as the boundary layer thickness, viscous effects are probably important. To expect the boundary layer to accelerate from the leading edge stagnation point (where it has zero velocity) to supersonic speeds in a distance of less than 1% of the axial chord would be unreasonable. Thus, the assumption that on each orthogonal the flow variables may be treated as independent of upstream conditions is obviously invalid.

Figure 41a shows the potential flow pressure variation with overall pressure ratio for an axial location of 0.14% chord. At this position, a curvature of approximately 8.0 inches^{-1} allowed the program to produce results, however, unrealistic. At points nearer the leading edge, higher curvatures produce programming mode errors as discussed previously.

Figure 41b shows that the curvatures were so high for the pressure surface leading edge that solutions could be obtained at only three positions for the lowest overall pressure ratio tested.

To use the results of the orthogonal generation program near the leading edge, requires a more sophisticated streamline curvature technique in which viscous flow boundary layer effects are included. Also the effect of upstream conditions will have to be considered in each orthogonal flow calculation.

TURBINE BLADE PROFILE AND COORDINATES

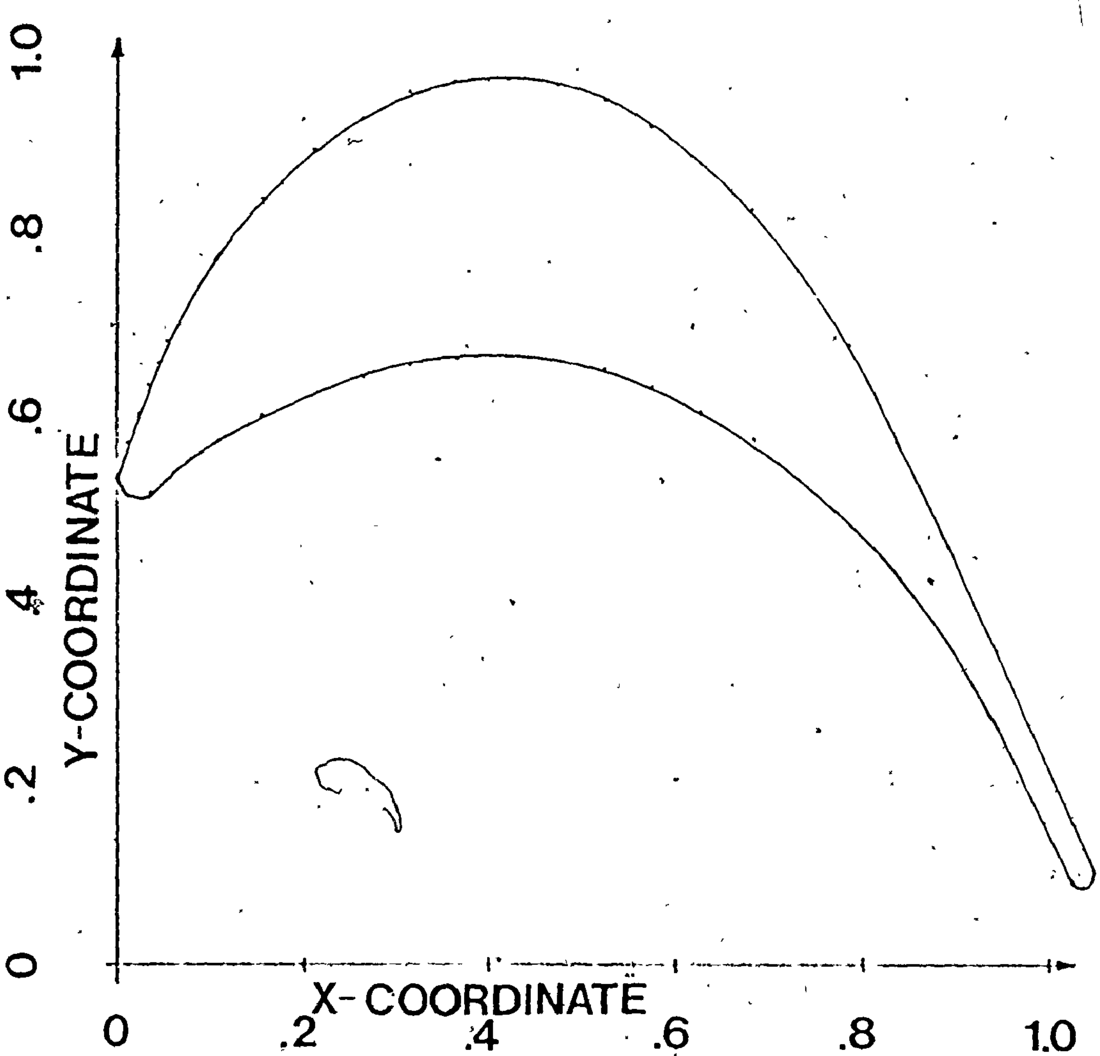

X-COORDINATE	Y-SUCTION SURFACE	Y-PRESSURE SURFACE
0.0000	0.5243	0.5243
0.0105	0.5655	0.5070
0.0210	0.5976	0.5049
0.0315	0.6255	0.5090
0.0420	0.6503	0.5173
0.0525	0.6726	0.5255
0.1050	0.7616	0.5623
0.1575	0.8281	0.5928
0.2100	0.8806	0.6172
0.2620	0.9187	0.6356
0.3150	0.9128	0.6483
0.3635	0.9553	0.6551
0.4200	0.9581	0.6562
0.4725	0.9515	0.6515

X-COORDINATE	Y-SUCTION SURFACE	Y-PRESSURE SURFACE
0.5250	0.9352	0.6408
0.5775	0.9083	0.6235
0.6300	0.8698	0.5993
0.6825	0.8180	0.5676
0.7350	0.7509	0.5276
0.7875	0.6665	0.4783
0.8400	0.5652	0.4181
0.8925	0.4532	0.3452
0.9450	0.3391	0.2575
0.9975	0.2224	0.1542
1.0290	0.1518	0.0906
1.0395	0.1282	0.0886
1.0500	0.1018	0.1018

APPENDIX IX

DIRECTIONS FOR FUTURE RESEARCH

These are three principal areas for future research in this field.

(a) Three Dimensional Effects

The existing cascade wind tunnel may be used to examine the effect of secondary flow induced by the inlet boundary layer. The larger three dimensional test rig currently under construction will also provide additional information on the effects of radial pressure gradients.

(b) The Streamline Curvature Program

The existing program should be expanded to allow the potential flow solution for three dimensional passages.

(c) The Orthogonal Generation Program

The speed of the search technique employed in this program may possibly be increased by the selection of a Newton-Raphson minimization approach. The section of the program in subroutine QUASI labelled [A] could be altered as follows: the equation for the length of the perpendicular from the pressure surface can be equated to that originating at the suction surface. The difference between the two can be minimized using a Newton-Raphson approach, with the pressure surface location as the iterating variable, until acceptable accuracy has been attained. For flow problems requiring a more accurate potential flow grid, an increase in the number of orthogonal defining points to eight (.'. number of spaces, NUS, = 16) could be investigated. This would likely require higher order polynomial fits close to the leading edge stagnation streamline.